Particle-number restoration within the energy density functional formalism

M. Bender,[1,2,3,4,*] T. Duguet,[1,2,5,†] and D. Lacroix[1,6,‡]

[1]*National Superconducting Cyclotron Laboratory, 1 Cyclotron Laboratory, East Lansing, Michigan 48824, USA*
[2]*CEA, Centre de Saclay, IRFU/Service de Physique Nucléaire, F-91191 Gif-sur-Yvette, France*
[3]*Université Bordeaux, Centre d'Etudes Nucléaires de Bordeaux Gradignan, UMR5797, F-33175 Gradignan, France*
[4]*CNRS/IN2P3, Centre d'Etudes Nucléaires de Bordeaux Gradignan, UMR5797, F-33175 Gradignan, France*
[5]*Department of Physics and Astronomy, Michigan State University, East Lansing, Michigan 48824, USA*
[6]*GANIL, CEA and IN2P3, Boîte Postale 5027, F-14076 Caen Cedex, France*

(Received 12 September 2008; published 23 April 2009)

We give a detailed analysis of the origin of spurious divergences and finite steps that have been recently identified in particle-number-restoration calculations within the nuclear energy density functional framework. We isolate two distinct levels of spurious contributions to the energy. The first one is encoded in the definition of the basic energy density functional itself, whereas the second one relates to the canonical procedure followed to extend the use of the energy density functional to multi-reference calculations. The first level of spuriosity relates to the long-known self-interaction problem and to the newly discussed self-pairing interaction process that might appear when describing paired systems with energy functional methods using auxiliary reference states of Bogoliubov or BCS type. A minimal correction to the second level of spuriosity to the multi-reference nuclear energy density functional proposed in [D. Lacroix, T. Duguet, and M. Bender, Phys. Rev. C **79**, 044318 (2009)] is shown to remove completely the anomalies encountered in particle-number-restored calculations. In particular, it restores sum rules over (positive) particle numbers that are to be fulfilled by the particle-number-restored formalism. The correction is found to be on the order of several hundreds of keVs up to about 1 MeV in realistic calculations, which is small compared to the total binding energy but often accounts for a substantial percentage of the energy gain from particle-number restoration and is on the same energy scale as the excitations one addresses with multi-reference energy density functional methods.

DOI: 10.1103/PhysRevC.79.044319 PACS number(s): 21.10.Re, 21.60.Ev, 21.60.Jz, 71.15.Mb

I. INTRODUCTION

Methods based on the use of energy density functionals (EDF) [1] currently provide the only set of theoretical tools that can be applied to all nuclei but the lightest ones in a systematic manner irrespective of their mass and isospin. Nuclear EDF methods coexist on two distinct levels. On the first level, that is traditionally and inappropriately called "self-consistent mean-field theory" or Hartree-Fock (HF) or Hartree-Fock-Bogoliubov (HFB), a single product state provides the normal and anomalous density matrices the energy is a functional of. We will call this type of method a single-reference (SR) EDF approach. On the second level, traditionally and inappropriately called "beyond-mean-field methods," i.e., symmetry restoration and configuration mixing in the spirit of the generator coordinate method (GCM), the set of transition density matrices defined from an appropriate ensemble of product states enter the EDF. We will call such a method a multi-reference (MR) EDF approach. Although SR-EDF calculations have many similarities with density functional theory (DFT) that is widely used in atomic, molecular, and condensed matter physics [2–8], they also present key differences, which prohibit the straightforward mapping of the concepts of electronic DFT to the nuclear case [9–11].

The reference state entering a SR-EDF calculation usually breaks several symmetries of the exact eigenstates of the nuclear Hamiltonian. This is done on purpose, as it allows one to incorporate so-called *static* correlations associated with collective modes [12–15] at moderate computational cost. One of the most important categories of correlations that can be grasped this way are those associated with the formation of neutron and proton Cooper pairs in the medium.

In an SR-EDF approach, pairing correlations are incorporated by making the energy a functional of the anomalous density matrix in addition to the normal one. This amounts to using an independent quasiparticle state (which will be called a quasiparticle vacuum in what follows) of BCS or Bogoliubov type as a reference state instead of a Slater determinant. The price to pay is breaking the $U(1)$ symmetry in gauge space that is a feature of eigenstates of the particle-number operator. As a result the SR state is spread in particle-number space, and one cannot associate the computed energy, even implicitly, to a state belonging to a specific irreducible representation of $U(1)$. In condensed matter physics, for which the BCS method was originally designed [16], this is usually not much of a problem. Nuclei, however, are small finite quantum many-body systems for which two problems arise in this context: (i) the SR approach does not grasp the so-called *dynamical* pairing correlations associated with the fluctuations of both the magnitude and the phase of the order parameter of the broken $U(1)$ symmetry. Correlations associated with this

*bender@cenbg.in2p3.fr
†thomas.duguet@cea.fr
‡lacroix@ganil.fr

zero-energy mode may affect any observable that probes the occupation of levels around the Fermi surface in a significant way; (ii) when the density of single-particle levels around the Fermi energy is below a critical value, pairing correlations are entirely *dynamical* and cannot be described by the SR method, in most cases in contradiction with experiment.

All of these limitations can be overcome by performing multi-reference EDF calculations. Those allow in particular the restoration of particle number [17–21]. It has been noticed for some time, however, that particle-number-restored energies might exhibit divergences [18,22,23] and finite steps [24,25] whenever a single-particle level crosses the Fermi energy as a function of a collective coordinate. This problem is particular to energy density functionals but absent in approaches based on the use of a genuine Hamiltonian and a correlated wave function. As pointed out by Anguiano *et al.* in Ref. [18], some of the common assumptions and approximations made in the construction of nuclear EDFs unavoidably lead to such anomalies, and these authors, as done earlier in Refs. [23,24] in a different context, advocate to use strict antisymmetric two-body vertices and to keep all exchange terms when computing the energy. However, and contrary to what is stated in Refs. [18,26], using antisymmetric but density-dependent two-body vertices is not free from pathologies, even when the divergence introduced by the density-dependent terms is integrable. There is an additional problem that arises particularly when such a dependence is taken under the form of a noninteger power of the density (matrix) [25,27].

Practitioners of EDF methods, however, recognize that it is desirable to use more general energy functionals. For those, particle-number restoration (PNR), and the MR formalism in general, still need to be formulated in a consistent and unambiguous manner that is free from pathologies. As a first step into that direction, a thorough analysis has been recently given by Dobaczewski *et al.* regarding the poles and steps contained in a particle-number-restored energy density functional [25]. In the first of our companion articles [28], hereafter referred to as Article I, we could connect those pathologies to an underlying level of spuriosity that is encoded in the SR energy functional. The associated spurious terms turn out to relate to *self-interaction* processes well known in DFT for condensed matter [29], a problem that was actually studied beforehand in the nuclear context [30] but was soon forgotten, as well as to spurious *self-pairing* processes, whose notion is introduced in the present article. The common source of both pathologies is the use of different and non-anti-symmetric vertices at different places in the EDF violating in this way the exchange symmetry of Fermi statistics. The existence of spurious self-interaction and self-pairing in the SR energy functional is indeed a prerequisite for the appearance of divergences and steps at the MR level, but it is not its origin as such. The pathologies that are particular to the MR level, e.g., particle-number restoration, turn out to be caused by an unphysical contribution to the *weight* of the self-interaction and self-pairing contributions in multi-reference energy kernels. This is an unforeseen consequence of the common practice of constructing the multi-reference energy functional kernel by replacing the density matrices entering a given SR energy functional by transition density matrices [31,32] in *analogy* to the application of the generalized Wick theorem (GWT) [33,34] within a Hamiltonian- and wave-function-based approach. Making reference to a Wick theorem in an energy density functional without having a genuine operator to relate to is necessarily outside the scope of that Wick theorem and might produce unexpected results. And, indeed, using the standard [35] and generalized [33,34] Wick theorems yields different weights to self-interaction and self-pairing contributions to the MR energy kernel as demonstrated in Article I. Only the GWT-motivated procedure produces the poles that are at the origin of the divergences and steps, thus introducing a second level of spuriosity. Using a Hamiltonian- and wave-function-based approach, no problem arises; the vertices at play are either zero or recombine in a particular way that cancels out dangerous poles. Our analysis in Article I was made without reference to a particular MR application and aimed at the introduction of a proper framework to identify and separate both levels of spuriosity within any MR-EDF calculation. It is the aim of the present article to apply the procedure proposed in Article I to correct for the unphysical weights in the special case of particle-number restoration using a particular energy functional the correction can be applied to. In a third article [27], hereafter called Article III, we analyze in detail in the context of PNR the reasons why the pathologies associated with more commonly used functionals containing noninteger powers of the density (matrix) [25] are very likely to be uncorrectable. Together with Ref. [25], Article III demonstrates that the density-dependent two-body forces that are advertised by some authors to be free of pathologies [18,21,26] also have their share of problems when used in MR calculations.

The article is organized as follows: In Sec. II, we introduce single-reference EDF calculations, paying particular attention to resemblances and key differences with the HFB method based on the use of a Hamilton operator. In Sec. III, we introduce multi-reference EDF calculations appropriate to restoring particle number, paying particular attention to resemblances and key differences with the strict particle-number-projected HFB (PNP-HFB) method based on the use of a Hamilton operator. In Sec. IV, we discuss the occurrence of spurious self-interaction and self-pairing processes in SR and MR calculations. Section V analyzes the occurrence of spurious self-interaction and self-pairing contributions to the particle-number-restored EDF using a complex plane analysis and specifies the correction designed in Article I to that particular case. Section VI applies the correction scheme to realistic calculations of finite nuclei. Finally, conclusions are drawn in Sec. VII. Several appendices complement the article with derivations and formulas useful for practical applications.

II. SINGLE-REFERENCE EDF APPROACH

Let us first present the basic elements of the single-reference EDF method that will be needed for our discussion. The HFB implementation of the single-reference EDF approach relies on the use of a quasiparticle vacuum $|\Phi_\varphi\rangle$ as a reference state from which the normal and anomalous one-body density matrices entering the energy density functional are calculated. In the

canonical basis $\{a_\mu, a_\mu^+\}$ that diagonalizes its one-body normal density matrix, the reference state reads

$$|\Phi_\varphi\rangle = \prod_{\mu>0}(u_\mu + v_\mu e^{2i\varphi} a_\mu^+ a_{\bar\mu}^+)|0\rangle, \tag{1}$$

where $|0\rangle$ is the particle vacuum. Throughout this article we limit ourselves to time-reversal invariant quasiparticle vacua $|0\rangle$ with even-number parity and thus only discuss explicitly the ground-state of even-even systems. In addition, we do not mix protons and neutrons when constructing quasiparticle operators. In particular, this limits the pairing interaction to particles of the same isospin. Identical assumptions are made in most, if not all, published work performed using particle-number-projected energy density functionals so far and are sufficient for the purpose of the present article.

The single-particle wave functions associated with the pair-conjugated canonical states $(\mu, \bar\mu)$ is denoted as ϕ_μ and $\phi_{\bar\mu}$. A quantum number η_μ can always be chosen to separate the single-particle basis into two halves, the "positive" and the "negative" ones, with each partner of a given conjugated pair associated to a different half. The normalization of $|\Phi_\varphi\rangle$ gives $|u_\mu^2| + |v_\mu^2 e^{2i\varphi}| = 1$. We use phase conventions where the u_μ and v_μ are real numbers; hence, $u_\mu^2 + v_\mu^2 = 1$, which also fixes the global phase of $|\Phi_\varphi\rangle$. The angle φ in the remaining phase factor denotes the orientation of the state in the $U(1)$ gauge space.

The exact eigenstates of the nuclear many-body problem belong to a specific irreducible representation of the $U(1)$ group. By contrast, the product state $|\Phi_\varphi\rangle$ behaves as a wave packet in gauge space as it mixes states belonging to different irreducible representations. The use of such Bogoliubov product states is at the heart of the symmetry-breaking description of static pairing correlations based on a single reference state. In spite of the broken symmetry of the product state, all observables that are scalars in gauge space still have to be independent on its orientation in gauge space. This allows one to choose a convenient angle on the level of SR calculations that simplifies the calculations, a procedure similar to choosing a major axis system for quadrupole deformed product states. In the case of gauge symmetry, a convenient orientation is provided by $\varphi = 0$. States at different angles are obtained from this state applying the rotation operator $e^{i\varphi\hat N}$ in gauge space

$$|\Phi_\varphi\rangle = e^{i\varphi\hat N}|\Phi_0\rangle = e^{i\varphi\hat N}\prod_{\mu>0}(u_\mu + v_\mu a_\mu^+ a_{\bar\mu}^+)|0\rangle. \tag{2}$$

A. Energy in the strict HFB approach

As a strict HFB approach, we denote the method that determines the energetically most favored quasiparticle vacuum $|\Phi_\varphi\rangle$ through the minimization of the expectation value of a given Hamiltonian $\hat H$ in that product state, without any approximations or generalizations. For the sake of transparency, the Hamiltonian

$$\hat H = \sum_{ij} t_{ij} c_i^+ c_j + \frac{1}{4}\sum_{ijkl}\bar v_{ijkl} c_i^+ c_j^+ c_l c_k \tag{3}$$

is assumed to be given by the sum of kinetic energy term and a two-body interaction. In Eq. (3) $\{c_i^+\}$ defines a complete set of single-particle states, whereas $\bar v_{ijkl}$ denotes antisymmetric matrix elements (or vertices) of the two-body interaction in that basis. The discussion below can be extended without difficulty to a Hamiltonian containing three-body or higher-body forces, but this becomes cumbersome and is not necessary for the purpose of this article.

An important point is that in the context of the strict HFB approach, we assume that the vertex $\bar v_{ijkl}$ does *not* depend on density. So-called density-dependent vertices of Skyrme and Gogny type are widely used in the literature. However, as pointed out in Ref. [25], discussed in the present article and insisted on further in Article III, *any* density-dependent effective vertices do provide MR energies with (at least) spurious finite contributions, even though the vertex is antisymmetric with respect to the remaining single-particle degrees of freedom and all associated exchange terms are exactly accounted for in the MR energy kernels.

Using the standard Wick theorem (SWT) [35–37], the expectation value of $\hat H$ in the product state $|\Phi_\varphi\rangle$ can be evaluated as

$$\begin{aligned} E[\rho^{\varphi\varphi}, \kappa^{\varphi\varphi}, \kappa^{\varphi\varphi *}] &\equiv \frac{\langle\Phi_\varphi|\hat H|\Phi_\varphi\rangle}{\langle\Phi_\varphi|\Phi_\varphi\rangle} \\ &= \sum_\mu t_{\mu\mu}\rho_{\mu\mu}^{\varphi\varphi} + \sum_{\mu\nu}\left[\frac{1}{2}\bar v_{\mu\nu\mu\nu}\rho_{\mu\mu}^{\varphi\varphi}\rho_{\nu\nu}^{\varphi\varphi} + \frac{1}{4}\bar v_{\mu\bar\mu\nu\bar\nu}\kappa_{\mu\bar\mu}^{\varphi\varphi *}\kappa_{\nu\bar\nu}^{\varphi\varphi}\right] \\ &= \sum_\mu t_{\mu\mu} v_\mu^2 + \sum_{\mu\nu}\left[\frac{1}{2}\bar v_{\mu\nu\mu\nu} v_\mu^2 v_\nu^2 + \frac{1}{4}\bar v_{\mu\bar\mu\nu\bar\nu} u_\mu v_\mu u_\nu v_\nu\right], \end{aligned} \tag{4}$$

where $\rho^{\varphi\varphi}$ and $\kappa^{\varphi\varphi}$ are the normal density matrix and anomalous density matrix (pairing tensor) constructed from $|\Phi_\varphi\rangle$, respectively. In the canonical basis of the Bogoliubov transformation defining $|\Phi_\varphi\rangle$, these take the simple form

$$\rho_{\mu\nu}^{\varphi\varphi} \equiv \frac{\langle\Phi_\varphi|a_\nu^\dagger a_\mu|\Phi_\varphi\rangle}{\langle\Phi_\varphi|\Phi_\varphi\rangle} = v_\mu^2\,\delta_{\mu\nu}, \tag{5}$$

$$\kappa_{\mu\nu}^{\varphi\varphi} \equiv \frac{\langle\Phi_\varphi|a_\nu a_\mu|\Phi_\varphi\rangle}{\langle\Phi_\varphi|\Phi_\varphi\rangle} = u_\mu v_\mu e^{2i\varphi}\,\delta_{\nu\bar\mu}, \tag{6}$$

$$\kappa_{\mu\nu}^{\varphi\varphi *} \equiv \frac{\langle\Phi_\varphi|a_\mu^\dagger a_\nu^\dagger|\Phi_\varphi\rangle}{\langle\Phi_\varphi|\Phi_\varphi\rangle} = u_\mu v_\mu e^{-2i\varphi}\delta_{\nu\bar\mu}. \tag{7}$$

The expectation value given in Eq. (4) can be seen as a particular functional of $\rho^{\varphi\varphi}$, $\kappa^{\varphi\varphi}$, and $\kappa^{\varphi\varphi *}$. The symmetries of the Hamiltonian lead of course to a number of specific properties of this functional. In particular, because the Hamiltonian commutes with the particle-number operator, one finds that

$$E[\rho^{\varphi\varphi}, \kappa^{\varphi\varphi}, \kappa^{\varphi\varphi *}] = E[\rho^{00}, \kappa^{00}, \kappa^{00 *}], \tag{8}$$

which underlines that all states that differ only by a rotation in gauge space are degenerate. In other words, the energy functional behaves as a scalar in gauge space as expected.

B. Energy in the SR energy functional approach

In nuclear physics, strict HFB-type approaches are frequently applied in a restricted shell-model space using parametrized single-particle energies and an effective Hamiltonian as a residual interaction [38–40]. For a multitude of reasons outlined in Article I and references given therein, methods using the full model space of occupied particles had to resume so far to the use of (phenomenological) density-dependent effective interactions [41,42], which sets the stage for what is nowadays recognized as an approximation to a more general single-reference EDF formalism. This framework shares many features with the density functional theory (DFT) widely used for description of electronic many-body systems [2–8] but also displays key differences that prohibit the straightforward mapping of all concepts of electronic DFT to the nuclear case [9–11].

In the DFT for many-electron systems, constructive schemes have been established to design the energy functional; see, for instance, Ref. [5] and references given therein. In nuclear physics, such a procedure that would suggest the structure of the functional is still missing, already on a qualitative level. The reasons are the complexity of the nucleon-nucleon interaction, on the one hand, and that in-medium correlations are never small corrections, on the other hand. In the absence of a constructive scheme, all widely used nuclear energy functionals were set up keeping an underlying two-body and sometimes three-body interaction as guiding principle, making generalizations suggested by phenomenology and approximating or even omitting terms that are small but difficult to evaluate. As a consequence, the structure of these functionals resembles that of Eq. (4), except that the expectation value $E[\rho,\kappa,\kappa^*]$ is replaced by a functional $\mathcal{E}[\rho,\kappa,\kappa^*]$. Considering the simple case of a bilinear functional for simplicity and comparison purposes, such a functional can be written as

$$\begin{aligned}\mathcal{E}[\rho,\kappa,\kappa^*] &\equiv \mathcal{E}^{\rho}+\mathcal{E}^{\rho\rho}+\mathcal{E}^{\kappa\kappa}\\ &=\sum_{\mu} t_{\mu\mu} v_\mu^2+\frac{1}{2}\sum_{\mu\nu}\bar{v}^{\rho\rho}_{\mu\nu\mu\nu}\, v_\mu^2 v_\nu^2\\ &\quad+\frac{1}{4}\sum_{\mu\nu}\bar{v}^{\kappa\kappa}_{\mu\bar{\mu}\nu\bar{\nu}}\, u_\mu v_\mu u_\nu v_\nu. \end{aligned} \tag{9}$$

This might appear as an unsusual way to write standard energy functional but will turn out to be very useful below. The corresponding explicit expressions for a Skyrme energy functional are given in Appendix A. The crucial point for our discussion is that the matrix elements of the effective vertex $\bar{v}^{\rho\rho}$ are in general not necessarily antisymmetric for these energy functionals. Also, for Skyrme functionals, one almost always chooses different vertices in the particle-hole ($\bar{v}^{\rho\rho}_{\mu\nu\mu\nu}$) and particle-particle ($\bar{v}^{\kappa\kappa}_{\mu\bar{\mu}\nu\bar{\nu}}$) channels and exploits broken antisymmetry of $\bar{v}^{\rho\rho}_{\mu\nu\mu\nu}$ to obtain a more versatile effective interaction, for example, in the spin-orbit [43,44] or spin-spin parts [45]. The situation is similar for the functionals by Fayans *et al.* [46]. By contrast, the philosophy of the Gogny force is to use the same antisymmetrized density-dependent vertex anywhere, although in actual calculations terms that are very small in SR calculations and at the same time very time-consuming to evaluate are often omitted [47]. As all standard parametrizations of the Skyrme and Gogny interactions use density-dependent vertices, they cannot be mapped on a functional that is the strict expectation value of a many-body Hamiltonian (4). Almost all relativistic mean-field models that are widely used in the literature are explicitly set up as Hartree approaches [1,48] without any explicit exchange terms at all, using phenomenological density dependencies and nonrelativistic pairing energy functionals.

Note that *any* local or nonlocal energy functional that contains only terms proportional to integer powers of the density matrices can be put into the form of Eq. (9) plus similar higher-order terms. For the rest of this article, however, we will assume idealized energy functionals that are linear and bilinear in the density matrix of a given isospin projection, and possibly trilinear with the two isospin projections necessarily involved. We postpone the discussion of functionals with noninteger powers of the density matrices to Article III.

We will not assume antisymmetry of $\bar{v}^{\rho\rho}$ in the formal manipulations throughout the article. Owing to the intrinsic antisymmetry of κ, however, only the antisymmetric part of the vertex is probed in the last term of Eq. (9) and one can always take $\bar{v}^{\kappa\kappa}$ to be antisymmetric, which we do here. The results based on a strict HFB method can always be easily recovered from those derived for a more general bilinear functional simply by enforcing the antisymmetry of $\bar{v}^{\rho\rho}$ and by taking $\bar{v}^{\rho\rho}=\bar{v}^{\kappa\kappa}=\bar{v}$.

III. PARTICLE-NUMBER RESTORATION

To restore good particle number and include the correlations associated with the corresponding Nambu-Goldstone mode, it is necessary to extend the EDF framework to a multi-reference formalism. This extension requires the explicit treatment of the fluctuations of the gauge angle of the gap field. This is particularly crucial for situations where the symmetry breaking is weak or even absent at the SR level, as it is the case, for instance, around closed shells or at high spin. The variation after projection (VAP) method [18,26,49–52] is superior in that respect to the projection after variation (PAV) one because the latter cannot compensate for the spurious sharp phase transition occurring at the SR level in the weak symmetry-breaking regime [18,36,50–52]. An intermediate treatment consists of performing a projection after a SR+Lipkin-Nogami (HFBLN) calculation [17,19,20,50]. This corrects for the principal defect of the PAV method as it guarantees the presence of pairing correlations in the SR state in the weak-pairing regime. However, some doubts have been raised in the literature about the quantitative reliability of this method [50,53]. The MR calculation could be extended further to incorporate dynamical pairing correlations associated with fluctuations of the magnitude of an order parameter that quantifies the amount of pairing correlations present in the SR state [53–56].

An operator that projects out an eigenstate of the particle-number operator $\hat{N}$ with an eigenvalue N from any many-body wave function is provided by [57]

$$\hat{P}^N=\frac{1}{2\pi}\int_0^{2\pi} d\varphi\; e^{i\varphi(\hat{N}-N)}. \tag{10}$$

For the purpose of the present article, it is sufficient to consider the simple case of particle-number restoration after variation. For the sake of transparent notation we discuss the formal framework assuming one type of particles only. The extension to two types of particles is straightforward and will be mentioned only whenever necessary. A normalized projected HFB state is given by

$$|\Psi^N\rangle = \int_0^{2\pi} d\varphi \, \frac{e^{-i\varphi N}}{2\pi c_N} |\Phi_\varphi\rangle, \tag{11}$$

where the real and positive $c_N = \langle\Phi_0|\Psi^N\rangle$ that reads

$$c_N^2 = \langle\Phi_0|\hat{P}^N|\Phi_0\rangle = \frac{1}{2\pi}\int_0^{2\pi} d\varphi e^{-i\varphi N} \langle\Phi_0|\Phi_\varphi\rangle \tag{12}$$

provides the weight of the normalized projected state in the normalized SR state it is projected from, whereas

$$\langle\Phi_0|\Phi_\varphi\rangle = \prod_{\mu>0} \left(u_\mu^2 + v_\mu^2 e^{2i\varphi}\right) \tag{13}$$

denotes the overlap of a gauge-space-rotated state with the unrotated one. The integration interval in Eq. (11) can be reduced to $[0, \pi]$ using symmetries of the integral whenever the SR state $|\Phi_\varphi\rangle$ has a good number parity quantum number [36,39,58].

A. Energy in the strict PNP-HFB approach

In the strict PNP-HFB method, the energy is calculated as the expectation value of the Hamilton operator in the normalized projected state $|\Psi^N\rangle$

$$E^N = \langle\Psi^N|\hat{H}|\Psi^N\rangle = \int_0^{2\pi} d\varphi \frac{e^{-i\varphi N}}{2\pi c_N^2} E[\varphi]\langle\Phi_0|\Phi_\varphi\rangle, \tag{14}$$

where we have used that $\hat{H}$ and $\hat{N}$ commute and that $\hat{P}^N$ is a projector $\hat{P}^N\hat{P}^N = \hat{P}^N$. The energy kernel $E[\varphi]$ can be easily evaluated with the help of the GWT [33,34], which in the canonical basis of $|\Phi_0\rangle$ gives

$$\begin{aligned} E[\varphi] &\equiv \frac{\langle\Phi_0|\hat{H}|\Phi_\varphi\rangle}{\langle\Phi_0|\Phi_\varphi\rangle} \\ &= \sum_\mu t_{\mu\mu}\rho^{0\varphi}_{\mu\mu} + \frac{1}{2}\sum_{\mu\nu} \bar{v}_{\mu\nu\mu\nu}\rho^{0\varphi}_{\mu\mu}\rho^{0\varphi}_{\nu\nu} \\ &\quad + \frac{1}{4}\sum_{\mu\nu} \bar{v}_{\mu\bar{\mu}\nu\bar{\nu}}\,\kappa^{\varphi 0*}_{\mu\bar{\mu}}\kappa^{0\varphi}_{\nu\bar{\nu}}. \end{aligned} \tag{15}$$

In this expression, the normal and anomalous *transition* density matrices between the ket $|\Phi_\varphi\rangle$ and the bra $\langle\Phi_0|$ are defined as

$$\rho^{0\varphi}_{\mu\nu} \equiv \frac{\langle\Phi_0|a^\dagger_\nu a_\mu|\Phi_\varphi\rangle}{\langle\Phi_0|\Phi_\varphi\rangle} = \frac{v_\mu^2 e^{2i\varphi}}{u_\mu^2 + v_\mu^2 e^{2i\varphi}}\delta_{\nu\mu}, \tag{16}$$

$$\kappa^{0\varphi}_{\mu\nu} \equiv \frac{\langle\Phi_0|a_\nu a_\mu|\Phi_\varphi\rangle}{\langle\Phi_0|\Phi_\varphi\rangle} = \frac{u_\mu v_\mu e^{2i\varphi}}{u_\mu^2 + v_\mu^2 e^{2i\varphi}}\delta_{\nu\bar{\mu}}, \tag{17}$$

$$\kappa^{\varphi 0*}_{\mu\nu} \equiv \frac{\langle\Phi_0|a^\dagger_\mu a^\dagger_\nu|\Phi_\varphi\rangle}{\langle\Phi_0|\Phi_\varphi\rangle} = \frac{u_\mu v_\mu}{u_\mu^2 + v_\mu^2 e^{2i\varphi}}\delta_{\nu\bar{\mu}}. \tag{18}$$

The functional kernel $E[\varphi]$ defined by Eq. (15) has the exact same form as the strict HFB energy functional $E[\rho, \kappa, \kappa^*]$ given by Eq. (4) except that the SR density matrix and pairing tensor [Eqs. (5)–(7)] have been replaced by the transition ones [Eqs. (16)–(18)]. Also, the HFB functional is recovered from Eq. (15) for $\varphi = 0$, which amounts to connecting the SR energy and MR energy kernels through $E[0] = E[\rho, \kappa, \kappa^*]$.

B. Energy in the PNR energy functional approach

Difficulties arise when trying to construct the multi-reference energy kernel $\mathcal{E}[\varphi]$ within a true functional framework and connect it to the single-reference one. At present, there is no *ab initio* formalism to derive MR energy functional kernels, of which the SR functional would be a special case, and one can only reverse engineer the procedure and extend the SR energy density functional to the MR level by analogy with the strict Hamiltonian case. Based on the strict HFB and PNP-HFB methods described above, EDF practitioners have used a procedure where $\mathcal{E}[\varphi] \equiv \mathcal{E}[\rho^{0\varphi}, \kappa^{0\varphi}, \kappa^{\varphi 0*}]$ is postulated to be the MR energy kernel that corresponds to a given SR functional [17,18,20,21,25]. In this case, the MR energy corresponding to particle-number restoration takes the form

$$\mathcal{E}^N \equiv \int_0^{2\pi} d\varphi \, \frac{e^{-i\varphi N}}{2\pi c_N^2} \mathcal{E}[\varphi]\langle\Phi_0|\Phi_\varphi\rangle, \tag{19}$$

where $\mathcal{E}[\varphi]$ denotes the set of MR energy functional kernels associated with each gauge angle φ. A kernel $\mathcal{E}[\varphi]$ is a functional of the bra $\langle\Phi_0|$ and of the ket $|\Phi_\varphi\rangle$ in such a way that $\mathcal{E}^N$ depends only implicitly on the projected state [59] and cannot be factorized into a form similar to the left-hand side of Eq. (14). We will call this procedure the "use of the GWT" below, although strictly speaking it is not the GWT that is applied but a formal analogy to the extension at play in the strict Hamiltonian case when using the GWT that is exploited.

On the one hand, the standard strategy based on the GWT analogy to define the nondiagonal functional energy kernel $\mathcal{E}[\varphi]$ from the single-reference functional replacing SR density matrices by the transition ones guarantees that the MR energy functional passes all consistency requirements thought of so far [21]. On the other hand, this procedure is also at the origin of the divergences and finite steps discussed in Ref. [18,25]. In Article I we proposed the general formalism appropriate for a remedy of these problems. The remedy is valid for any type of multi-reference calculation but is limited to EDFs depending on integer powers of the density matrices as is further elaborated on in Article III. The goal of the following sections is to discuss the origin of the problem further and to illustrate the general regularization procedure in its application to PNR.

We note in passing that in PNR and all other MR-EDF calculations the energy is the only observable that is currently determined from a functional; all other observables that are routinely calculated within such an approach are obtained as matrix elements of the corresponding operator between projected states such that they do not contain spurious contributions.

IV. SELF-INTERACTION AND SELF-PAIRING

A. Single-reference level

1. Self-interaction

Microscopic methods for low-energy nuclear structure physics usually describe a self-bound nucleus in terms of nucleons characterized by their experimental mass. In such an approach, a nucleon should not gain energy by interacting with itself. Its so-called *self-interaction* energy, which can be extracted from the one-orbital limit of the interaction part of the energy functional $\mathcal{E}_\mu \equiv \mathcal{E}[\rho^{\varphi\varphi}_{\mu\mu}, 0, 0]$ in the canonical basis, should be strictly zero. This requirement is, however, not fulfilled for most functionals used in electronic DFT [5,6,29,60–62] or nuclear EDF methods [30]. Energy functionals with higher-order density dependencies than those discussed here might also exhibit multiparticle self-energies, not having the proper n-particle limit of the energy functional [62].

Let us consider the energy $\mathcal{E}_\mu$ of a single Fermion occupying the canonical state ϕ_μ, divided by the probability $\rho^{\varphi\varphi}_{\mu\mu} = v^2_\mu$ of this state to be occupied in the auxiliary state $|\Phi_0\rangle$

$$\frac{\mathcal{E}_\mu}{v^2_\mu} = t_{\mu\mu} + \frac{1}{2}\bar{v}^{\rho\rho}_{\mu\mu\mu\mu} v^2_\mu. \tag{20}$$

This expression shows that a self-interaction arises whenever the vertex $\bar{v}^{\rho\rho}$ is not antisymmetric, $\bar{v}^{\rho\rho}_{\mu\mu\mu\mu} \neq 0$, which is impossible when calculating the exact matrix element of a Hamilton operator but happens for general energy density functionals. The total one-body self-interaction energy is obtained summing all individual contributions $\mathcal{E}_\mu$.

2. Self-pairing

Beyond the well-known problem of spurious self-interactions, there exists a similar problem of spurious *self-pairing* processes that may arise whenever superfluidity is incorporated into an energy functional in a DFT or EDF framework. The rationale behind it is that two Fermions occupying a pair of conjugated states should not gain extra binding through the pairing interaction by scattering onto themselves. This requirement constrains the two-particle limit of the theory and the contribution of a conjugated pair to the many-body energy. To the best of our knowledge, the possibility of self-pairing has never been addressed before.

Self-pairing can be easily identified when isolating the energy of two fermions occupying a pair of conjugated states $\{\phi_\mu, \phi_{\bar{\mu}}\}$ in the canonical basis. We define the *direct* interaction energy of such a pair by removing the one-body contributions defined through Eq. (20) to $\mathcal{E}_{\mu\bar{\mu}} \equiv \mathcal{E}[\{\rho^{\varphi\varphi}_{\mu\mu}, \rho^{\varphi\varphi}_{\bar{\mu}\bar{\mu}}\}, \{\kappa^{\varphi\varphi}_{\mu\bar{\mu}}, \kappa^{\varphi\varphi}_{\bar{\mu}\mu}\}, \{\kappa^{\varphi\varphi *}_{\mu\bar{\mu}}, \kappa^{\varphi\varphi *}_{\bar{\mu}\mu}\}]$ and by dividing the result by the probability $P^\Phi_{\mu\bar{\mu}}$ to occupy the pair in the auxiliary state $|\Phi_0\rangle$

$$\frac{\mathcal{E}_{\mu\bar{\mu}} - \mathcal{E}_\mu - \mathcal{E}_{\bar{\mu}}}{P^\Phi_{\mu\bar{\mu}}} = \frac{1}{2}\left(\bar{v}^{\rho\rho}_{\mu\bar{\mu}\mu\bar{\mu}} + \bar{v}^{\rho\rho}_{\bar{\mu}\mu\bar{\mu}\mu}\right) v^2_\mu + \bar{v}^{\kappa\kappa}_{\mu\bar{\mu}\mu\bar{\mu}} u^2_\mu. \tag{21}$$

The probability $P^\Phi_{\mu\bar{\mu}}$ to occupy the pair

$$P^\Phi_{\mu\bar{\mu}} \equiv \frac{\langle\Phi_\varphi|a^\dagger_\mu a^\dagger_{\bar{\mu}} a_{\bar{\mu}} a_\mu|\Phi_\varphi\rangle}{\langle\Phi_\varphi|\Phi_\varphi\rangle} = v^2_\mu \tag{22}$$

is equal to the probability of each state to be occupied, which is a particularity of fully paired quasiparticle vacua, Eq. (1). In the strict HFB case where $\bar{v}^{\rho\rho}_{\mu\bar{\mu}\mu\bar{\mu}} = \bar{v}^{\rho\rho}_{\bar{\mu}\mu\bar{\mu}\mu} = \bar{v}^{\kappa\kappa}_{\mu\bar{\mu}\mu\bar{\mu}} \equiv \bar{v}_{\mu\bar{\mu}\mu\bar{\mu}}$, the two terms on the right-hand side of Eq. (21) combine into

$$\frac{E_{\mu\bar{\mu}} - E_\mu - E_{\bar{\mu}}}{P^\Phi_{\mu\bar{\mu}}} = \bar{v}_{\mu\bar{\mu}\mu\bar{\mu}}, \tag{23}$$

using $u^2_\mu + v^2_\mu = 1$. The same result is obtained in a strict HF method without explicit treatment of pairing correlations. The equality of the two-body interaction energy (23) in the HF and HFB case means that a conjugated pair of states $\{\mu, \bar{\mu}\}$ does not gain extra *direct* binding by scattering onto itself. Genuine pairing correlations originate from scattering to different pairs of conjugated states and back.

For most of the standard SR energy density functionals used for nuclear structure calculations, however, the three terms in Eq. (21) can in general not be recombined into a single one because the vertices entering $\mathcal{E}^{\rho\rho}$ and $\mathcal{E}^{\kappa\kappa}$ are not related, either by construction or due to approximations. Consequently, the direct interaction energy of the conjugated pair is not equal to its zero-pairing limit as it should be, which gives rise to a spurious self-pairing interaction where one has a contribution to the energy functional from the scattering of a pair of conjugated states onto itself.

3. Further discussion

In a composite system consisting of two particle species such as atomic nuclei, the like-particle self-interaction for a given particle species is obtained as the one-particle limit of the interaction energy for this particle species, while keeping the particle number of the other particle species unchanged. Otherwise self-interactions in the terms that couple the two particle species will be missed.

The existence of spurious self-interactions was first recognized in Kohn-Sham DFT for electronic systems [29]. In this context, the construction of self-interaction-free functionals has been studied in some detail; see Refs. [6,29,60–62] and references given therein. It turns out to be not trivial at all knowing that the standard correction method is formulated within the frame of so-called orbital-dependent energy density functionals [63,64] and significantly complexifies the calculations through the modification of both the total energy and the single-particle equations of motion. The (unknown) exact Hohenberg-Kohn functional of DFT is of course self-interaction free. The spurious terms arise when constructing approximate energy functionals that are tractable for the use in actual calculations; i.e., self-interaction is one of the prices to pay for replacing the exact many-body problem by a much simpler set of coupled one-body problems. It is of course desirable to work within a theory that conserves the Pauli principle, but its restoration is mandatory only when its violation affects observables of interest on a scale comparable

with or larger than the precision desired and reachable within a given method. The situation is thus similar to the necessity to restore other broken symmetries. As a matter of fact, the merits of self-interaction corrected energy functionals for electronic DFT are still debated from a phenomenological point of view, as they improve some observables but at the same time degrade others when compared to uncorrected functionals; see Ref. [62] and references given therein.

The same remarks apply to self-pairing. Both self-interaction and self-pairing processes are actually rooted in a violation of the Pauli principle at the level of the two-body (or even higher-order) density matrix in the definition of the energy functional. It is important to stress that they are solely a shortcoming of common energy functionals and not of the auxiliary states of reference used, as the latter are set up as antisymmetrized product states. In particular, all observables other than the energy, which are customarily calculated as expectation values of the corresponding operators, do not exhibit any explicit spurious contributions, although they might be indirectly affected through the use of density matrices that are determined from the solution of a variational equation that uses an energy functional containing spurious contributions as an input.

In the nuclear context, the possible contamination of nuclear energy density functionals by spurious self-energies has been noticed before [1,30,65,66] but was never studied in quantitative detail so far.

It has to be stressed that using self-interaction and self-pairing free energy functionals is not *per se* equivalent to the use of an effective Hamilton operator. Indeed, self-interaction, as usually characterized, and self-pairing, as presently defined, probe only the exchange symmetry of a particle in the canonical basis with itself and its conjugate partner, not the exchange symmetry between all particles. Asking for a full restoration of the Pauli principle necessarily leads to using a genuine Hamilton operator [30].

B. multi-reference level

The appearance of self-interaction and self-pairing processes persists to MR calculations whereas new spurious contributions particular to the MR level arise from the construction of nondiagonal energy kernels. The extension of the self-interaction and self-pairing concepts to the multi-reference framework, however, is not at all straightforward. For instance, the very notion of "occupied" orbitals is ill defined for transition density matrices between arbitrary quasiparticle vacua. In the case of particle-number restoration, the situation is significantly simplified owing to the fact that all vacua entering the PNR energy (19) share the same canonical single-particle basis, which consequently also is the canonical basis of the Bogoliubov transformation linking any pair of these vacua. As demonstrated in Article I it is precisely the latter canonical basis of the transformation connecting a given pair of mixed vacua that must be used to meaningfully identify self-interaction and self-pairing contributions to the corresponding multi-reference energy kernel.

1. "Naive" extension of self-interaction

In the context of PNR multi-reference calculations, the energy of a single Fermion occupying the canonical orbital ϕ_μ divided by the probability $\rho^{\Psi^N}_{\mu\mu}$ to occupy that orbital in the projected state $|\Psi^N\rangle$ is given by

$$\frac{\mathcal{E}^N_\mu}{\rho^{\Psi^N}_{\mu\mu}} = t_{\mu\mu} + \frac{1}{2}\bar{v}^{\rho\rho}_{\mu\mu\mu\mu}\frac{1}{\rho^{\Psi^N}_{\mu\mu}}\int_0^{2\pi} d\varphi \frac{e^{-i\varphi N}}{2\pi c_N^2}\frac{v_\mu^4 e^{4i\varphi}}{u_\mu^2 + v_\mu^2 e^{2i\varphi}} \times \prod_{\substack{\nu>0\\ \nu\neq\mu}}\left(u_\nu^2 + v_\nu^2 e^{2i\varphi}\right). \tag{24}$$

The one-body density matrix ρ^{Ψ^N} of the projected state

$$\begin{aligned}\rho^{\Psi^N}_{\mu\mu} &\equiv \frac{\langle\Psi^N|a^\dagger_\mu a_\mu|\Psi^N\rangle}{\langle\Psi^N|\Psi^N\rangle}\\ &= \int_0^{2\pi} d\varphi\, \frac{e^{-i\varphi N}}{2\pi c_N^2}\rho^{0\varphi}_{\mu\mu}\langle\Phi_0|\Phi_\varphi\rangle\\ &= v_\mu^2\int_0^{2\pi} d\varphi\, \frac{e^{-i\varphi N}}{2\pi c_N^2}e^{2i\varphi}\prod_{\substack{\nu>0\\ \nu\neq\mu}}\left(u_\nu^2 + v_\nu^2 e^{2i\varphi}\right),\end{aligned} \tag{25}$$

is diagonal in the canonical basis of the HFB state it is projected from, which means that the canonical basis of the underlying HFB state is also the natural basis of the projected one.

As for the SR case, the energy (24) reduces to kinetic energy when antisymmetric vertices $\bar{v}^{\rho\rho}$ are used. However, an important aspect specific to the MR case is that the integrand appearing in Eq. (24) contains a potential (simple) pole for $\varphi = \pi/2$ and $v_\mu^2 = u_\mu^2 = 1/2$, i.e., when the state μ is located at the Fermi level and is not more than twofold degenerate in terms of occupation numbers v_μ^2. If the states present a higher degree of degeneracy, an additional factor in the norm overlap will cancel out the dangerous denominator.

2. "Naive" extension of self-pairing

In multi-reference EDF calculations, the direct interaction energy of a conjugated pair as defined above takes the form

$$\frac{\mathcal{E}^N_{\mu\bar{\mu}} - \mathcal{E}^N_\mu - \mathcal{E}^N_{\bar{\mu}}}{P^{\Psi^N}_{\mu\bar{\mu}}} = \int_0^{2\pi} d\varphi\, \frac{e^{-i\varphi N}}{2\pi\, c_N^2\, P^{\Psi^N}_{\mu\bar{\mu}}}\left[\frac{1}{2}\left(\bar{v}^{\rho\rho}_{\mu\bar{\mu}\mu\bar{\mu}} + \bar{v}^{\rho\rho}_{\bar{\mu}\mu\bar{\mu}\mu}\right)v_\mu^2 e^{2i\varphi} + \bar{v}^{\kappa\kappa}_{\mu\bar{\mu}\mu\bar{\mu}}\,u_\mu^2\right]\frac{v_\mu^2\, e^{2i\varphi}}{u_\mu^2 + v_\mu^2\, e^{2i\varphi}}\prod_{\substack{\nu>0\\ \nu\neq\mu}}\left(u_\nu^2 + v_\nu^2\, e^{2i\varphi}\right), \tag{26}$$

where

$$P^{\Psi^N}_{\mu\bar{\mu}} = \frac{\langle\Psi^N|a^\dagger_\mu a^\dagger_{\bar{\mu}} a_{\bar{\mu}} a_\mu|\Psi^N\rangle}{\langle\Psi^N|\Psi^N\rangle} = \rho^{\Psi^N}_{\mu\mu} \tag{27}$$

is the occupation probability of the pair $(\mu, \bar{\mu})$ in the projected HFB state. The probability $P^{\Psi^N}_{\mu\bar{\mu}}$ is equal to the probability $\rho^{\Psi^N}_{\mu\mu}$ of each state to be occupied as we assume the underlying SR state to be a fully paired quasiparticle vacuum with even number parity.

Using a genuine Hamilton operator, for which $\bar{v}^{\rho\rho}_{\mu\bar{\mu}\mu\bar{\mu}} = \bar{v}^{\rho\rho}_{\bar{\mu}\mu\bar{\mu}\mu} = \bar{v}^{\kappa\kappa}_{\mu\bar{\mu}\mu\bar{\mu}} \equiv \bar{v}_{\mu\bar{\mu}\mu\bar{\mu}}$ the matrix elements entering Eq. (26) can be recombined in such a way that the potential pole disappears [18] and that the zero-pairing limit is again recovered

$$\frac{E^N_{\mu\bar{\mu}} - E^N_\mu - E^N_{\bar{\mu}}}{P^{\Psi^N}_{\mu\bar{\mu}}} = \bar{v}_{\mu\bar{\mu}\mu\bar{\mu}}. \tag{28}$$

In the EDF formalism, however, the recombination of terms in Eq. (26) that gives Eq. (28) can no longer be achieved. In this case, the integrand in Eq. (26) contains the same kind of pole as the integrand in Eq. (24).

C. Poles versus "true" self-interaction and self-pairing

In the previous section, we have shown how the self-interaction and self-pairing persist to the multi-reference EDF framework in the case of particle-number restoration. What cannot be deduced from such an extension of the single-reference case, Eqs. (20) and (21), to the multi-reference case, Eqs. (24) and (26), is if self-interaction and self-pairing processes are actually responsible for the poles. Indeed, recalling our general analysis of possible spurious terms in MR energy density functionals from Article I, there are in fact two distinct levels of spuriosity contained in Eqs. (24) and (26), which are of different origins.

The first level is a consequence of using effective vertices that are not antisymmetrized, and/or that are different on the particle-hole and particle-particle channels. In the MR framework, such spurious contributions appear in the diagonal energy kernels, which are equivalent to the self-interaction and self-pairing contributions to the SR energy density functional discussed in Sec. IV A and also enter the off-diagonal kernels. Neither contain poles; hence they cannot be at the origin of the divergences and steps which are the target of the present work.

In addition to that, a second level of spuriosity arises as a consequence of constructing nondiagonal energy kernels in analogy with the generalized Wick theorem, although strictly speaking the GWT applies only to matrix elements of operators. As a matter of fact, and as demonstrated in Article I, using a SWT-motivated procedure rather than a GWT-motivated one does not lead to the second level of spuriosity. Taking the example of a bilinear EDF, the use of the GWT instead of the SWT gives an additional contribution of the form

$$\begin{aligned}\mathcal{E}^N_{\rm CG} &\equiv \int_0^{2\pi} d\varphi\, \frac{e^{-i\varphi N}}{2\pi\, c^2_N} \left(\mathcal{E}^{\rho\rho}_{\rm CG}[\varphi] + \mathcal{E}^{\kappa\kappa}_{\rm CG}[\varphi]\right) \langle\Phi_0|\Phi_\varphi\rangle \\ &= \sum_{\mu>0} \left[\frac{1}{2}\left(\bar{v}^{\rho\rho}_{\mu\mu\mu\mu} + \bar{v}^{\rho\rho}_{\bar{\mu}\bar{\mu}\bar{\mu}\bar{\mu}} + \bar{v}^{\rho\rho}_{\mu\bar{\mu}\mu\bar{\mu}} + \bar{v}^{\rho\rho}_{\bar{\mu}\mu\bar{\mu}\mu}\right) - \bar{v}^{\kappa\kappa}_{\mu\bar{\mu}\mu\bar{\mu}}\right] (u_\mu v_\mu)^4 \int_0^{2\pi} d\varphi\, \frac{e^{-i\varphi N}}{2\pi\, c^2_N} \frac{(e^{2i\varphi}-1)^2}{u^2_\mu + v^2_\mu\, e^{2i\varphi}} \prod_{\substack{\nu>0\\ \nu\neq\mu}} \left(u^2_\nu + v^2_\nu\, e^{2i\varphi}\right)\end{aligned} \tag{29}$$

that is absent in a SWT-motivated procedure and which contains a pole clearly similar to those discussed in connection with Eqs. (24)–(26). Having identified the contribution (29) caused by the use of the GWT, we defined in Article I the *regularized* MR energy and energy kernels, respectively, as

$$\mathcal{E}^N_{\rm REG} \equiv \mathcal{E}^N - \mathcal{E}^N_{\rm CG}, \tag{30}$$

$$\mathcal{E}_{\rm REG}[\varphi] \equiv \mathcal{E}[\varphi] - \mathcal{E}_{\rm CG}[\varphi]. \tag{31}$$

Removing $\mathcal{E}^N_{\rm CG}$ from Eqs. (24) and (26), one obtains the "true" MR self-interaction

$$\begin{aligned}\mathcal{E}^N_{\rm SI} &\equiv \int_0^{2\pi} d\varphi\, \frac{e^{-i\varphi N}}{2\pi\, c^2_N}\, \mathcal{E}^{\rho\rho}_{\rm SI}[\varphi]\, \langle\Phi_0|\Phi_\varphi\rangle \\ &= \sum_{\mu>0} \frac{1}{2}\left(\bar{v}^{\rho\rho}_{\mu\mu\mu\mu} + \bar{v}^{\rho\rho}_{\bar{\mu}\bar{\mu}\bar{\mu}\bar{\mu}}\right) \int_0^{2\pi} d\varphi\, \frac{e^{-i\varphi N}}{2\pi\, c^2_N} \left[v^4_\mu \left(u_\mu{}^2 + v_\mu{}^2 e^{2i\varphi}\right) + 2\, u^2_\mu v^4_\mu (e^{2i\varphi} - 1)\right] \prod_{\substack{\nu>0\\ \nu\neq\mu}} \left(u^2_\nu + v^2_\nu\, e^{2i\varphi}\right).\end{aligned} \tag{32}$$

and the "true" self-pairing contribution

$$\mathcal{E}^N_{\rm SP} \equiv \int_0^{2\pi} d\varphi\, \frac{e^{-i\varphi N}}{2\pi\, c_N^2}\, \mathcal{E}^{\kappa\kappa}_{\rm SP}[\varphi]\, \langle\Phi_0|\Phi_\varphi\rangle$$
$$= \sum_{\mu>0}\left[\bar{v}^{\kappa\kappa}_{\mu\bar{\mu}\mu\bar{\mu}} - \frac{1}{2}\left(\bar{v}^{\rho\rho}_{\mu\bar{\mu}\mu\bar{\mu}} + \bar{v}^{\rho\rho}_{\bar{\mu}\mu\bar{\mu}\mu}\right)\right]\int_0^{2\pi} d\varphi\, \frac{e^{-i\varphi N}}{2\pi\, c_N^2}\, \left[u_\mu^2\, v_\mu^2\, \left({u_\mu}^2 + {v_\mu}^2 e^{2i\varphi}\right) + \left(u_\mu^4 v_\mu^2 - u_\mu^2 v_\mu^4\right)(e^{2i\varphi} - 1)\right]\prod_{\substack{\nu>0\\ \nu\neq\mu}}\left(u_\nu^2 + v_\nu^2\, e^{2i\varphi}\right). \tag{33}$$

both of which belong to the first level of spuriosity and contain no dangerous poles. The expressions (32) and (33) could also have been obtained directly from Eqs. (79) and (80) of Article I.

D. Impact of the poles on PNR energies

In the previous section, we demonstrated that the spurious contribution $\mathcal{E}^N_{\rm CG}$ contains poles. Figure 1 illustrates, through a realistic calculation of the particle-number-restored deformation energy surface of ^{18}O, the impact of such poles for a functional containing a fractional power of the density matrix. The SLy4 parametrization of the standard Skyrme EDF is used in connection with a density-dependent pairing energy functional, which was used in many MR calculations before [67–73]. In practice, the integral over the gauge angle appearing in Eq. (19) is discretized into a sum using the Fomenko expansion, as will be explained in Sec. VI B below. It is important to stress that all observables calculated as operator matrix elements, e.g., particle number, quadrupole moment, radius, etc., are converged using five integration points. The particle-number-restored energy functional, however, does not converge. Instead, one observes the development of several localized divergences as one increases the precision of the calculation, which appear exactly where neutron or proton levels cross the Fermi energy; i.e., where their occupation probability is $v^2 = 0.5$. In spite of the evidence for their appearance presented in Refs. [18,23–25], the divergences remained undetected so far in our PAV calculations, because, on the one hand, the appearance of the divergence requires a number of integration points far above the one used in practical calculations, and beyond what is tractable in connection with other projections and mixing of different deformations, and because, on the other hand, the divergences are sufficiently localized in deformation space that the area obviously affected by the pathology is smaller than the typical distance of states commonly used when calculating energy surfaces and when mixing states with different deformations.

At this point, three questions arise: (i) do the divergences seen in Fig. 1 constitute the only pathological manifestation of the poles? (ii) Do divergences manifest for any type of functional, i.e., irrespective of the fact that it is bilinear or trilinear or contains noninteger powers of the density matrices? (iii) Is the spurious contribution isolated in Eq. (29) responsible for all problems associated with the poles; i.e., would removing it from PNR energy kernels properly regularize the MR-EDF calculation? Answering theses questions will be the aim of

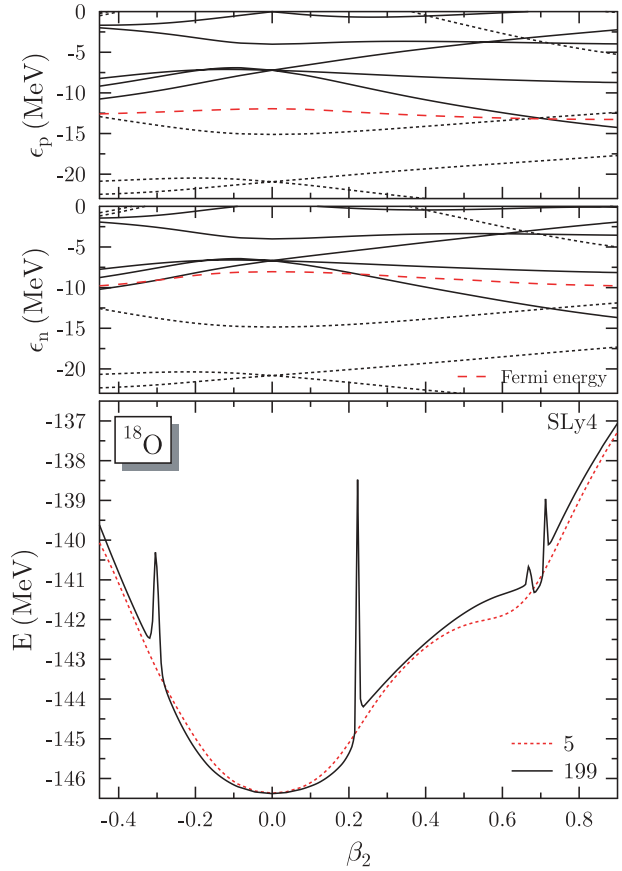

FIG. 1. (Color online) Particle-number-restored deformation energy surface of ^{18}O calculated with SLy4 and a density-dependent pairing interaction and the corresponding single-particle spectra of protons and neutrons as a function of the axial quadrupole deformation for $L = 5$ and 199 discretization points of the integral over the gauge angle (lowest panel). There are clear anomalies that appear when either a proton or neutron single-particle level crosses the Fermi energy. The dimensionless quadrupole deformation β_2 is defined in Eq. (66).

Sec. VI. Before discussing the results obtained using the method proposed in Article I to regularize MR energy kernels, we discuss the pathological manifestations of the poles in more detail through a complex plane analysis, following Ref. [25].

V. COMPLEX PLANE ANALYSIS

The integral over the real gauge angle can be reformulated as a contour integral in the complex plane, which allows the analysis of the energy functional in terms of its poles within the integration contour [25]. In fact, particle-number projection was first introduced through such complex contour integrals [57,74]. It was only after Fomenko [75] demonstrated that a simple trapezoidal rule gives a very efficient discretization of integrals over the gauge angle that Eq. (11) became the standard way to formulate and evaluate PNR observables.

A. Analytic continuation

To that aim, one introduces the complex variable $z = e^{i\varphi}$. As a result, quantities used in the PNR method involve an integration over the unit circle $C_1(|z| = 1)$[1]

$$|\Psi^N\rangle = \oint_{C_1} \frac{dz}{2i\pi c_N} \frac{1}{z^{N+1}} |\Phi_z\rangle, \tag{34}$$

$$\mathcal{E}^N = \oint_{C_1} \frac{dz}{2i\pi c_N^2} \frac{\mathcal{E}[z]}{z^{N+1}} \langle\Phi_1|\Phi_z\rangle, \tag{35}$$

$$c_N^2 = \oint_{C_1} \frac{dz}{2i\pi} \frac{1}{z^{N+1}} \langle\Phi_1|\Phi_z\rangle, \tag{36}$$

whereas the overlap now reads

$$\langle\Phi_1|\Phi_z\rangle = \prod_{\mu>0} \left(u_\mu^2 + v_\mu^2 z^2\right). \tag{37}$$

Finally, the transition density matrix and pairing tensor extended to the complex plane become

$$\rho_{\mu\nu}^{1z} = \frac{v_\mu^2 z^2}{u_\mu^2 + v_\mu^2 z^2} \delta_{\nu\mu}, \tag{38}$$

$$\kappa_{\mu\nu}^{1z} = \frac{u_\mu v_\mu}{u_\mu^2 + v_\mu^2 z^2} \delta_{\nu\bar{\mu}}, \tag{39}$$

$$\kappa_{\mu\nu}^{z1*} = \frac{u_\mu v_\mu z^2}{u_\mu^2 + v_\mu^2 z^2} \delta_{\nu\bar{\mu}}. \tag{40}$$

B. Energy functional kernels

Taking advantage of the Cauchy residue theorem, going to the complex plane allows the calculation of all quantities of interest in terms of poles of the integrand located inside the integration contour. For the norm

$$c_N^2 = \mathcal{R}es(0) \left[\frac{1}{z^{N+1}} \prod_{\mu>0} \left(u_\mu^2 + v_\mu^2 z^2\right) \right] \tag{41}$$

or any other operator matrix elements between projected states, only the pole at $z = 0$ contributes.

The situation is different for the PNR energy as additional poles at finite $z_\mu^\pm = \pm i|u_\mu|/|v_\mu|$ enter the energy kernel $\mathcal{E}[z]$. Thus, Eq. (35) takes the form

$$\mathcal{E}^N = \sum_{z_i=0, |z_\mu^\pm|<1} \frac{1}{c_N^2} \mathcal{R}es(z_i) \left[\frac{\mathcal{E}[z]}{z^{N+1}} \prod_{\mu>0} \left(u_\mu^2 + v_\mu^2 z^2\right) \right] \tag{42}$$

with contributions from the pole at the origin and from all pairs of "hole-like" poles at $z_\mu^\pm$. The situation is schematically depicted in Fig. 2. The location of the pole associated to a given pair $(\mu, \bar{\mu})$ moves along the imaginary axis as the occupation v_μ^2 changes with deformation. When the corresponding pole crosses the unit circle, either entering or leaving the Fermi sea, the integrand is nonanalytical on the integration contour and the integral diverges.

The point has now come to realize that the divergences constitute the most obvious part of the problem but do not contain the entire problem. As can be seen from Eq. (42), the poles at $|z_\mu^\pm| < 1$ contribute to the energy when using an energy functional that contains self-interactions and self-pairing. On the other hand, only the pole at the origin contributes in the strict PNP-HFB/Hamiltonian framework as the poles at $|z_\mu^\pm|$ do

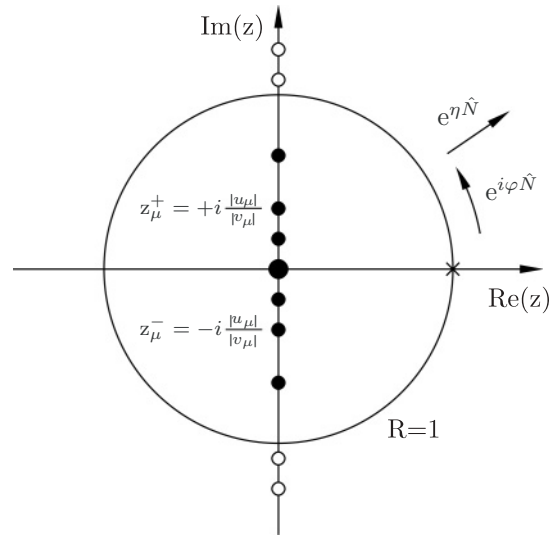

FIG. 2. Schematic view of the analytical structure of the transition densities defined in Eqs. (38)–(40) and of the PNR functional energy kernel $\mathcal{E}[\varphi]$ in the complex plane. Poles marked with filled circles are within the standard circular integration contour of radius $R = 1$, whereas those outside are marked with open circles. The cross marks the location of the SR energy functional at $z = 1$. The operator $e^{i\varphi\hat{N}}$ produces a rotation in gauge space, whereas $e^{\eta\hat{N}}$ is a shift transformation as defined in Eq. (45).

[1] We abusively replace the gauge angle φ by the complex variable z in all our expressions; i.e., SR states characterized by the gauge angle φ, $|\Phi_\varphi\rangle$, are extended into $|\Phi_z\rangle$ to denote SR states anywhere on the complex plane. In particular, the unrotated SR state, denoted as $|\Phi_0\rangle$ when using φ as a variable, is written as $|\Phi_1\rangle$ when using z as a more general variable.

not exist in this case. Consequently, one has to ask the question whether the contributions from the poles at $0 < |z_\mu^\pm| < 1$ to the projected energy are physical, in particular when realizing that the contribution of a given pole can be many orders of magnitude larger than the total energy gain from PNR [25]. In addition, a pole at finite $|z_\mu^\pm|$ entering or leaving the integration circle not only provokes a divergence but also provides the PNR energy with a finite step after the crossing is completed [25]. Looking carefully at the potential energy surface obtained using $L = 199$ integration points, such a step can be seen in Fig. 1; i.e., compare the energy before and after the crossings at $\beta_2 = +0.22$ and $\beta_2 = -0.3$. As a matter of fact, the binding energy jumps from one potential energy surface to another.

C. Spurious contributions

In Sec. IV C, we have identified $\mathcal{E}^N_{\rm CG}$ as the only possible source of spurious poles. In order to obtain a deeper insight to its content, we rewrite Eq. (29) as

$$\begin{aligned}
&\mathcal{E}^N_{\rm CG} \\
&\equiv \oint_{C_1} \frac{dz}{2i\pi c_N^2} \frac{\mathcal{E}_{\rm CG}[z]}{z^{N+1}} \prod_{\mu>0} \left(u_\mu^2 + v_\mu^2 z^2\right) \\
&= \sum_{\mu>0} \left[\frac{1}{2}\left(\bar{v}^{\rho\rho}_{\mu\mu\mu\mu} + \bar{v}^{\rho\rho}_{\bar{\mu}\bar{\mu}\bar{\mu}\bar{\mu}} + \bar{v}^{\rho\rho}_{\mu\bar{\mu}\mu\bar{\mu}} + \bar{v}^{\rho\rho}_{\bar{\mu}\mu\bar{\mu}\mu}\right) - \bar{v}^{\kappa\kappa}_{\mu\bar{\mu}\mu\bar{\mu}} \right] \\
&\quad \times \frac{(u_\mu v_\mu)^4}{2i\pi c_N^2} \oint_{C_1} \frac{dz}{z^{N+1}} \frac{\left(z^2-1\right)^2}{u_\mu^2 + v_\mu^2 z^2} \prod_{\substack{\nu>0 \\ \nu\neq\mu}} \left(u_\nu^2 + v_\nu^2 z^2\right), \qquad (43)
\end{aligned}$$

and define in passing the spurious contribution $\mathcal{E}_{\rm CG}[z]$ to the MR energy kernel over the entire complex plane. From Eq. (43), the spurious contribution of each pole to the PNR energy can be calculated. As for the total energy, the poles of the integrand are located at $z_0 = 0$ and $z_\mu^\pm = \pm i|u_\mu|/|v_\mu|$. This has the important consequence that removing $\mathcal{E}^N_{\rm CG}$ from $\mathcal{E}^N$ does not only extract the contribution of the poles at $|z_\mu^\pm| < 1$ but also a spurious contribution of each conjugated pair $(\mu, \bar{\mu})$ to the physical pole at $z_0 = 0$. The latter could not have simply been guessed from the analysis of the analytical structure of $\mathcal{E}[z]$ in the complex plane. As a matter of fact, the spurious contribution from the pole at $z_0 = 0$ is absolutely essential for the internal consistency of $\mathcal{E}^N_{\rm CG}$. On the one hand, it was shown in Ref. [25] that the energy associated with a single pole at $|z_\mu^\pm| < 1$ can be gigantic (away from where it might be divergent). On the other hand, the total spurious energy hidden in a PNR method cannot be larger than the energy gain from particle-number restoration itself, which is on the order of at most a few MeV. It is only the combined contribution from the poles at $z_0 = 0$ and $z_\mu^\pm$, which nearly cancel each other, that will give reasonable values to the total spurious energy $\mathcal{E}^N_{\rm CG}$ as will be exemplified below.

The residue for the pair of poles at $|z_\mu^\pm|$ contained in Eq. (43) can be evaluated analytically

$$\begin{aligned}
\mathcal{R}e^N_{\rm CG}(z_\mu^\pm) &\equiv \sum_{z_i = z_\mu^\pm} \mathcal{R}es(z_i) \left[\frac{(z^2-1)^2 \prod_{\substack{\nu>0 \\ \nu\neq\mu}} \left(u_\nu^2 + v_\nu^2 z^2\right)}{v_\mu^2 z^{N+1} \left(z - i\frac{|u_\mu|}{|v_\mu|}\right)\left(z + i\frac{|u_\mu|}{|v_\mu|}\right)} \right] \\
&= -\frac{1}{v_\mu^6} \left(\frac{v_\mu}{u_\mu}\right)^{N+2} \frac{1 + (-1)^N}{2i^N} \prod_{\substack{\nu>0 \\ \nu\neq\mu}} \frac{u_\nu^2 v_\mu^2 - v_\nu^2 u_\mu^2}{v_\mu^2}. \qquad (44)
\end{aligned}$$

Note that $\mathcal{R}e^N_{\rm CG}(z_\mu^\pm)$ is zero if projecting on an odd particle number N as the underlying reference state (1) has been chosen to have an even number-parity quantum number [39,58]. The generalization of the present discussion to the case one- (or $2n + 1$) quasiparticle states with an odd number parity is straightforward but not important for the purpose of this article.

The total contribution from the pair of poles $0 < |z_\mu^\pm| < 1$ to the PNR energy is then obtained by replacing the integral in Eq. (43) by $2i\pi\mathcal{R}e^N_{\rm CG}(z_\mu^\pm)$, where $\mathcal{R}e^N_{\rm CG}(z_\mu^\pm)$ is given by Eq. (44). We will discuss the individual contributions from the poles in Sec. VI below. Note that calculating the residue of the pole at z_0 is much more involved because it is a pole of order $N + 1$. Its residue can in fact be calculated analytically through a recursive formula, which, however, involves a sum over such a large number of terms that it is of no practical use and is not reported here. In any case, one can access the spurious contribution from the pole z_0 by subtracting the analytic expression of Eq. (44) from a numerical evaluation of the full expression given by Eq. (29).

D. Properties under shift transformation

The interpretation of the poles at $z_\mu^\pm \neq 0$ becomes clearer when looking at the properties of the PNR energy functional under a so-called shift transformation [25]. In the present article, we choose a slightly different definition of the shift transformation from the one used in Ref. [25]

$$|\Phi_{\varphi - i\eta}\rangle \equiv e^{\eta\hat{N}} |\Phi_\varphi\rangle, \qquad (45)$$

such that the shift transformation operator $e^{(\eta + i\varphi)\hat{N}}$ used in Ref. [25] is the product of ours (45) and a rotation in gauge space.[2] In contrast to a gauge-space rotation that is unitary, the shift transformation (45) is nonunitary and changes the norm of the product state.

In the complex plane, the shift transformation (45) corresponds to a radial shift of z from $z = e^{i\varphi}$ to $z' = e^\eta e^{i\varphi}$; see Fig. 2. Thus, projecting a shifted HFB state on particle number amounts to changing the radius of the integration circle from

[2]Starting from a circular contour, the additional rotation in the definition of Ref. [25] does not make any difference. The situation would have been different if we had started from a noncircular contour.

$R = 1$ to $R = e^{\eta}$ [25]

$$\hat{P}^N|\Phi_{\varphi-i\eta}\rangle = \oint_{C_1} \frac{dz'}{2i\pi}\frac{1}{(z')^{N+1}}|\Phi_{Rz'}\rangle = \oint_{C_R} \frac{dz}{2i\pi}\frac{R^N}{z^{N+1}}|\Phi_z\rangle, \quad (46)$$

where we have made the substitution $z' = e^{i\varphi}$ in the first line and the substitution $z = Rz'$ in the second one. Both expressions will turn out to be useful below. The overlap between the non-normalized projected SR state and its counterpart shifted along the real axis is given by

$$c_N^2(R) \equiv \langle\Phi_1|\hat{P}^N|\Phi_R\rangle = c_N^2 R^N \quad (47)$$

with c_N^2 as defined through Eq. (12); i.e., $c_N^2 \equiv c_N^2(1)$.

All normalized projected matrix elements are shift invariant if the operator $\hat{O}$ in question commutes with $\hat{N}$. Just as the exact ground-state energy, its approximation obtained through the particle-number-restored expectation value of the Hamilton operator is shift invariant. On the other hand, this is not the case for standard particle-number-restored energy density functionals [25]. The violation of shift invariance is obviously a consequence of the presence of the poles at finite $z_\mu^\pm$ contained in the PNR energy kernel constructed on the basis of the GWT. For a given spectrum of poles $z_\mu^\pm$ the energy $\mathcal{E}^N$ changes by a finite quantity whenever the integration circle crosses a pair of poles $|z_\mu^\pm|$ in the course of a shift transformation. As a result, the PNR-EDF is shift invariant only over a finite range of values of the shift parameter η [25]. This result clearly points to the unphysical nature of these poles.

E. Sum rules

One might wonder where the energy that is added/removed when crossing a pole with the integration contour comes from/goes to. In the present section, two different sum rules involving PNR energies $\mathcal{E}^N$ extracted from a given SR functional are carefully derived and discussed to answer such a question.

1. *Radius-weighted sum rule*

As it is introduced in Ref. [25], we first discuss the characteristics of the radius-weighted sum rule $\sum c_N^2(R)\mathcal{E}^N(R)$, although we already insist here that the physical sum rule of interest is the non-radius-weighted one discussed in Sec. V E2 below. The number R appearing in the sum rule is taken to be real even though it is possible to formulate the sum rule using an arbitrary complex number of norm R [25]. Our conclusions will be insensitive to this detail.

First, let us recall how such sum rules arise in the operator- and wave-function-based context. Inserting the complete set of normalized particle-number-projected states[3]

$$\sum_{N\geqslant 0}|\Psi^N\rangle\langle\Psi^N| = \sum_{N\geqslant 0}\hat{P}^N = 1 \quad (48)$$

into an unprojected shifted matrix element of an operator $\hat{O}$ that commutes with $\hat{N}$ gives

$$\langle\Phi_1|\hat{O}|\Phi_R\rangle = \langle\Phi_1|\hat{O}e^{\eta\hat{N}}|\Phi_1\rangle = \sum_{N\geqslant 0}\langle\Phi_1|\hat{O}e^{\eta\hat{N}}|\Psi^N\rangle\langle\Psi^N|\Phi_1\rangle = \sum_{N\geqslant 0} c_N^2(R)\,O^N, \quad (49)$$

where we have used that $e^{\eta\hat{H}}|\Psi^N\rangle = R^N|\Psi^N\rangle$ and define $O^N = \langle\Phi_1|\hat{O}|\Psi^N\rangle/\langle\Phi_1|\Psi^N\rangle$. Equation (49) expands the shifted SR matrix element $O[R] \equiv \langle\Phi_1|\hat{O}|\Phi_R\rangle$ in terms of average values O^N of the operator in all normalized projected states. Applied to the Hamilton operator, Eq. (49) reads

$$E[R] = \sum_{N>0} c_N^2(R)E^N, \quad (50)$$

and provides for $\eta = 0\,(R = 1)$ that the strict HFB energy decomposes into strict PNP-HFB energies (with $N > 0$) weighted by the probability to find the normalized projected states into the SR state. In Eq. (50), the sum could be further reduced to $N > 0$ as the contribution from the term $N = 0$ is strictly zero, i.e., $c_0^2E^0 = E[z = 0]\prod_{\nu>0}u_\nu = 0$. Such a result relies on the fact that only the physical pole at $z = 0$ contributes to the integral providing E^N.

Let us now come to the EDF context and lay out some specificities that are crucial to provide a meaningful discussion of sum rules. (i) In Eq. (50), it was not necessary to specify the integration contour used to calculate E^N as the latter is shift invariant. In the EDF context where the shift invariance might be broken, it is mandatory to specify the contour employed. Consequently, the notation $\mathcal{E}^N(R)$ is used whenever necessary to characterize that a circular contour C_R of radius R is employed to calculate PNR energies. (ii) There is no equivalent to "inserting a complete set of states" in the EDF context as one directly postulates the PNR energy under the form of a functional built from one-body transition density matrices and integrated over the gauge angle and not from the expectation value of a Hamilton operator in projected many-body wave functions. As a consequence, the existence of a sum rule similar to the one discussed for operators is neither obvious nor trivial. By contrast to the above derivation, one has to start from the weighted sum over PNR energies and see if and how it recombines in the same manner as for an operator matrix element. To obey a sum rule analogous to the one provided by Eq. (50) can thus be demanded as a

[3]The fact that one does not need to sum over $N < 0$ can be seen as a consequence of the fact that $|\Psi^N\rangle = 0$ for $N < 0$ as a result of the disappearance of the physical pole at $z = 0$ in the contour integral of Eq. (34). Note that the normalized projected-state on $N = 0$ is $|\Psi^0\rangle = |0\rangle$.

consistency requirement for MR energy density functionals. To recover the SR energy from such a sum rule, it is a necessary condition (but not sufficient) that the MR energy kernel $\mathcal{E}[z]$ is set up such that it gives back the SR energy functional $\mathcal{E}[\rho,\kappa,\kappa^*]$ for $z=1$, as assumed throughout this article. (iii) The sum rule considered in the present section actually differs from the one discussed in Ref. [25]. Indeed, it is mandatory in the EDF context to make the sum running over both positive *and* negative "particle numbers." As will be shown below, the latter is crucial to establish the expected sum rule when individual particle-number-restored energies $\mathcal{E}^N$ are not shift invariant, i.e., when MR energy kernels $\mathcal{E}[z]$ possess spurious poles at finite $z_\mu^\pm$. Indeed, the product $c_N^2(R)\,\mathcal{E}^N(R)$ is different from zero in this case for $N\leqslant 0$ because, although the physical pole at $z=0$ disappears from the integrand as it should, the poles at finite $z_\mu^\pm$ contribute. This is certainly the most direct proof of the nonphysical nature of such poles and nonregularized energy functionals. In the context of the real-space derivation of Ref. [25], obtaining the appropriate sum rule calls for using the correct Fourier decomposition of the periodic delta function over *all* irreducible representations of $U(1)$ including those characterized by negative integers N; i.e., $\sum_{N=-\infty}^{+\infty} e^{-i\varphi N}=2\pi\delta_{2\pi}(\varphi)$. In the following we proceed in the complex plane to establish the needed sum rules.

First, the change of variable $z=Rz'$ is performed to recover an integration over the unit circle

$$\sum_{N=-\infty}^{+\infty} c_N^2(R)\mathcal{E}^N(R)=\sum_{N=-\infty}^{+\infty}\oint_{C_1}\frac{dz}{2i\pi}\frac{\mathcal{E}[Rz]}{z^{N+1}}\langle\Phi_1|\Phi_{Rz}\rangle. \tag{51}$$

We recall that $\mathcal{E}^N(R)$ is proportional to $1/c_N^2(R)$, Eq. (19). As a consequence, $c_N^2(R)=0$ alone is not a sufficient condition that the contribution of a given N to the left-hand side of Eq. (51) vanishes, as $c_N^2(R)\mathcal{E}^N(R)$ might remain finite. We will come back to this below.

To invert the summation and the integral in Eq. (51) and perform the summation explicitly, the power series must be (uniformly) converging on the integration contour. To ensure this property, one has to separate the sums over positive and negative N and use the (local) shift invariance of $\mathcal{E}^N$ to scale the integration radius appropriately in each of the two terms thus generated. Using two infinitesimal shift transformations characterized by $\eta_+>0\,(\eta_-<0)$ for $N>0$ $(N\leqslant 0)$, the right-hand side of Eq. (51) splits into two geometric series converging separately and uniformly on the corresponding integration contours $C_{1^+}(C_{1^-})$. Performing the summation of both geometric series, one obtains

$$\sum_{N=-\infty}^{+\infty} c_N^2(R)\mathcal{E}^N(R)=\left[\oint_{C_{1^+}}-\oint_{C_{1^-}}\right]\frac{dz}{2i\pi}\frac{\mathcal{E}[Rz]}{z(z-1)}\langle\Phi_1|\Phi_{Rz}\rangle. \tag{52}$$

The physical pole at $z=0$, which is of order $N+1$ in $\mathcal{E}^N$, has transformed into two simple poles at $z=0$ and $z=1$ in both integrals in Eq. (52). Note in passing that the pole at $z=0$ would have not appeared if we had grouped the component $N=0$ to the sum over positive numbers. The pole at $z=1$ is on the unit circle and is thus located inside of C_{1^+}, but outside of C_{1^-}. Thus, it contributes to the first integral only in Eq. (52) and provides the sum rule with the contribution $\mathcal{E}[R]\langle\Phi_1|\Phi_R\rangle$ that represents the transition kernel involving the original HFB state $|\Phi_1\rangle$ and the state $|\Phi_R\rangle$ shifted along the real axis to $z=R$.

In the strict PNP-HFB method, this is the only contribution to Eq. (52) as the residue of the simple pole at $z=0$, which corresponds to the contribution from the $N=0$ component, is zero for the reason explained earlier. In any case, such a pole contributes to both integrals in Eq. (52) such that any finite residue would have canceled out anyway. Thus, the sum rule (50) is recovered.

The question is whether this still holds in the EDF context As a matter of fact, the contribution from the poles of $\mathcal{E}[z]$ at $z_\mu^\pm$ depends on the original contour C_R and on the infinitesimal shift transformations leading to Eq. (52). If the shift transformations are such that no pole appears in between the two contours C_{1^-} and C_{1^+}, all poles with $|z_\mu^\pm|<R$ contribute to both integrals and cancel out in Eq. (52), whereas all poles with $|z_\mu^\pm|>R$ do not contribute to either of them. This proves that, except for the ill-defined case of a pair of poles sitting on the original integration circle C_R, one can always perform two infinitesimal shift transformations to prove that

$$\sum_{N=-\infty}^{+\infty} c_N^2(R)\mathcal{E}^N(R)=\mathcal{E}[R]\langle\Phi_1|\Phi_R\rangle. \tag{53}$$

Equation (53) thus expresses that the expected sum rule is found to be valid, even for contaminated and yet uncorrected EDFs, i.e., using energy kernels constructed on the basis of the GWT, at the price of including the contributions from unphysical components $(N\leqslant 0)$.

Applying the same derivation as above to the spurious contribution isolated in Eq. (43), one obtains

$$\sum_{N=-\infty}^{+\infty} c_N^2(R)\,\mathcal{E}_{\rm CG}^N(R)=\mathcal{E}_{\rm CG}[R]\,\langle\Phi_1|\Phi_R\rangle$$
$$=(R^2-1)^2\sum_{\mu>0}\left[\frac{1}{2}\left(\bar v^{\rho\rho}_{\mu\mu\mu\mu}+\bar v^{\rho\rho}_{\bar\mu\bar\mu\bar\mu\bar\mu}+\bar v^{\rho\rho}_{\mu\bar\mu\mu\bar\mu}+\bar v^{\rho\rho}_{\bar\mu\mu\bar\mu\mu}\right)-\bar v^{\kappa\kappa}_{\mu\bar\mu\mu\bar\mu}\right]\frac{(u_\mu\,v_\mu)^4}{u_\mu^2+R^2\,v_\mu^2}\prod_{\substack{\nu>0\\ \nu\neq\mu}}\left(u_\nu^2+R^2\,v_\nu^2\right), \tag{54}$$

which is zero for $R = 1$ as $z = 1$ is the only point in the complex plane where the GWT-related spurious contributions to the MR energy kernel is zero.

It is crucial to analyze further the cancellation of the contribution of spurious poles in Eqs. (52) and (53). Indeed, such a cancellation relies on the original summation over *both* positive and negative "particle numbers" in the definition of the sum rule. If one sums over positive particle numbers only, all pairs of poles situated inside C_R contribute to the sum rule. This is puzzling as it is clearly unphysical to consider negative "particle numbers." Indeed, one necessarily has $c_N^2(R)E^N(R) = 0$ for $N \leqslant 0$ when employing a genuine Hamiltonian. However, the product $c_N^2(R)\mathcal{E}^N(R)$ is different from zero for $N \leqslant 0 if \mathcal{E}[z]$ possesses poles at finite $|z_\mu^\pm| < R$. This is to our opinion the most direct way of stating the nonphysical nature of those poles. In any case, and as proven above, one can at least recover a sum rule for uncorrected functionals at the price of summing over both positive and negative particle numbers. If summing over positive values only, one obtains, using our example of a bilinear functional,

$$\begin{aligned}
&\sum_{N>0} c_N^2(R)\mathcal{E}^N(R) - \mathcal{E}[R]\langle\Phi_1|\Phi_R\rangle \\
&\quad= \sum_{|z_\mu^\pm|<R} \mathcal{R}es(z_\mu^\pm/R)\left[\frac{\mathcal{E}[Rz]}{z(z-1)}\prod_{\mu>0}\left(u_\mu^2 + v_\mu^2 R^2 z^2\right)\right] \\
&\quad= \sum_{\substack{\mu>0 \\ |z_\mu^\pm|<R}} \left[\frac{1}{2}\left(\bar{v}^{\rho\rho}_{\mu\mu\mu\mu} + \bar{v}^{\rho\rho}_{\bar{\mu}\bar{\mu}\bar{\mu}\bar{\mu}} + \bar{v}^{\rho\rho}_{\mu\bar{\mu}\mu\bar{\mu}} + \bar{v}^{\rho\rho}_{\bar{\mu}\mu\bar{\mu}\mu}\right) - \bar{v}^{\kappa\kappa}_{\mu\bar{\mu}\mu\bar{\mu}}\right] \\
&\qquad\times \frac{u_\mu^2 R^2 v_\mu^2}{u_\mu^2 + R^2 v_\mu^2}\prod_{\substack{\nu>0 \\ \nu\neq\mu}} \frac{u_\nu^2 v_\mu^2 - v_\nu^2 u_\mu^2}{v_\mu^2},
\end{aligned} \tag{55}$$

which shows that the physical sum rule ($N > 0$) is broken by a finite amount that relates directly to the presence of spurious poles at finite $z_\mu^\pm$ inside the original integration circle C_R. Note again that the simple pole at $z = 0$ does not contribute as its residue is zero. Equation (55) proves that the sum rule derived in Ref. [25] is incorrect for the cases of interest. In particular, computing Eq. (55) for $R = 1$ provides the nonzero amount by which the decomposition of the SR-EDF into its *physical* PNR components ($N > 0$) is broken, already for the standard integration circle. However, as we will show in Sec. VI D4 below, the contribution from $N \leqslant 0$ is several orders of magnitude smaller than the contribution from $N > 0$ in realistic cases, such that it might pass as numerical noise to the unsuspecting eye.

Subtracting Eq. (54) from Eq. (53) provides the quantity $\sum_{-\infty}^{+\infty} c_N^2(R)[\mathcal{E}^N(R) - \mathcal{E}_{\rm CG}^N(R)]$ by which the sum rule is modified when regularizing the MR energy kernels. One observes that the nonphysical components are zero, i.e., $c_N^2(R)\mathcal{E}_{\rm REG}^N(R) = 0$ for $N \leqslant 0$, and that the sum rule matches the *regularized* kernel at $z = R\mathcal{E}_{\rm REG}[R]\,\langle\Phi_1|\Phi_R\rangle$.

2. *Non-radius-weighted sum rule*

The sum rule (53) is of particular interest when the unit circle C_1 is used as an integration contour to define PNR energies. Indeed, Eq. (53) reduces in this case to

$$\sum_{N=-\infty}^{+\infty} c_N^2 \mathcal{E}^N(R = 1) = \mathcal{E}[z = 1] = \mathcal{E}[\rho, \kappa, \kappa^*], \tag{56}$$

which expresses that the SR-EDF decomposes into PNR energies obtained for all possible "particle numbers" $N \gtrless 0$. This decomposition actually relies on the (required) connection between the SR-EDF and the MR energy functional kernel; i.e., $\mathcal{E}[z = 1] = \mathcal{E}[\rho, \kappa, \kappa^*]$. Equation (56) is valid prior to any regularization of the PNR energy kernel, as long as the sum runs over both positive and negative particle numbers. The null sum rule (54) at $R = 1$ shows that regularizing the PNR-EDF method through the removal of $\mathcal{E}_{\rm CG}^N$ from $\mathcal{E}^N$ consists, for this radius, of reshuffling contributions among different particle-number-restored energies, in such a way that the decomposition of the SR-EDF into its *physical* PNR components ($N > 0$) is fulfilled. Note that the regularized sum rule matches the SR-EDF precisely because the regularization does not modify the energy kernel $\mathcal{E}[z]$ for $z = 1$.

Still, the radius-weighted sum rule considered in Sec. V E2 and in Ref. [25] does not allow us to study the shift invariance of Eq. (56), which is the real question of interest. Indeed, what matters is whether the standard decomposition of the SR-EDF into c_N^2-weighted PNR energies is valid independently on the radius of integration chosen initially to compute $\mathcal{E}^N$. In a Hamiltonian and wave-function-based framework, such an invariance reflects the trivial identity

$$\begin{aligned}
\langle\Phi_1|\hat{H}|\Phi_1\rangle &= \sum_{N>0} \frac{\langle\Phi_1|\hat{H}|\Psi^N\rangle}{\langle\Phi_1|\Psi^N\rangle}\,|\langle\Phi_1|\Psi^N\rangle|^2 \\
&= \sum_{N>0} \frac{\langle\Phi_1|\hat{H}e^{i\eta\hat{N}}|\Psi^N\rangle}{\langle\Phi_1|e^{i\eta\hat{N}}|\Psi^N\rangle}\,|\langle\Phi_1|\Psi^N\rangle|^2.
\end{aligned} \tag{57}$$

Translated to the functional framework, this amounts to considering the non-radius-weighted sum rule

$$\sum_{N=-\infty}^{+\infty} c_N^2(1)\mathcal{E}^N(R) = \sum_{N=-\infty}^{+\infty} \oint_{C_R} \frac{dz}{2i\pi}\,\frac{\mathcal{E}[z]}{z^{N+1}}\,\langle\Phi_1|\Phi_z\rangle, \tag{58}$$

where $c_N^2(1) = c_N^2$ and where the circle of integration C_R is the one chosen to calculate PNR energies. Again, the power series must be split into two parts to perform the summation over particle numbers explicitly. The initial circle of integration C_R being above/below the unit circle, one needs to perform a finite shift transformation to bring the circle associated with negative/positive particle numbers on the other side of the unit circle to make the corresponding series convergent. If particle-number-restored energies are shift invariant, one can proceed without any difficulty and obtain the trivial result that the sum rule $\sum_{N=-\infty}^{+\infty} c_N^2 \mathcal{E}^N(R) = \mathcal{E}[\rho, \kappa, \kappa^*]$ is valid independently on the original radius R. This is of course the case for a Hamiltonian- and wave-function-based PNR method that, once again, would only require the summation over positive particle numbers in the first place.

Of course, problems arise if particle-number-restored energies are not invariant as the shifted circle crosses a spurious pole at $z_\mu^\pm$, i.e., if there are poles $z_\mu^\pm$ located in between C_R and C_1. Indeed, proceeding to the required shift transformation brings an extra contribution to the sum rule in this case. Exemplifying the problem for a bilinear functional and an initial radius $R > 1$, one obtains

$$\sum_{N=-\infty}^{+\infty} c_N^2\, \mathcal{E}^N(R) = \left[\oint_{C_R} - \oint_{C_{1^-}}\right] \frac{dz}{2i\pi}\, \frac{\mathcal{E}[z]}{z(z-1)}\, \langle \Phi_1 | \Phi_z \rangle + 2i\pi \sum_{N=-\infty}^{0} \sum_{1<|z_\mu^\pm|<R} \mathcal{R}es(z_\mu^\pm) \left[\frac{\mathcal{E}[z]}{z^{N+1}} \prod_{\mu>0} \left(u_\mu^2 + v_\mu^2 z^2\right) \right]$$

$$= \mathcal{E}[\rho, \kappa, \kappa^*] + \sum_{N=-\infty}^{+\infty} c_N^2\, \mathcal{E}_{\rm CG}^N(R), \tag{59}$$

with

$$\sum_{N=-\infty}^{+\infty} c_N^2\, \mathcal{E}_{\rm CG}^N(R) = \sum_{\substack{\mu>0 \\ 1<|z_\mu^\pm|<R}} \left[\frac{1}{2}\left(\bar{v}_{\mu\mu\mu\mu}^{\rho\rho} + \bar{v}_{\bar{\mu}\bar{\mu}\bar{\mu}\bar{\mu}}^{\rho\rho} + \bar{v}_{\mu\bar{\mu}\mu\bar{\mu}}^{\rho\rho} + \bar{v}_{\bar{\mu}\mu\bar{\mu}\mu}^{\rho\rho}\right) - \bar{v}_{\mu\bar{\mu}\mu\bar{\mu}}^{\kappa\kappa} \right] u_\mu^2\, v_\mu^2 \prod_{\substack{\nu>0 \\ \nu\neq\mu}} \frac{u_\nu^2 v_\mu^2 - v_\nu^2 u_\mu^2}{v_\mu^2}$$

$$+ \sum_{\substack{\mu>0 \\ 1<|z_\mu^\pm|<R}} \left[\frac{1}{2}\left(\bar{v}_{\mu\mu\mu\mu}^{\rho\rho} + \bar{v}_{\bar{\mu}\bar{\mu}\bar{\mu}\bar{\mu}}^{\rho\rho} + \bar{v}_{\mu\bar{\mu}\mu\bar{\mu}}^{\rho\rho} + \bar{v}_{\bar{\mu}\mu\bar{\mu}\mu}^{\rho\rho}\right) - \bar{v}_{\mu\bar{\mu}\mu\bar{\mu}}^{\kappa\kappa} \right] (u_\mu v_\mu)^4 \sum_{N=-\infty}^{0} \mathcal{R}e_{\rm CG}^N(z_\mu^\pm), \tag{60}$$

where $\mathcal{R}e_{\rm CG}^N(z_\mu^\pm)$ is given by Eq. (44) and where the sums run over all pairs of poles located in between the unit circle C_1 and the integration circle C_R. Note that, in agreement with Eq. (54), the sum rule (60) is zero for $R = 1$ as no pole resides between C_R and C_1 in this case. However, it is easy to see from Eq. (44) that $\sum_{N\leqslant 0} \mathcal{R}e_{\rm CG}^N(z_\mu^\pm)$ is a diverging geometric series of common ratios $|z_\mu^\pm| > 1$ for $R > 1$; i.e., the sum rule is broken by a diverging amount as soon as poles are located in between the integration circle C_R and the unit circle C_1. One can check that the situation is similar if $R < 1$ and the conclusion identical. Regularizing the PNR-EDF through the removal of $\mathcal{E}_{\rm CG}^N(R)$ amounts to transferring the second term in the right-hand side of Eq. (59) to the left-hand side. Doing so restores the physical value ($\mathcal{E}[\rho, \kappa, \kappa^*]$) and the shift invariance of the sum rule as the shift invariance of each individual PNR energy $\mathcal{E}^N(R)$ is actually restored. As $c_N^2 \mathcal{E}_{\rm REG}^N(R) = 0$ for $N \leqslant 0$, the sum rule is in fact restored and made shift invariant by summing over positive particle numbers only

$$\sum_{N>0} c_N^2 \mathcal{E}_{\rm REG}^N(R) = \mathcal{E}[\rho, \kappa, \kappa^*]. \tag{61}$$

Last but not least, it is of interest to look at the nonregularized sum rule obtained by summing over physical components only ($N > 0$). In this case, the physical sum rule calculated for $R > 1$ is broken by a finite amount

$$\sum_{N=1}^{+\infty} c_N^2 \mathcal{E}^N(R) = \oint_{C_R} \frac{dz}{2i\pi}\, \frac{\mathcal{E}[z]}{z(z-1)} \langle \Phi_1 | \Phi_z \rangle$$

$$= \mathcal{E}[\rho, \kappa, \kappa^*] + \sum_{N=1}^{+\infty} c_N^2 \mathcal{E}_{\rm CG}^N(R), \tag{62}$$

with

$$\sum_{N=1}^{+\infty} c_N^2 \mathcal{E}_{\rm CG}^N(R)$$

$$= \sum_{\substack{\mu>0 \\ |z_\mu^\pm|<R}} \left[\frac{1}{2}\left(\bar{v}_{\mu\mu\mu\mu}^{\rho\rho} + \bar{v}_{\bar{\mu}\bar{\mu}\bar{\mu}\bar{\mu}}^{\rho\rho} + \bar{v}_{\mu\bar{\mu}\mu\bar{\mu}}^{\rho\rho} + \bar{v}_{\bar{\mu}\mu\bar{\mu}\mu}^{\rho\rho}\right) - \bar{v}_{\mu\bar{\mu}\mu\bar{\mu}}^{\kappa\kappa} \right] u_\mu^2\, v_\mu^2 \prod_{\substack{\nu>0 \\ \nu\neq\mu}} \frac{u_\nu^2 v_\mu^2 - v_\nu^2 u_\mu^2}{v_\mu^2}, \tag{63}$$

where the sum runs over all pairs of poles located inside the integrations circle C_R. This time, however, and as already made clear above, the sum rule (56) is *not* even recovered for $R = 1$ as the last term of Eq. (62) does not go to zero. Regularizing the PNR-EDF through the removal of $\mathcal{E}_{\rm CG}^N$ amounts to transferring the second term in the right-hand side of Eq. (62) to the

left-hand side. Once again, doing so restores the physical value, i.e., $\mathcal{E}[\rho,\kappa,\kappa^*]$, and the shift invariance of the sum rule.

3. Main conclusions

The first conclusion is that the decomposition of the SR energy $\mathcal{E}[\rho,\kappa,\kappa^*]$ into its *physical* ($N>0$) particle-number-restored components is (i) always fulfilled for a Hamiltonian- and wave-function-based method, whatever the chosen integration circle is, whereas it is (ii) broken by an amount that depends on the chosen integration contour for an EDF-based PNR method if MR energy kernels $\mathcal{E}[z]$ contain poles at finite $z_\mu^\pm$ but (iii) recovered for any value of R after regularizing $\mathcal{E}^N$ through the removal of $\mathcal{E}^N_{\rm CG}$.

The second conclusion is that the decomposition of $\mathcal{E}[\rho,\kappa,\kappa^*]$ involving *unphysical* components ($N\leqslant 0$) is (i) always fulfilled in a Hamiltonian- and wave-function-based PNR method as unphysical components do not contribute anyway (ii) fulfilled in the EDF context if integrating over the unit circle C_1, even for MR energy kernels $\mathcal{E}[z]$ plagued by poles at finite $z_\mu^\pm$ (iii) fulfilled for any integration circle C_R by the regularized EDF-based PNR method, noting in addition that unphysical components no longer contribute.

VI. APPLICATIONS

A. General remarks

As seen in Sec. IV there are two distinct classes of spurious contributions to a multi-reference energy density functional. The first one represents the "true" self-interaction and self-pairing processes that already appear at the single-reference level. It does not provide MR energy kernels with poles; hence, it does not cause divergences or steps in the PNR energy and does not break its shift invariance. The second one is due to the use of the GWT out of its context to define MR energy functional kernels from an underlying SR-EDF that contains self-interaction and self-pairing contributions.

As outlined in Sec. IV A1, correcting consistently for the standard (true) self-interaction $\mathcal{E}^N_{\rm SI}$, Eq. (32), is not an easy task; the correction enters the variational equations already on the single-reference level and leads to a state-dependent single-particle field [29,60–62]. The same would hold regarding the correction for true spurious self-pairing $\mathcal{E}^N_{\rm SP}$, Eq. (33). For that reason, and because such spurious contributions are not responsible for divergences and steps in the PNR energy, we concentrate here on $\mathcal{E}^N_{\rm CG}$, Eq. (29) which is at the origin of the specific and dramatic pathologies encountered in PNR-EDF calculations. Note that subtracting $\mathcal{E}^N_{\rm CG}$ from the PNR energy will also modify the variational equations of a VAP calculation. Here, we confine ourselves to an analysis of the poles and of their impact on the particle-number-restored energy after the variation. In this case, $\mathcal{E}^N_{\rm CG}$ is easily subtracted *a posteriori*.

There is one important limitation to the applicability of the regularization method proposed in Article I and applied in the present work. Although it is straightforward to extend Eq. (29) to an EDF depending on any integer powers of the density matrices, this is not the case for EDFs depending on noninteger powers of the densities. This is a significant limitation, considering that most successful modern functionals use density dependencies of noninteger power.[4] Indeed, this allows them to provide a good description of the most important nuclear matter properties with a very small number of terms and coupling constants to be adjusted phenomenologically [1]. Also the widely used Slater approximation to the Coulomb exchange term falls into the category of a density-dependent term of noninteger power. We analyze the spurious contributions to such category of functionals in Article III, complementing the study of Dobaczewski *et al.* [25]. In the present work, however, we use instead the particular early parametrization SIII [77] of the Skyrme EDF that contains only bilinear and trilinear terms in the normal density matrix. We complement the SIII energy functional with a density-independent local pairing functional that is bilinear in either the neutron or proton anomalous density matrix. For the Coulomb energy functional, we consider only the direct term and neglect the approximate exchange term that was considered in the fit of SIII. As a consequence, all calculated nuclei will be underbound by a few MeV, but this is of no importance for the purpose of the present article. Having said that, it is clear that the construction of high-precision *correctable* EDFs, i.e., only containing integer powers of the density matrices, represents an important task for the future.[5]

The calculation of the various contributions to the correction $\mathcal{E}^N_{\rm CG}$ is outlined in Appendix A. The trilinear terms in the SIII functional are motivated by a local zero-range three-body force that excludes terms of third order in the same nucleon density; it only contains terms of the kind $\rho_n^2(\mathbf{r})\rho_p(\mathbf{r})$ and $\rho_p^2(\mathbf{r})\rho_n(\mathbf{r})$. From a practical point of view, the absence of a genuine term of third power in the same density matrix has the advantage that we do not have to invoke the corresponding correction term outlined in Article I. Instead, the correction of the trilinear terms has the structure of the one of bilinear terms times the projected density of the other species as outlined in Appendix B1.

B. Numerical implementation

In practice, the integrals over gauge angles are discretized with a simple n-point trapezoidal formula

$$\frac{1}{\pi}\int_0^\pi d\varphi\ f(e^{i\varphi}) \Rightarrow \frac{1}{L}\sum_{l=1}^{L} f\left(e^{i\frac{\pi l}{L}}\right), \tag{64}$$

where we assume the projection of a state with even number parity on even particle number to reduce the integration interval to $[0,\pi]$. As was shown by Fomenko [75], this simple scheme

[4] An exception is the relativistic functional [76] used in the MR calculations of Nikšić *et al.* [20].

[5] In practice, one will have to restrict the form to rather low orders in the density matrices. For example, the EDF recently proposed by Baldo *et al.* [78] includes terms up to fifth power in the total density $\rho(\mathbf{r})$, which clearly lead to self-interaction terms [30] that will require a regularization containing quadruple sums over single-particle states, which might be too costly in realistic calculations.

eliminates exactly all components from the SR state that differ from the desired particle number N by up to $\pm 2(L-1)$ particles. Although the spread in particle number is large compared to the total particle number, even small values for L, ranging from 5 in light nuclei to 13 in heavy ones, are sufficient to obtain a converged projected state.

It is customary to use an odd number of discretization points L in the interval $[0, \pi]$ to avoid numerical problems that may appear at $\phi = \pi/2$. This practice does not relate to the real divergences of the energy functional contained in $\mathcal{E}^N_{\rm CG}$ that we discuss here but avoids the implicit division of $u^2_\mu + v^2_\mu e^{i\pi/2}$ contained in an operator kernel by the same factor in the normalization factor c^2_N when evaluating projected operator matrix elements (as, for example, particle number, deformation, or radii), which numerically will not give the analytical result 1 when u^2_μ comes very close to v^2_μ. Of course, the numerical representation of the pole contained in the energy functional would not be very precise in this case either.

With a small modification, the discretization (64) can also be used to represent complex contour integrals with an arbitrary radius R

$$\oint_{C_R} \frac{dz}{2i\pi} f(z) = \int_0^\pi \frac{d\varphi}{\pi} f(R\, e^{i\varphi}) \Rightarrow \frac{1}{L}\sum_{l=1}^{L} f\left(R\, e^{i\frac{\pi l}{L}}\right), \quad (65)$$

which we will use to examine the properties of the energy functional under shift transformations.

For all results shown below, the SR calculations used as a starting point were performed with an approximate particle-number projection before variation within the Lipkin-Nogami approach to ensure that pairing correlations are present in all SR states. Otherwise, pairing correlations would collapse in the SR state whenever there is a large gap in the single-particle spectrum around the Fermi surface.

The dependence of various quantities on axial quadrupole deformation is shown in function of the dimensionless deformation of the mass density distribution β_2 defined as

$$\beta_2 = \sqrt{\frac{5}{16\pi}} \frac{4\pi}{3R^2A} \langle 2z^2 - y^2 - x^2 \rangle, \quad (66)$$

where $R = 1.2A^{1/3}$ fm.

C. ^{18}O

As a first example we discuss ^{18}O. It has the advantage that the density of single-particle levels around the Fermi energy is sufficiently low that the impact of the spurious contribution brought by each single-particle level to the projected energy can be studied separately without having them interfere too much. The integration radius $R_q = 1$ is used until we come to discussing shift invariance.

1. Convergence of operator matrix elements

Before we enter the discussion of the energy functional, we demonstrate the convergence of the particle-number projection method for observables that are calculated as expectation values of the corresponding operators in the projected states.

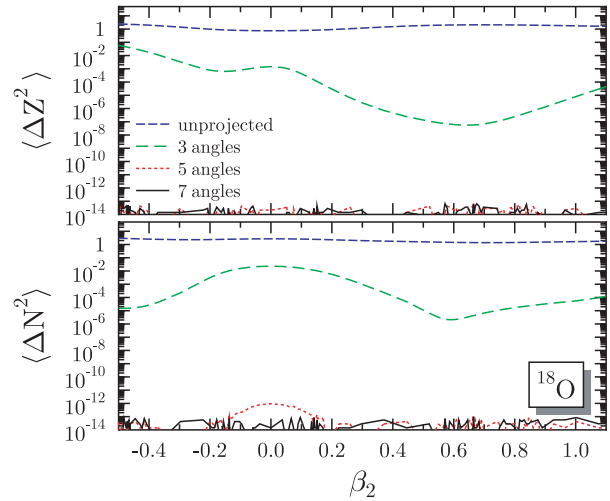

FIG. 3. (Color online) Dispersion of the proton and neutron number of the unprojected SR state and the particle-number-projected SR using 3, 5, or 7 discretization points of the gauge-space integrals as a function of their deformation. For 5 points the projected state is sufficiently converged; for 7 and more points (not shown) the dispersion cannot be distinguished from numerical noise.

In the context of particle-number projection, the most sensitive observable is the dispersion of particle number $\langle \Delta N^2 \rangle = \langle \hat{N}^2 \rangle - \langle \hat{N} \rangle^2$, a two-body operator that provides a measure for the quality of the particle-number-projected state as it has to be zero for an eigenstate of the particle-number operator. For an (unprojected) SR state, $\langle \Delta N^2 \rangle$ is proportional to its spread in particle-number space [79]. One can see in Fig. 3 that the Fomenko discretization converges quickly, already $L = 5$ gives excellent results for ^{18}O, and for $L \geqslant 7$ the dispersion of particle number cannot be distinguished from numerical noise.

2. Regularized PNR energy

Unlike any operator expectation value, particle-number-restored energies do not converge when increasing the number of discretization points in the gauge-space integrals, as already demonstrated in Fig. 1 for the parametrization SLy4. Figure 4 shows the projected deformation energy curve of ^{18}O, now calculated with SIII. What appears to be a smooth deformation energy curve when calculating it with $L = 5$ develops steps and discontinuities when increasing the number of discretization points to 199, i.e., when one starts to resolve the poles at finite $z^\pm_\mu$ close to the integration contour [25]. For example, at small prolate and oblate deformation $\beta_2 \approx \pm 0.15$, the energy jumps from a lower deformation curve around the spherical point to a higher-lying one at larger deformation. Using a small number of discretization points provides a curve that smoothly interpolates between the two energy curves distinguished with $L = 199$. Figure 4 also displays, as a function of the deformation, the poles at $|z^\pm_\mu| = |u_\mu/v_\mu|$ that enter uncorrected energy kernels for protons and neutrons. We follow Dobaczewski *et al.* [25] and plot $z^\pm$ instead of a Nilsson diagram of single-particle energies, as divergences and steps appear where poles cross the integration contour. Note

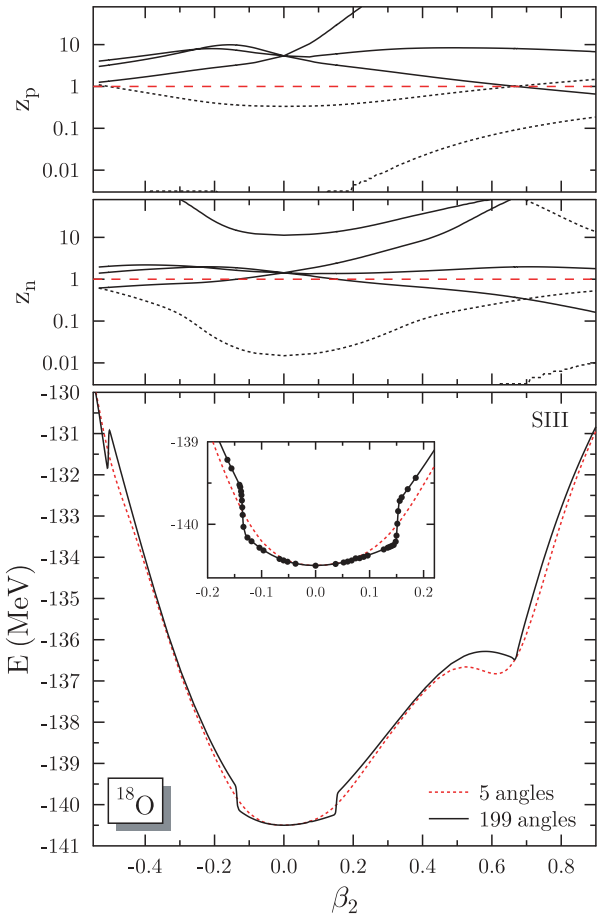

FIG. 4. (Color online) Spectrum of poles $z_\mu = |u_\mu/v_\mu|$ for protons (top panel) and neutrons (middle panel), which for levels in the vicinity of the Fermi energy resembles a stretched and slightly distorted Nilsson diagram. The dashed red line at $z = 1$ denotes the radius of the standard integration contour $R = 1$. The bottom panel shows the particle-number-projected quadrupole deformation energy for $L = 5$ and 199 discretization points for the integral in gauge space. The insert shows a close-up of the steps at small deformation.

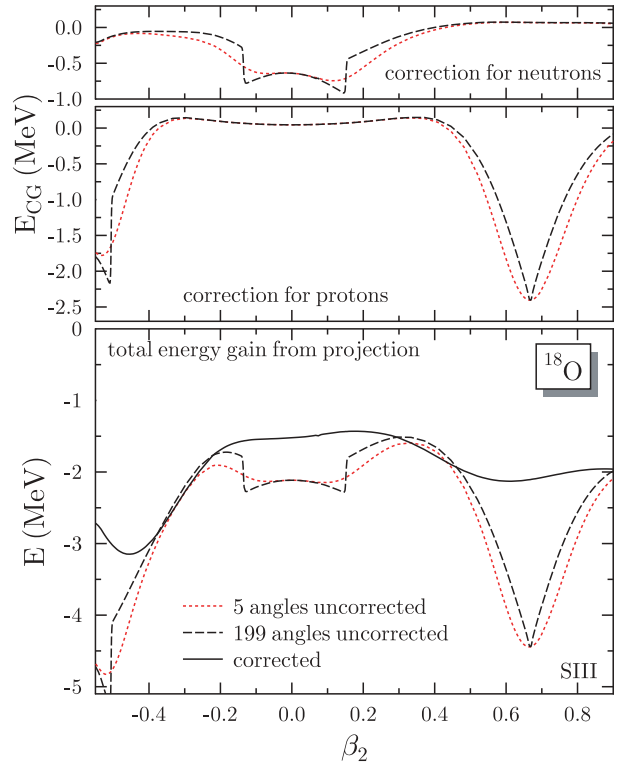

FIG. 5. (Color online) Correction for neutrons (top panel) and protons (middle panel) and energy gain from projection without and with correction for ^{18}O as a function of quadrupole deformation for 5 and 199 discretization points for the integrals in gauge space. The corrected energy gain in independent on the discretization of the integrals when 5 or more angles are used. All panels share the same energy scale.

again that the radius of the latter can be chosen to be different from the standard value $R_q = 1$ that is equivalent to the Fermi energy.

In Fig. 4, however, we do not yet make use of the freedom to modify the integration contour and use the standard values $R_p = R_n = 1$. It can be seen that the two steps developing at $\beta_2 \approx \pm 0.15$ coincide with a pair of neutron levels originating from the spherical $\nu d_{5/2^+}$ shell that enters the integration contour either at the prolate or the oblate deformation. It is noteworthy that the steps are not completely sharp even when using $L = 199$ points for the calculation, as can be seen from the markers in the insert in the lowest panel. There also is a step at $\beta_2 = -0.5$ that coincides with a pair of proton levels from the $\pi p_{1/2^-}$ shell leaving the integration contour. A particular case is the discontinuity at $\beta_2 = 0.7$ that coincides with the crossing of two different pairs of proton levels right on the integration contour.

It is worth noting that no divergence is seen in the PNR energy surface displayed in Fig. 4. This is at variance to Fig. 1. Indeed, SIII corresponds to a specific functional form such that poles at $z = z_\mu^\pm$ are simple poles. This is due to the fact that the trilinear terms entering SIII do not contain products of three density matrices referring to the same isospin. As explained in Article III, this leads to a finite Cauchy principal value as the poles cross the integration circle. Divergences appear only for poles of higher order.

The effects of particle-number restoration on the energy is partly masked in Fig. 4 by the genuine evolution of the energy with deformation. To obtain a clearer picture, we show in the lower panel of Fig. 5 the energy gain from particle-number restoration, obtained as the difference between the MR and SR energy functionals for a given deformation of the SR state. For a cleaner comparison, the LN correction is removed from the SR energy. The steps and discontinuities already seen in Fig. 4 appear when increasing L from 5 to 199. The two upper panels show the correction $\mathcal{E}^N_{\rm CG}$, Eq. (29), separately for protons and neutrons. The lower panel also shows the energy gain for the regularized PNR energy surface $\mathcal{E}^N_{\rm REG}$ obtained by subtracting the neutron and proton corrections $\mathcal{E}^N_{\rm CG}$ from the uncorrected PNR energy $\mathcal{E}^N$ for a given value of L. The correction has many interesting and appealing features

(i) The regularized PNR energy $\mathcal{E}^N_{\rm REG}$ is independent on the discretization of the integral; it is identical, within the

numerical accuracy, for $L = 5$ and 199. As a result, only one curve is shown in Fig. 5.

(ii) The previous result confirms that the entire dependence of the (uncorrected) PNR energy on the discretization of the gauge space integral is contained in $\mathcal{E}^N_{\rm CG}$.

(iii) Looking separately at protons and neutrons, the corresponding correction $\mathcal{E}^N_{\rm CG}$ is largest when a pole of a given nucleon species is close to the integration contour ($R = 1$ here). However, the correction is different from zero for the deformations in between; i.e., the spurious nature of the poles is also felt when being away from divergences and steps.

(iv) All terms in the energy functional (central, spin-orbit, pairing, Coulomb, etc.) contribute to $\mathcal{E}^N_{\rm CG}$, with slightly different magnitudes and different signs, so one has to strictly correct for all of them. This is not unexpected as the source of the spuriosity we focus on here is the weight the matrix elements $\bar{v}^{\rho\rho}$ and $\bar{v}^{\kappa\kappa}$ are multiplied with in Eq. (29), not the matrix elements themselves.

(v) The correction depends strongly on the deformation and will have a non-negligeable impact on the topology of the deformation energy curve. The regularized energy gain from projection is a much smoother function of deformation than the uncorrected one, meaning that regularized particle-number restoration will provide potential energy surfaces with less pronounced structures than uncorrected PNR.

(vi) The correction $\mathcal{E}^N_{\rm CG}$ is of the order of 1 MeV. Of course it has to be smaller than the energy gain from particle-number restoration, which is a few MeV. For ^{18}O, however (and when calculated with SIII), the spurious contribution to the uncorrected energy can be as large as 50% of the total energy gain at some deformations. Also, one MeV error on the mass is larger than the targeted accuracy from EDF methods. In addition, and as exemplified below, the correction to the mass varies from nucleus to nucleus.

(vii) The regularized PNR energy gain can be both larger and smaller than the uncorrected one. In all cases we have looked at so far, however, an increase obtained from the correction rests always very small, while a reduction from correction might be quite substantial, but this might not always be the case.

The corrected deformation energy surface of ^{18}O is shown in Fig. 6 together with the uncorrected ones obtained with $L = 5$ and 199 as was already displayed in Fig. 4. It is striking to see that the corrected PNR energy surface has less structure than the uncorrected ones; its curvature changes now monotonically and the shoulder at $\beta_2 = 0.6$, which always appears as a secondary minimum in SR calculations without pairing for oxygen isotopes, disappears completely. The latter does not mean *a priori* that a regularized PNR plus configuration mixing calculation will no longer give a collective state located at this deformation as it was obtained for ^{16}O [71] and ^{20}O [72] using SLy4. This question needs to be addressed in the near future by performing regularized MR calculations including quadrupole shape configuration mixing.

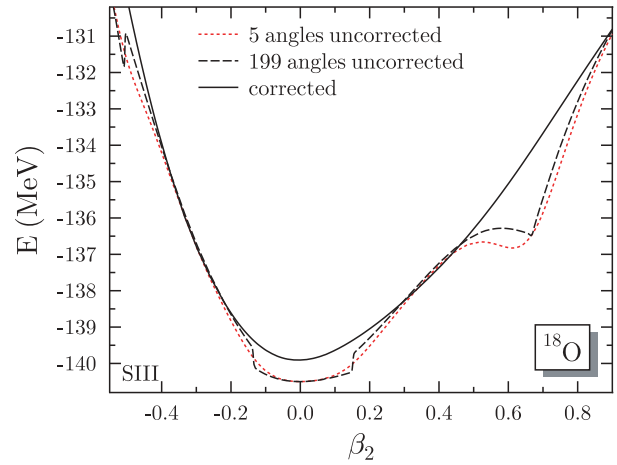

FIG. 6. (Color online) Corrected (solid line) and uncorrected (dotted and dashed lines) particle-number-projected quadrupole deformation energy for ^{18}O, calculated with $L = 5$ and 199 discretization points of the integral in gauge space. The corrected curves are identical.

D. Detailed analysis of spurious contributions

1. *Contributions of individual poles*

After discussing the behavior of the contaminated and regularized PNR energies of a nucleus as a function of its quadrupole deformation, it is instructive to investigate the contribution ε_μ of each canonical pair $(\mu, \bar{\mu})$ to the unphysical energy $\mathcal{E}^N_{\rm CG}$ that contaminate uncorrected MR energies $\mathcal{E}^N$. Formally, each pair of single-particle levels provides a spurious contribution ε^0_μ through the pole at $z = 0$, in addition to the contribution $\varepsilon^\pm_\mu$ associated with the unphysical poles at finite $z^\pm_\mu = \pm i|u_\mu/v_\mu|$, if the latter are located inside of the integration contour of radius R_q. In the end, one can rewrite Eq. (43) as

$$\mathcal{E}^N_{\rm CG} \equiv \sum_{\mu>0} \varepsilon_\mu \equiv \sum_{\mu>0} \varepsilon^0_\mu + \sum_{\substack{\mu>0 \\ |z^\pm_\mu|<R}} \varepsilon^\pm_\mu. \tag{67}$$

The total contribution ε_μ is calculated numerically through Eq. (29) and might depend on the number of discretization points L used for the gauge-space integral. The partial contribution $\varepsilon^\pm_\mu$ can be evaluated using the analytical expression for the residue of the poles, Eq. (44), which does not depend on the discretization of the gauge-space integrals. Finally, ε^0_μ is equal to ε_μ when $|z^\pm_\mu| > R$, whereas for $|z^\pm_\mu| < R$ it can be estimated through $\varepsilon^0_\mu = \varepsilon_\mu - \varepsilon^\pm_\mu$. As $\varepsilon^\pm_\mu$ is calculated analytically while ε_μ is obtained numerically, the values obtained for ε^0_μ might not be very precise when $|z^\pm_\mu| \approx R$.

It turns out that only a few pairs of levels located close to the Fermi level give a nonzero contribution to $\mathcal{E}^N_{\rm CG}$. The relative size and behavior of these contributions as the spectrum of poles changes can be understood by analyzing Eqs. (43) and (44) for a few idealized cases. For this discussion, the combination of matrix elements entering the expression of $\mathcal{E}^N_{\rm CG}$ can be ignored. The values of the matrix elements depend of course on the actual pair of conjugated states they refer to and thereby scale the contribution of a given level to $\mathcal{E}^N_{\rm CG}$. However,

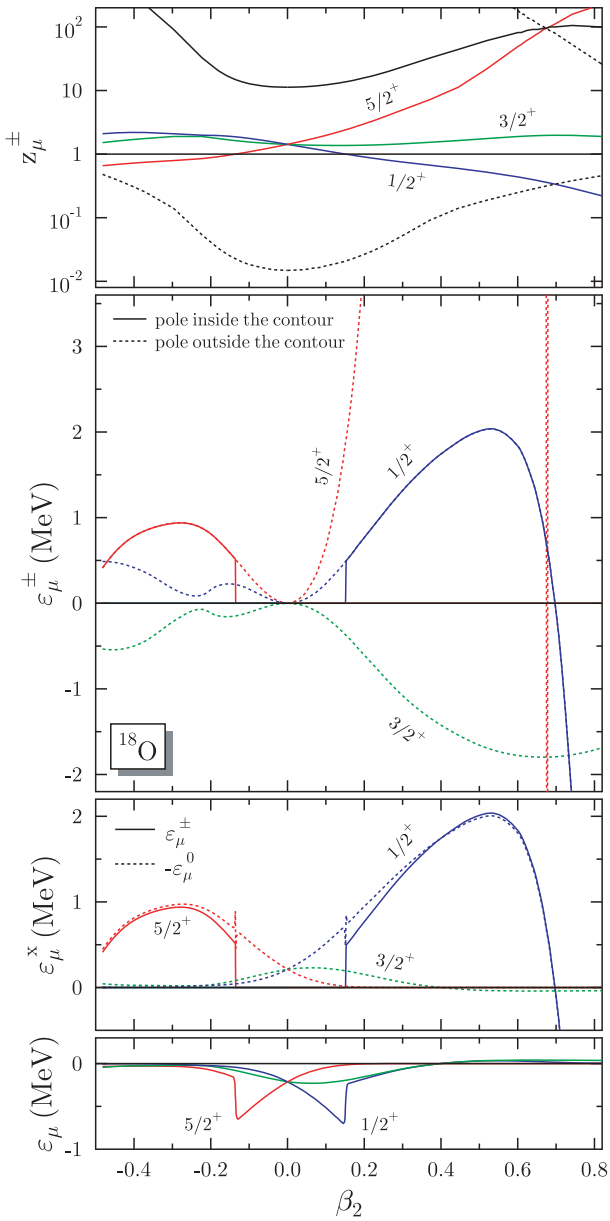

FIG. 7. (Color online) Spurious energy from the single-particle orbits that correspond to the spherical neutron $d_{5/2^+}$ level in ^{18}O as a function of quadrupole deformation (see text).

the matrix elements do not show a particular dependence on μ that determines the limit of ε_μ for completely occupied or unoccupied levels. Therefore it is sufficient to concentrate on the occupation-number-dependent weight factors in Eqs. (43) and (44).

Figure 7 separates the various contributions to $\mathcal{E}^N_{\rm CG}$ for the three pairs of canonical orbits that originate from the spherical neutron $d_{5/2^+}$ level in ^{18}O. The top panel of Fig. 7 displays the location of the three poles of interest on the imaginary axis. Those three pairs of poles are explicitly labeled by the j_z quantum number denoting the projection of the angular momentum on the symmetry axis. Other poles are left unmarked. The three other panels show ε_μ, ε^0_μ, and $\varepsilon^\pm_\mu$ for the three pairs of $d_{5/2^+}$ levels only, as these entirely determine the neutron contribution to $\mathcal{E}^N_{\rm CG}$ for the deformations shown.[6]

The second panel from the top shows $\varepsilon^\pm_\mu$. Solid lines denote $\varepsilon^\pm_\mu$ when the corresponding pole is inside the integration contour ($R_n = 1$ here), while dotted lines denote $\varepsilon^\pm_\mu$ when the pole is outside. Only the former of the two contributes to $\mathcal{E}^N_{\rm CG}$. As $\varepsilon^\pm_\mu$ is usually finite when the corresponding pole crosses the integration contour, its size determines the step left in the PNR deformation energy curve. To understand how $\varepsilon^\pm_\mu$ changes as a function of the location of the corresponding pole $z^\pm_\mu$ within the spectrum of the other poles, Eq. (44) has to be analyzed further. The product over $\nu \neq \mu$ in this expression can be estimated by first considering that there are k_r pairs of levels with $|z^\pm_\xi| \ll |z^\pm_\mu|$, such that their contribution to the product can be approximated by

$$\prod_{\xi=1}^{k_r} \frac{u^2_\xi v^2_\mu - v^2_\xi u^2_\mu}{v^2_\mu} \approx (-)^{k_r} |z^\pm_\mu|^{2k_r} \prod_{\xi=1}^{k_r} v^2_\xi. \tag{68}$$

For a small number k_f of pairs of levels, $|z^\pm_\nu|$ is of the same order as $|z^\pm_\mu|$ such that the full factor in the product has to be kept. Finally, all remaining levels are such that $|z^\pm_\mu| \ll |z^\pm_\lambda|$ and the product can again be simplified

$$\prod_{\lambda=k_r+k_f+1}^{\infty} \frac{u^2_\lambda v^2_\mu - v^2_\lambda u^2_\mu}{v^2_\mu} \approx \prod_{\lambda=k_r+k_f+1}^{\infty} u^2_\lambda. \tag{69}$$

In practical calculations one works with a limited number of pairs of levels k_t in the basis. This cutoff, however, has no consequence for the contribution $\varepsilon^\pm_\mu$ from a pair of levels $(\mu, \bar\mu)$ below the cutoff, as for all reasonable cutoffs the discarded pairs of levels contribute a factor 1 to the product in Eq. (44). Altogether one obtains

$$\begin{aligned}\varepsilon^\pm_\mu &\propto u^4_\mu v^4_\mu \, \mathcal{R}e\mathcal{E}^N_{\rm CG}(z^\pm_\mu) \\ &\approx (-)^{k_r+N/2+1} \, u^2_\mu \, |z^\pm_\mu|^{2k_r-N} \prod_{\substack{\xi=1 \\ |z^\pm_\xi| \ll |z^\pm_\mu|}}^{k_r} v^2_\xi \\ &\quad \times \prod_{\substack{\nu=k_r+1 \\ \nu\neq\mu}}^{k_r+k_f+1} u^2_\nu \left(1 - \frac{|z^\pm_\mu|^2}{|z^\pm_\nu|^2}\right) \prod_{\substack{\lambda=k_r+k_f+1 \\ |z^\pm_\mu| \ll |z^\pm_\lambda|}}^{k_t} u^2_\lambda,\end{aligned} \tag{70}$$

where we assume even particle number N. Equation (70) allows for the complete explanation of the global behavior of $\varepsilon^\pm_\mu$ seen in Fig. 7.

First, for a bilinear functional as discussed here, $\varepsilon^\pm_\mu$ is zero whenever the pair of levels $(\mu, \bar\mu)$ is degenerate with another pair $(\nu, \bar\nu)$, i.e., $|z^\pm_\mu| = |z^\pm_\nu|$, as in this case the middle product in Eq. (70) contains a factor zero. In fact, this is a direct consequence of the disappearance of the pole at $z^\pm_\mu$ in the PNR energy kernel, as the dangerous remaining denominator is now

[6] At large oblate and prolate deformation, the $\varepsilon^\pm_\mu$ of the other levels approaching $z = 1$ are of the same order as those shown but make the plot difficult to read and do not add crucial information.

canceled by an additional factor in the norm kernel.[7] This alone already indicates that the contribution $\varepsilon_\mu^\pm$ of a given pair of levels might fluctuate rapidly when the spectrum of poles $|z_\mu^\pm|$ changes as a function of a collective coordinate. The $(-)^{k_r}$ factor in Eq. (70), whose sign depends on the number of pairs of levels k_r located below the pair $(\mu, \bar{\mu})$, makes $\varepsilon_\mu^\pm$ to change sign through a crossing with another pair. Figure 7 contains several such examples. The downsloping $j_z = 1/2^+$ substate from the $d_{5/2}$ spherical shell crosses with an upsloping level at large prolate deformation. There, $\varepsilon_\mu^\pm$ changes its sign as k_r changes by 1 through the crossing. At spherical deformation, where the three pairs of $d_{5/2}$ levels are degenerate, each of them crosses with the two others and k_r changes either by 2 (for the $j_z = 1/2^+$ and $j_z = 5/2^+$) or 0 (for the $j_z = 3/2^+$), such that the corresponding $\varepsilon_\mu^\pm$ do not change their sign. A very particular case is the subsequent crossing of the upsloping $j_z = 5/2^+$ level with two other levels within a very small interval around $\beta_2 \approx 0.63$. As the three levels do not cross at exactly the same deformation, $\varepsilon_\mu^\pm$ changes its sign twice in a tiny deformation interval, oscillating between values far outside the vertical energy interval shown, that cannot be resolved by what appears as a single vertical (red) dotted line in the plot at $\beta_2 = 0.67$.

Second, let us consider the case of a pair $(\mu, \bar{\mu})$ that is well separated from all others. Thus, there remains only two categories of "other" states in Eq. (70), k_r pairs of levels $(\xi, \bar{\xi})$ with $|z_\xi^\pm| \ll |z_\mu^\pm|$ and $k_t - k_r - 1$ pairs of levels $(\lambda, \bar{\lambda})$ with $|z_\lambda^\pm| \gg |z_\mu^\pm|$. One has still to distinguish between the two cases where $|z_\mu^\pm|$ is larger or smaller than 1.

We start with the case $|z_\mu^\pm| = |u_\mu/v_\mu| > 1$ for which the u_μ^2 factor in Eq. (70) rapidly converges toward 1 as $|z_\mu^\pm|$ increases. In this case, the number of pairs below the pair $(\mu, \bar{\mu})$ is larger than half the particle number; i.e., $k_r > N/2$. For $k_r = N/2 + 1$, $|\varepsilon_\mu^\pm|$ grows linearly with $|z_\mu^\pm|$ for $|z_\mu^\pm| > 1$, for $k_r = N/2 + 2$ it grows quadratically, etc., but always only until it approaches another level, where $|\varepsilon_\mu^\pm|$ goes back to 0 as a consequence of the degeneracy as described above. After the crossing, however, $|\varepsilon_\mu^\pm|$ grows again, although one of the $u_\lambda^2 \approx 1$ factors in Eq. (70) has changed into a $v_\xi^2 \ll 1$ factor at the crossing. At the same time, the number of pairs k_r below the pair $(\mu, \bar{\mu})$ has grown by one such that after the crossing there is an additional $|z_\mu^\pm|^2 = u_\mu^2/v_\mu^2$ factor that overcompensates the effect of the occupation factor v_ξ^2 from the level just crossed, as $v_\xi^2 > v_\mu^2$ and $v_\mu^2 < 1/2$ give $v_\xi^2 u_\mu^2/v_\mu^2 > 1$. For the simultaneous crossing with more than one level, the net effect is the product of the change brought by each crossed level. For poles far from the Fermi level, the values of $\varepsilon_\mu^\pm$ can be very large. For example, the $\varepsilon_\mu^\pm$ of the $j_z = 5/2^+$ level reaches about 550 MeV around $\beta_2 = 0.42$ where the corresponding pole $|z_\mu^\pm|$ is well isolated in the spectrum, drops below zero, and rises immediately back when it crosses a pair from a higher-lying spherical j shell and quickly rises to values larger than 10^5 MeV, dropping back to zero right away as the pole crosses the next pair and quickly gaining a value again several orders of magnitude larger. The sheer size of these values that quickly grow beyond any physical scale that appears in the EDF description of nuclei clearly shows that $\varepsilon_\mu^\pm$ alone cannot be a meaningful quantity in a well-defined theory. The only reason why the $\varepsilon_\mu^\pm$ of these high-lying levels with $|z_\mu^\pm| \gg 1$ do not make $\mathcal{E}_{\rm CG}^N$ incommensurably large is that the corresponding poles are outside of the standard integration circle and thus do not contribute. We will come back to this when discussing PNR with shifted contour integrals below.

For a sufficiently isolated level below the Fermi level, $|z_\mu^\pm| = |u_\mu/v_\mu| < 1$, $|\varepsilon_\mu^\pm|$ also tentatively grows when $|z_\mu^\pm|$ goes toward 0. This is now a consequence of the fact that $k_r \leqslant N/2$, such that $\varepsilon_\mu^\pm$ scales with powers of the inverse of $|z_\mu^\pm|$. At each crossing with a lower lying pair of levels, the additional $u_\lambda^2 \ll 1$ factor is overcompensated by the additional $|z_\mu^\pm|^{-2}$ factor from the decreasing number of pairs k_r below. Again, $\varepsilon_\mu^\pm$ goes to 0 at level crossings and changes its sign depending on the number of pairs crossed.

An important consequence of Eq. (70) and the discussion above is that the $\varepsilon_\mu^\pm$ of an isolated pair is smallest when there are exactly $k_r = N/2$ pairs of other levels below it, which is usually the case for a level with its pole $z_\mu^\pm$ close to the Fermi level. A side effect is that the spurious step due to a pair crossing the integration contour remains rather small when the latter is chosen as the unit circle. This is to put in perspective with the rather small spurious steps observed in Fig. 5 and contaminating the unregularized PNR energy computed using a unit integration circle. We will see in the following that the situation would have been more dramatic if we had used different contours.

As discussed in Sec. V, poles at finite $z_\mu^\pm$ entering or leaving the integration contour are the origin of the spurious steps in PNR energy surfaces, as the corresponding (usually finite) $\varepsilon_\mu^\pm$ is suddenly added to or removed from $\mathcal{E}_{\rm CG}^N$, respectively. In the second panel of Fig. 7, contributions from poles inside or outside the standard integration contour of radius $R = 1$ are plotted as solid or dotted lines, respectively, to make this distinction. The third panel from the top also shows $\varepsilon_\mu^\pm$ with solid lines but now only when it actually contributes to $\mathcal{E}_{\rm CG}^N$. The dotted lines represent $-\varepsilon_\mu^0$ such that the distance between the curves for $\varepsilon_\mu^\pm$ and $-\varepsilon_\mu^0$ provides the total contribution ε_μ from the pair $(\mu, \bar{\mu})$ to $\mathcal{E}_{\rm CG}^N$.[8]

The results for the neutron levels depicted in Fig. 7 suggest that $\varepsilon_\mu^\pm$ converges toward $-\varepsilon_\mu^0$ when $z_\mu^\pm$ goes to zero, i.e., for deeply bound levels far below the Fermi energy, such that the

[7] This results holds for any bilinear functional in the density matrix of a given isospin, even if it is multiplied with the densities of the other one. When allowing for higher-order functionals, however, a term of order n in the density matrix can generate a pole at $z_\mu^\pm$ of order (at most) $(n-1)$. For $\varepsilon_\mu^\pm$ to be 0, one needs the pole at $z_\mu^\pm$ to disappear altogether, which requires $(n-1)$ additional factors from the norm kernel to cancel the denominator $(u_\mu^2 + v_\mu^2 z^2)^{-(n-1)}$. Thus, the pair of interest $(\mu, \bar{\mu})$ needs to be degenerated (at least) with $(n-1)$ other pairs for $\varepsilon_\mu^\pm$ to be 0. As a consequence, $\varepsilon_\mu^\pm$ will *not* be 0 at a simple level crossing when working with a trilinear (or higher-order) energy functional in the same isospin.

[8] The spikes of ε_μ^0 at the deformations where the contribution from $\varepsilon_\mu^\pm$ to $\mathcal{E}_{\rm CG}^N$ jumps to 0 are of numerical origin.

total contribution ε_μ is zero for deeply bound levels. When $z_\mu^\pm$ approaches the Fermi energy from below, $\varepsilon_\mu^\pm$ and $-\varepsilon_\mu^0$ slowly grow apart. Still, for all examples we have looked at, ε_μ^0 and $\varepsilon_\mu^\pm$ remain of similar size, but opposite sign, and have a similar dependence on deformation around the Fermi energy, $z_\mu^\pm \approx 1$. They do not cancel exactly when the pole at $z_\mu^\pm$ approaches the Fermi level but the difference between $\varepsilon_\mu^\pm$ and $-\varepsilon_\mu^0$ remains much smaller than the individual contributions and provides the finite and smoothly varying spurious energy $\mathcal{E}_{\rm CG}^N$ between the steps. For levels far above the Fermi level, ε_μ^0 goes to zero. Also, the pole $z_\mu^\pm$ is beyond the integration contour and $\varepsilon_\mu^\pm$ does not contribute to ε_μ either. Consequently, levels far above the Fermi energy do not contribute to $\mathcal{E}_{\rm CG}^N$ for standard integration contours at $R_q = 1$.

The behaviors described above can be understood as limiting cases of the factor $u_\mu^4 v_\mu^4$ times the contour integral in Eq. (43). Omitting unimportant prefactors, one obtains for $|z_\mu^\pm| \to 0$, that is, for $u_\mu^2 \approx 0$ and $v_\mu^2 \approx 1$, that

$$\begin{aligned}\varepsilon_\mu &= \varepsilon_\mu^0 + \varepsilon_\mu^\pm \\ &\propto u_\mu^4 v_\mu^4 \oint_{C_1} \frac{dz}{2i\pi} \frac{1}{z^{N+1}} \frac{(z^2-1)^2}{v_\mu^4 z^4} \prod_{\nu>0} \left(u_\nu^2 + v_\nu^2 z^2\right) \\ &\propto |z_\mu^\pm|^4 \left(c_N^2 - 2c_{N+2}^2 + c_{N+4}^2\right) \\ &\to 0, \end{aligned} \tag{71}$$

whereas for $|z_\mu^\pm| \to \infty$, that is, for $u_\mu^2 \approx 1$ and $v_\mu^2 \approx 0$, one has

$$\begin{aligned}\varepsilon_\mu &= \varepsilon_\mu^0 \\ &\propto u_\mu^4 v_\mu^4 \oint_{C_1} \frac{dz}{2i\pi} \frac{1}{z^{N+1}} \frac{(z^2-1)^2}{u_\mu^4} \prod_{\nu>0} \left(u_\nu^2 + v_\nu^2 z^2\right) \\ &\propto |z_\mu^\pm|^{-4} \left(c_{N-4}^2 - 2c_{N-2}^2 + c_N^2\right) \\ &\to 0. \end{aligned} \tag{72}$$

where the c_N denote in both cases the amplitudes of the normalized projected states with particle number N in the SR state, Eq. (42), all of which are usually nonzero and independent of μ. The key element to obtain both limits is that the integral over the gauge angle becomes simply proportional to $v_\mu^{-4} \approx 1$ or $u_\mu^{-4} \approx 1$, respectively. As a result, the prefactor $u_\mu^4 v_\mu^4$ dominates and drives ε_μ toward zero in both cases. As a consequence, one indeed finds as a general rule that

$$\varepsilon_\mu = \varepsilon_\mu^0 \to 0 \quad \text{for} \quad z_\mu^\pm \to \infty, \tag{73}$$

$$\varepsilon_\mu = \varepsilon_\mu^\pm + \varepsilon_\mu^0 \to 0 \quad \text{for} \quad z_\mu^\pm \to 0, \tag{74}$$

as suggested by the numerical results in Fig. 7.

Unlike $\varepsilon_\mu^\pm$, the contribution ε_μ^0 to the physical pole at $z = 0$ is not *a priori* suppressed for degenerate levels and might have a nonzero value. For deep-hole states, this seems contradictory with the previous proof that $\varepsilon_\mu = \varepsilon_\mu^\pm + \varepsilon_\mu^0$ goes to zero. In fact, when the pair $(\mu, \bar{\mu})$ crosses another one $(\zeta, \bar{\zeta})$, not only the pole at $z_\mu^\pm$ is removed but the residue of the pole at $z = 0$ is strongly affected by the disappearance of the corresponding denominator. As a result, ε_μ^0 also goes toward zero as $\varepsilon_\mu^\pm$ goes to zero. Indeed, ε_μ right at the crossing behaves as

$$\begin{aligned}\varepsilon_\mu &= \varepsilon_\mu^0 \\ &\propto u_\mu^4 v_\mu^4 \oint_{C_1} \frac{dz}{2i\pi} \frac{1}{z^{N+1}} (z^2-1)^2 \prod_{\substack{\nu>0 \\ \nu\neq\mu,\zeta}} \left(u_\nu^2 + v_\nu^2 z^2\right) \\ &= u_\mu^4 v_\mu^4 \left(c_{N-4}^2[\mu,\zeta] - 2c_{N-2}^2[\mu,\zeta] + c_N^2[\mu,\zeta]\right), \end{aligned} \tag{75}$$

where $c_N^2[\mu,\zeta]$ denotes a modified norm obtained by removing the contributions of both pairs $(\mu, \bar{\mu})$ and $(\zeta, \bar{\zeta})$ from the usual norm kernel

$$c_N^2[\mu,\zeta] \equiv \oint_{C_1} \frac{dz}{2i\pi} \frac{1}{z^{N+1}} \prod_{\substack{\nu>0 \\ \nu\neq\mu,\zeta}} \left(u_\nu^2 + v_\nu^2 z^2\right). \tag{76}$$

Considering either rather deep-hole or highly lying single-particle states, the prefactor $(u_\mu v_\mu)^4$ appearing in Eq. (75) makes $\varepsilon_\mu = \varepsilon_\mu^0$ to be small.

The bottom panel of Fig. 7 shows the total contribution ε_μ of each selected pairs to $\mathcal{E}_{\rm CG}^N$. One can now clearly see that there is more to the spurious energy than just the steps and the divergences (the latter of which do not appear for the particular functional used here). The poles $z_\mu^\pm$ associated to the $j_z = 3/2^+$ pair remain outside the integration contour for all deformations. Thus, it does not produce a step as the corresponding $\varepsilon_\mu^\pm$ never contributes to $\mathcal{E}_{\rm CG}^N$. Still, this level gives a small contribution ε_μ^0 to the spurious energy through the pole at $z = 0$, which happens to be slightly larger for prolate deformations than for oblate ones.

Starting on the oblate side, only the pole at $z = 0$ contributes at first to the spurious energy from the $j_z = 1/2^+$ pair of levels. The corresponding ε_μ^0 increases slowly from zero with increasing β_2. The moment the corresponding poles $z_\mu^\pm$ enter the integration contour at $\beta_2 = 0.15$, $\varepsilon_\mu^\pm$ suddenly contributes to the spurious energy. We already saw that the finite value of $\varepsilon_\mu^\pm$ at this point determines the step. As $\varepsilon_\mu^\pm$ approaches $-\varepsilon_\mu^0$ when the $1/2^+$ levels become more and more occupied with increasing prolate deformation, the total contribution ε_μ of the $1/2^+$ pair to $\mathcal{E}_{\rm CG}^N$ now decreases after the step. With the total contribution ε_μ increasing on one side of the step and suddenly decreasing on the other, the curvature of the spurious energy is different on both sides of a step. As a consequence, removing $\mathcal{E}_{\rm CG}^N$ modifies the improper curvature of the uncorrected deformation energy surface that is visible in Fig. 6, even when the steps themselves are not numerically resolved. The regularized deformation energy surfaces show much less structure; in ^{18}O to the extreme that the curvature of the corrected energy surface is now positive for all deformations as shown in Fig. 6. The contribution from the $5/2^+$ levels to the spurious energy behaves very much as the one from the $1/2^+$ levels with oblate and prolate sides exchanged. The sum of the three individual contributions gives the neutron correction shown in the top panel of Fig. 5 for $L = 199$.

We have seen that for a bilinear functional, the steps are always the consequence of a pair of single poles $z_\mu^\pm$ crossing the integration contour and have the size of the corresponding $\varepsilon_\mu^\pm$ at that crossing. The steps cannot add up for a bilinear functional as, for degenerate poles with $\mu \neq \mu'$, $z_\mu^\pm = z_{\mu'}^\pm$

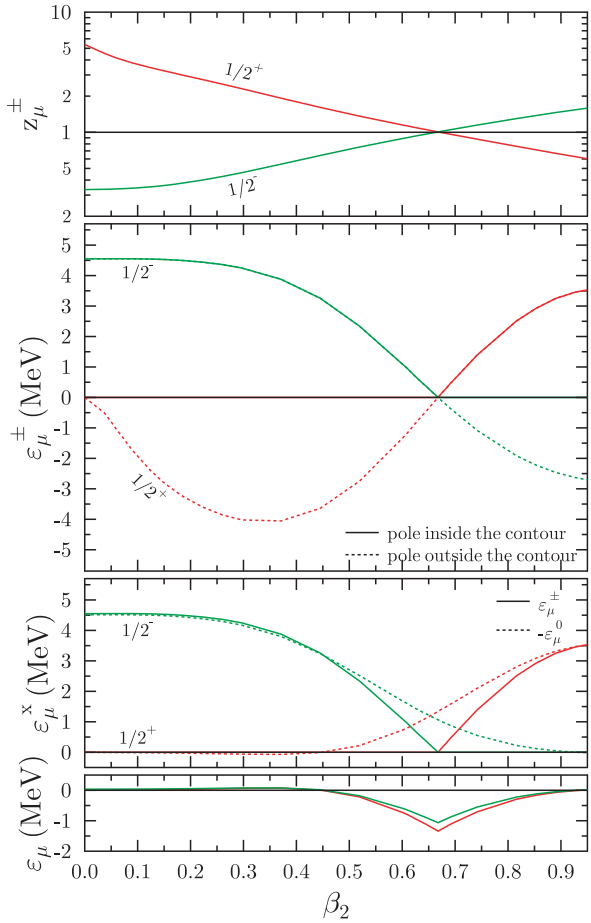

FIG. 8. (Color online) Same as Fig. 7, but for the proton $1/2^+$ and $1/2^-$ levels that give the dominant contributions to the proton correction at prolate deformation and cross at the Fermi energy at $\beta_2 = 0.67$.

directly lead to $\varepsilon_\mu^\pm = \varepsilon_{\mu'}^\pm = 0$. This does not mean, however, that there is no spurious contribution to the PNR energy when two poles cross the integration contour simultaneously, as the corresponding ε_μ^0 and $\varepsilon_{\mu'}^0$ are in general nonzero. In fact, Fig. 5 demonstrates clearly that, in our calculation of ^{18}O with SIII, the spurious energy $\mathcal{E}_{\rm CG}^N$ is largest exactly where two proton levels cross at the Fermi energy at $\beta_2 = 0.67$. The contribution of these two pairs of levels to $\mathcal{E}_{\rm CG}^N$, which also happen to be the only proton levels that have a finite contribution at prolate deformation, is analyzed in Fig. 8. There are a number of interesting differences with Fig. 7: (i) The contribution $\varepsilon_\mu^\pm$ does not vanish at spherical shape for the $1/2^-$ levels for a bilinear functional. Indeed, the spherical $p_{1/2}$ shell is only doubly degenerate, which does not suppress the corresponding $\varepsilon_\mu^\pm$. In fact, only $s_{1/2}$ and $p_{1/2}$ levels with poles $z_\mu^\pm$ below the integration contour provide nonzero $\varepsilon_\mu^\pm$ at spherical shape. (ii) Both pairs cross right at the Fermi energy at $\beta_2 = 0.67$. For the standard choice $R_p = 1$, their poles $z_\mu^\pm$ thus cross on the integration contour. As a result, $\varepsilon_\mu^\pm$ from both pairs are zero and change sign at the crossing. (iii) The derivative of $\varepsilon_\mu^\pm$ is not zero for both pairs when they simultaneously cross the Fermi energy. By contrast, ε_μ^0 slowly approaches zero such that the total contribution ε_μ is quite large for the two proton pairs. When the poles $z_\mu^\pm$ approach the integration contour from below, the distance between $\varepsilon_\mu^\pm$ and ε_μ^0 grows for both pairs. After the poles have crossed the contour, only the ε_μ^0 contribute. Finally, the total contribution ε_μ from each pair that crosses with another at the integration contour is largest at the crossing and decreases toward zero on both sides. The sum of the two individual contributions gives the proton correction shown in the middle panel of Fig. 5 for $L = 199$; all other proton levels are too far away from the Fermi level to provide any visible contribution.

One can take advantage of the fact that only a very limited number of levels actually contributes to $\mathcal{E}_{\rm CG}^N$ to reduce the numerical effort. Evaluating the necessary matrix elements $\bar{v}^{\rho\rho}$ and $\bar{v}^{\kappa\kappa}$ only for those levels for which the weight is significantly different from zero is particularly welcome for the expensive contribution from the Coulomb interaction.

2. *Shift invariance*

In their recent article, Dobaczewski *et al.* [25] pointed out that the (uncorrected) PNR energy density functional is not shift invariant, i.e., PNR energies depend on the radius chosen for the contour integral in the complex plane. As outlined in Secs. V D and V E, the source of violation of the shift invariance is the contribution $\varepsilon_\mu^\pm$ from the poles at $z_\mu^\pm$ inside the integration contour C_R to the spurious energy $\mathcal{E}_{\rm CG}^N$ in Eq. (67). Each time a pole $z_\mu^\pm$ enters or leaves the integration contour when changing its radius, $\mathcal{E}_{\rm CG}^N$ changes by the amount $\varepsilon_\mu^\pm$. This is illustrated in Fig. 9 for ^{18}O at $\beta_2 = 0.371$. The radius of the contour used for neutrons is held fixed at $R_n = 1$, whereas the radius of the contour used for the protons is varied. The three steps visible in Fig. 9 correspond to the three proton poles

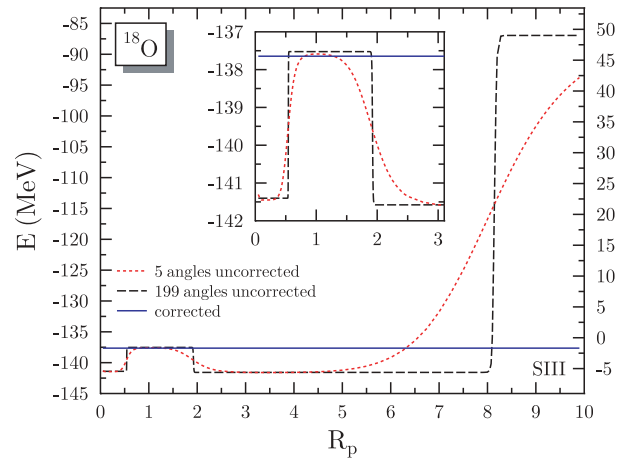

FIG. 9. (Color online) Projected energy for ^{18}O at the deformation $\beta_2 = 0.371$ as a function of the radius R_p of the integration contour calculated without and with correction using 5 and 199 angles. The energy scale on the left gives the absolute energy, the scale on the right the energy gain from projection. The insert magnifies the curves around $R_p = 1$. The regularized PNR energy in independent on the discretization of the integrals when 5 or more angles are used. The integration contour for projection on neutron number is $R_n = 1$ in all cases.

located at $0.1 < z_\mu^\pm < 10$ visible in Fig. 4 for the deformation of interest.

An interesting feature of the steps is that their size grows as the integration contour is shifted away from $R_p = 1$ [25], i.e., away from the Fermi level. The reason is easy to understand from the discussion of Eq. (70) given in the previous section: $\varepsilon_\mu^\pm$ increases as $|z_\mu^\pm|$ moves away from 1 (as long as it is separated from other poles) and as the difference between the number k_r of pairs of states below $(\mu, \bar{\mu})$ and half the number of particles $N/2$ one is restoring grows.

Using the small number of $L = 5$ discretization points for the gauge-space integral does not resolve the steps in the uncorrected PNR energy; only with much larger L one obtains sharp steps. By contrast, and as seen in Fig. 9, the regularized PNR energy is constant within a numerical precision of the order 1 keV as R_p is modified and L increased beyond 5.

3. *Distribution of weighted PNR energies*

As a next step, we analyze how the spurious energy $\mathcal{E}^N_{\rm CG}(R)$ affects the distribution of non-normalized PNR energies $c^2_N(R)\mathcal{E}^N(R)$ and $c^2_N(1)\mathcal{E}^N(R)$ as a function of the particle number one restores. Of course, restoring other particle numbers than the one that the underlying SR state was constrained in average to is not very useful for practical applications. The purpose of the exercise, however, is to shed further light on the nature of the spurious energy $\mathcal{E}^N_{\rm CG}(R)$, especially through testing sum rules associated with such a decomposition over N. For the latter test to be meaningful, and as explained in Sec. V E, it is essential to include zero and negative particle numbers in the analysis.

Starting with a SR calculation for ^{18}O, the average proton and neutron number are small enough that nonzero values of the quantities of interest for negative particle numbers can be unambiguously detected in the tail of the distribution when performing a numerical calculation. Of course, an SR state with even number-parity quantum number, as assumed here, can only be projected on even particle number such that the weight $c^2_N(R)$ and any operator matrix elements are obviously zero for odd N. In addition, the contributions to $\mathcal{E}^N(R)$ from the spurious poles, see Eq. (44), and from the physical pole[9] are zero for odd N when restoring particle number from a SR state with an even-number parity quantum number. As a consequence, we can limit ourselves here to looking at even particle numbers.

For the sake of transparency, and to avoid double sums over N and Z as well as the interference of the corresponding terms when analyzing the sum rules, we limit ourselves to the restoration of proton number in this section and in the following one. We start with the same SR state calculated for ^{18}O with $\beta_2 = 0.371$ as in Fig. 9 but *without* restoring neutron number, which is constrained to an average value of $N = 10$. The restoration of proton number is performed using $L = 199$ integration points. In what follows, we discuss the *interaction* part of the EDF only, i.e., the EDF without kinetic energy and without the one-body center-of-mass correction used in connection with SIII. Both are expectation values of one-body operators and therefore free of spurious contributions. As before, the Coulomb exchange term is omitted from the energy functional.

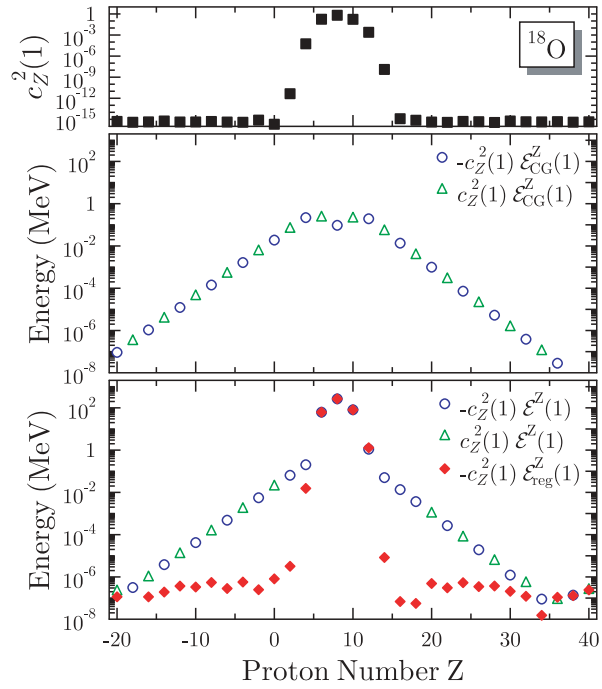

FIG. 10. (Color online) Weight $c^2_Z(R_p = 1) = |\langle\Psi^Z|\Phi_1\rangle|^2$ of the normalized proton-number-projected states in the SR HFB state (upper panel), the weighted spurious energy $c^2_Z(R_p = 1)\mathcal{E}^Z_{\rm CG}(R_p = 1)$ (middle panel), the nonregularized weighted PNR energies $c^2_Z(R_p = 1)\mathcal{E}^Z(R_p = 1)$ and regularized $c^2_Z(R_p = 1)\mathcal{E}^Z_{\rm REG}(R_p = 1)$ (lower panel). All results are obtained using the same SR state calculated for ^{18}O at a deformation of $\beta_2 = 0.371$ as auxiliary state. The neutron number is not restored.

First, we discuss the standard case with an integration contour at $R_p = 1$. The upper panel of Fig. 10 displays the distribution of the weights $c^2_Z(R_p = 1) = |\langle\Psi^Z|\Phi_{z_p=1}\rangle|^2$, Eq. (12), of the normalized proton-number projected states in the SR state. As expected, $c^2_Z(1)$ is peaked at $Z = 8$ and falls off quickly to numerical noise. Components with $Z > 14$ and $Z < 2$ cannot be numerically distinguished from zero. In the former case and for $Z = 0$ it is a consequence of these proton numbers being too far from the average proton number such that $c^2_Z(1)$ becomes too small to be distinguished from zero within the numerical precision of our code, while for $Z < 0$ the proton-number projected states $|\Psi^Z\rangle$ are strictly zero for analytical reasons.

The lower panel of Fig. 10 shows the interaction part of weighted PNR energies before and after applying the regularization method. The distribution of absolute values of $c^2_Z(1)\mathcal{E}^Z(1)$ does not follow the distribution of the weights $c^2_Z(1)$ displayed in the upper panel. Instead, it has a long tail that spreads visibly to $Z = -20$ and $Z = 34$, before it can no longer be distinguished from numerical noise. In these tails, the values of $c^2_Z(1)\mathcal{E}^Z(1)$ have alternating signs, which is clearly

[9]The Laurent series centered at $z = 0$ of the integrand in Eq. (35) does only contain even powers for odd N. As a result, such a pole does not contribute to $\mathcal{E}^N(R)$.

unphysical. Only the regularized quantity $c_Z^2(1)\mathcal{E}^Z_{\rm REG}(1)$ falls off in the same manner as $c_Z^2(1)$ does and is numerically zero for $Z \leqslant 0$. This underlines again the spurious nature of $\mathcal{E}^Z_{\rm CG}$, that is shown separately in the middle panel of Fig. 10. In the present example, $c_Z^2(1)\mathcal{E}^Z_{\rm CG}(1)$ has alternating signs throughout the entire interval of Z. This does not always have to be the case; in some other examples we have looked at, this happens only for particle numbers that are a at least a few units away from the average particle number of the underlying SR state.

For $Z \leqslant 0$, nonzero $c_Z^2(1)\mathcal{E}^Z(1)$ are entirely spurious with $\mathcal{E}^Z(1) = \mathcal{E}^Z_{\rm CG}(1)$; i.e., they originate entirely from spurious poles at finite $z_\mu^\pm$. The same situation applies to the tail of the distribution of $c_Z^2(1)\mathcal{E}^Z(1)$ for large positive Z.

As a second example, we show in the three upper panels of Fig. 11 the same quantities as in Fig. 10 but obtained employing an integration contour of radius $R_p = 2.5$. By contrast to before ($R_p = 1$), the poles $z_\mu^\pm$ from the $1/2^+$ substate of the $\pi d_{5/2^+}$ shell are located inside the integration contour, see

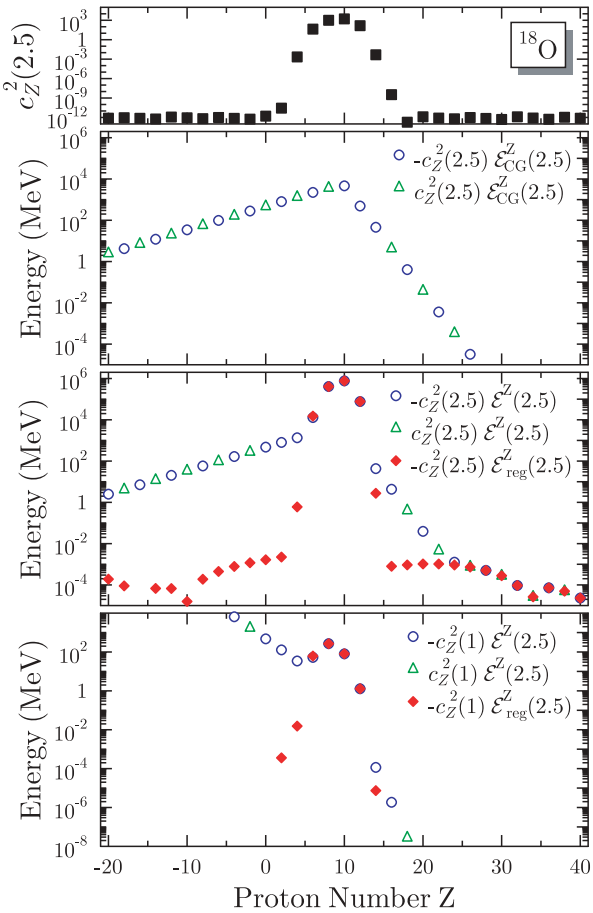

FIG. 11. (Color online) Weight $c_Z^2(R_p = 2.5) = |\langle\Psi^Z|\Phi_{R_p}\rangle|^2$ of the normalized proton-number-projected states into the radially shifted SR HFB state at $R_p = 2.5$ (upper panel), the weighted spurious energy $c_Z^2(R_p = 2.5)\mathcal{E}^Z_{\rm CG}(R_p = 2.5)$ (upper middle panel), the nonregularized $\mathcal{E}^Z(R_p = 2.5)$ and regularized $\mathcal{E}^Z_{\rm REG}(R_p = 2.5)$ PNR energies weighted by $c_Z^2(R_p = 2.5)$ (lower middle panel) and by $c_Z^2(R_p = 1)$ (lower panel). All results are obtained using the same SR state calculated for ^{18}O at a deformation of $\beta_2 = 0.371$ as auxiliary state. The neutron number is not restored.

Fig. 8. As a result, the spurious contribution $\varepsilon_\mu^\pm$ from those poles increases $\mathcal{E}^Z$ by about 4 MeV when projecting on $Z = 8$ using a nonregularized functional, see Fig. 9. We analyze now if and how the energy restored on other proton numbers are affected compared to using $R_p = 1$.

Compared to Fig. 10, the distribution of weights $c_Z^2(2.5)$ is distorted by the additional $R_p^Z = (2.5)^Z$ factor such that absolute values change by several orders of magnitude, and the maximum of the distribution is shifted to $Z = 10$. The main difference to the case using the standard integration contour $R_p = 1$ is that the distribution of the spurious energy $c_Z^2(2.5)\mathcal{E}^Z_{\rm CG}(2.5)$ is distorted in a different manner than the distribution of the norm, such that it falls off quicker for $Z > 8$, but much slower for $Z < 8$, including negative Z. Again, only the distribution of the regularized MR energy functional $\mathcal{E}^Z_{\rm REG}(2.5)$ follows that of the weights $c_Z^2(2.5)$.

The lowest panel of Fig. 11 shows the contributions to the non-radius-weighted energy sum rule discussed in Sec. V E2. The distribution $c_Z^2(1)\mathcal{E}^Z(R_p)$ is even more distorted than for the contributions to the radius-weighted sum rule shown in the panel above. For $R_p > 1$, $c_Z^2(1)\mathcal{E}^Z(R_p)$ falls off much quicker than $c_Z^2(R_p)\mathcal{E}^Z(R_p)$ for $Z > 8$ but much slower for $Z < 8$. For negative values of Z the missing factor $(2.5)^Z$ makes $c_Z^2(1)\mathcal{E}^Z(R_p)$ to grow so fast that it will be impossible to safely evaluate numerically the sum rules including negative particle numbers.

For $R_p < 1$, a case not discuss here, the situation is reversed such that $c_Z^2(1)\mathcal{E}^Z(R_p)$ falls off faster than $c_Z^2(R_p)\mathcal{E}^Z(R_p)$ for $Z < 8$, but slower for $Z > 8$, now with the impossibility to safely evaluate the sum rule when including positive Z.

To summarize, the contamination of the PNR-EDF by spurious contributions originating from the use of the GWT affects the decomposition of the (shifted) SR functional energy (kernel) into weighted PNR energies with different particle numbers such that energy is shifted out of the physical subspace corresponding to positive particle numbers. The impact of this finding on the fulfillment of basic sum rules is examined in the next section.

4. Sum rules

Now we turn to the sum rules, which are obtained by summing the weighted PNR energies shown in Figs. 10 and 11. Numerical summation is performed on a subset of even proton numbers in the interval $-20 \leqslant Z \leqslant 40$.

Again we begin with the case $R_p = 1$, for which the radius-weighted and non-radius-weighted sum rules are identical. The SR energy[10] that sets the reference is given by

$$\mathcal{E}[\rho, \kappa, \kappa^*] = -410.3403 \text{ MeV}. \tag{77}$$

In agreement with Eq. (52), the sum of $c_Z^2(1)\mathcal{E}^Z(1)$ over positive *and* negative Z reproduces this value better than 0.1 keV

$$\sum_{Z=-\infty}^{+\infty} c_Z^2(1)\mathcal{E}^Z(1) = -410.3403 \text{ MeV}. \tag{78}$$

[10]We recall that quoted energies are without the kinetic and center-of-mass correction energies.

When limiting the sum to "physical" proton numbers $Z > 0$, however, we obtain instead

$$\sum_{Z>0} c_Z^2(1)\mathcal{E}^Z(1) = -410.3550 \text{ MeV}. \quad (79)$$

With 14.7 keV, the numerical difference between Eq. (78) and Eq. (79), which constitutes the breaking of the physical sumrule, is quite small. Using the standard integration contour of $R_p = 1$, we find similar values for other deformations in ^{18}O, whereas for heavier nuclei this quantity becomes rapidly suppressed such that it cannot be unambiguously detected in a numerical calculation anymore.

The largest individual sum-rule breaking contribution is that for $Z = 0$, for which we obtain

$$c_Z^2(1)\mathcal{E}^{Z=0}(1) = c_Z^2(1)\mathcal{E}_{\text{CG}}^{Z=0}(1) = 0.0189 \text{ MeV}, \quad (80)$$

which is slightly larger than the entire sum over $Z \leqslant 0$. This is not unexpected in view of the alternating signs of the contributions pointed out in the previous section.

For $Z \leqslant 0$, nonzero $c_Z^2(1)\mathcal{E}^Z(1)$ are of course entirely spurious such that they equally contribute to the sum rule of $c_Z^2(1)\mathcal{E}_{\text{CG}}^Z(1)$. For $R_p = 1$, the right-hand-side of Eq. (54) is zero such that the sum of $c_Z^2(1)\mathcal{E}_{\text{CG}}^Z(1)$ over all Z is zero as well, which we do find numerically

$$\sum_{Z=-\infty}^{+\infty} c_Z^2(1)\mathcal{E}_{\text{CG}}^Z(1) = 0.0000 \text{ MeV}. \quad (81)$$

Although the alternating sign of $c_Z^2(1)\mathcal{E}_{\text{CG}}^Z(1)$ with Z indicates that a cancellation effect is at play, the result of Eq. (81) is not so obvious when looking at the middle panel of Fig. 10. Summing up $c_Z^2(1)\mathcal{E}_{\text{CG}}^Z(1)$ for positive values of Z gives -0.0146 MeV, which precisely is the difference between Eqs. (77) and (79).

The regularized energy $c_Z^2(1)\mathcal{E}_{\text{REG}}^Z(1)$ is numerically zero for $Z \leqslant 0$ as any meaningful particle-number-restored observable should be. The same holds for those large positive values of Z where $c_Z^2 > 0$. As a consequence, the sum over $c_Z^2(1)\mathcal{E}_{\text{REG}}^Z(1)$ can be limited to "physical" particle numbers. The numerical value for this sum

$$\sum_{Z=-\infty}^{+\infty} c_Z^2(1)\mathcal{E}_{\text{REG}}^Z(1) = \sum_{Z>0} c_Z^2(1)\mathcal{E}_{\text{REG}}^Z(1) = -410.3403 \text{ MeV} \quad (82)$$

gives back the SR energy, Eq. (77), within 0.1 keV as expected from Eq. (61).

When shifting one of the states to $R_p = 2.5$, the norm kernel is $\langle\Phi_1|\Phi_{2.5}\rangle = 2816.9760$, and the corresponding transition energy kernel is $\mathcal{E}[2.5] = -830.2386$ MeV. The reference for the radius-weighted sum rule is thus provided by

$$\mathcal{E}[2.5]\langle\Phi_1|\Phi_{2.5}\rangle = -1266844\text{MeV}, \quad (83)$$

where we limit ourselves again to seven digits. Summing $c_Z^2(2.5)\mathcal{E}^Z(2.5)$ over all Z reproduces this value with the same precision, while summing over positive Z only gives -1266546 MeV, which differs from the above value by -298 MeV, which is of similar order as in case of the unshifted integration contour.

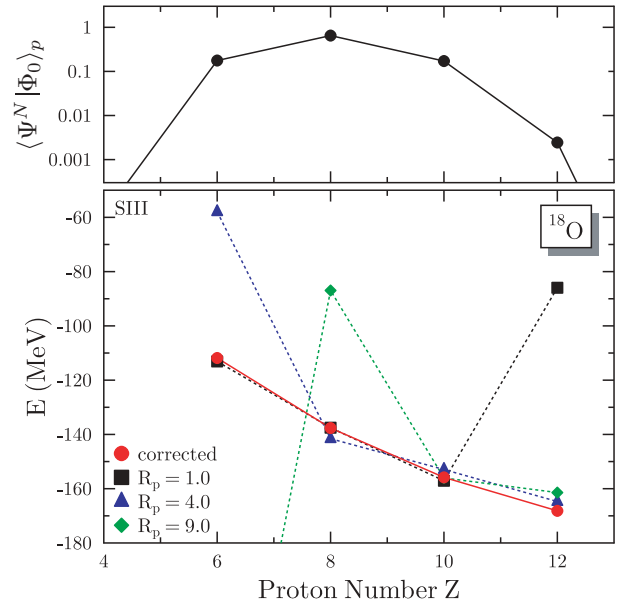

FIG. 12. (Color online) Weight of the normalized state projected on various values of Z in the SR vacuum (top panel) and decomposition of the energy into Z components for three different radii of the integration contour for protons (bottom panel) for ^{18}O at a deformation of $\beta_2 = 0.371$. All states are projected on the same neutron number $N = 10$ with an integration contour of radius $R_n = 1$, using $L = 199$ integration points for both protons and neutrons. Corrected PNR energies are the same for all values of R_p within numerical accuracy.

In the case of shifted contours, the non-radius-weighted sum rule is more interesting to look at. As became clear from the bottom panel of Fig. 11, the sum over all Z cannot be evaluated numerically. Let us anyway focus on the sum rule over positive Z only; i.e., Eq. (62). In this case, summing $c_Z^2(1)\mathcal{E}^Z(2.5)$ gives -309.4217 MeV that indeed decomposes into $\mathcal{E}[\rho, \kappa, \kappa^*] = -410.3403$ MeV plus the sum-rule breaking term obtained [either numerically or analytically through Eq. (63)] by summing $c_Z^2(1)\mathcal{E}_{\text{CG}}^Z(2.5)$ over $Z > 0$ and that equates $+100.9189$ MeV. Thus, one realizes that the most essential non-radius-weighted sum rule performed over physical components ($Z > 0$) is broken and not shift invariant. In particular, the breaking term can be very large as soon as the integration radius differs from 1. Of course, the small (nonzero) value of that sum-rule breaking term obtained from using the unit circle as an integration contour has masked the contamination of energy functionals with spurious terms for many years. Indeed, practitioners naturally interpreted that very tiny breaking as due to numerical noise.

5. *Energies of physical systems*

After looking into the contributions to the sum rules, we now turn our attention to normalized PNR energies pertaining to the physical subspace, i.e., addressing only those particle numbers that give a nonzero norm. Figure 12 shows PNR energies (now again completed by kinetic energy and center-of-mass correction) for three values of the integration contour

radius R_p. With each step in the uncorrected projected energy of the $Z = 8$ component seen for $R_p = 1.9$ and $R_p = 8.2$ in Fig. 9, the energy of all other Z components changes as well. For each radius of the integration contour there is at least one Z component that has an obviously unphysical uncorrected PNR energy.

The breaking of the physical sum rule for the nonregularized PNR-EDF discussed above is much smaller than the energy scale of the changes we observe in Fig. 9 when shifting R_p. Still, we can argue with the help of the sum rules for the regularized and nonregularized PNR-EDF that any small spurious energy in a Z component with large weight c_Z^2 might have to be compensated by a very large spurious energy in a Z component with small weight, as it happens in Fig. 12 for the $Z = 12$ component at $R_p = 1.0$ and the $Z = 6$ component at $R_p = 4.0$. As a consequence, the moderate energy scale found for the spurious energy along a deformation energy surface when projecting on the same nucleon number that SR vacua were constrained to does not apply to the spurious energies entering other Z components. Although this usually has no particular consequences for particle restoration calculations where one is in most cases interested in projecting out the one particle number that the SR HFB state was constrained to and which can be expected to have a comparatively small contamination of spurious energy, the spurious redistribution of energy might seriously compromise angular-momentum restoration, where one is often interested in producing the entire spectrum of low-lying states.

E. ^{76}Kr

With the next example ^{76}Kr, a medium heavy nucleus located in a region of shape coexistence, we examine how the spurious contributions to the particle-number-restored energy evolve when increasing the density of single-particle levels. This nucleus is one of the series of neutron-deficient Kr isotopes that were recently studied [73] with GCM mixing of quadrupole deformed axial particle-number- and angular-momentum-restored states using SLy6.[11]

Figure 13 shows the location of the poles at $z_\mu^\pm$ for protons and neutrons, the energy gain from PNR and the absolute PNR energy as a function of quadrupole deformation, both with and without correction and both calculated with $L = 9$ and 99 discretization points of the gauge-space integrals. We have checked that all observables calculated as operator matrix elements are converged for $L = 9$. The main difference to ^{18}O is the much larger overall density of poles. This has two consequences. (i) It increases the number of poles crossing the integration contour when deforming the nucleus and thus the number of steps. (ii) Poles crossing the Fermi level are hardly isolated from other poles; this limits the size of the steps through the factors entering the middle product in Eq. (70). As

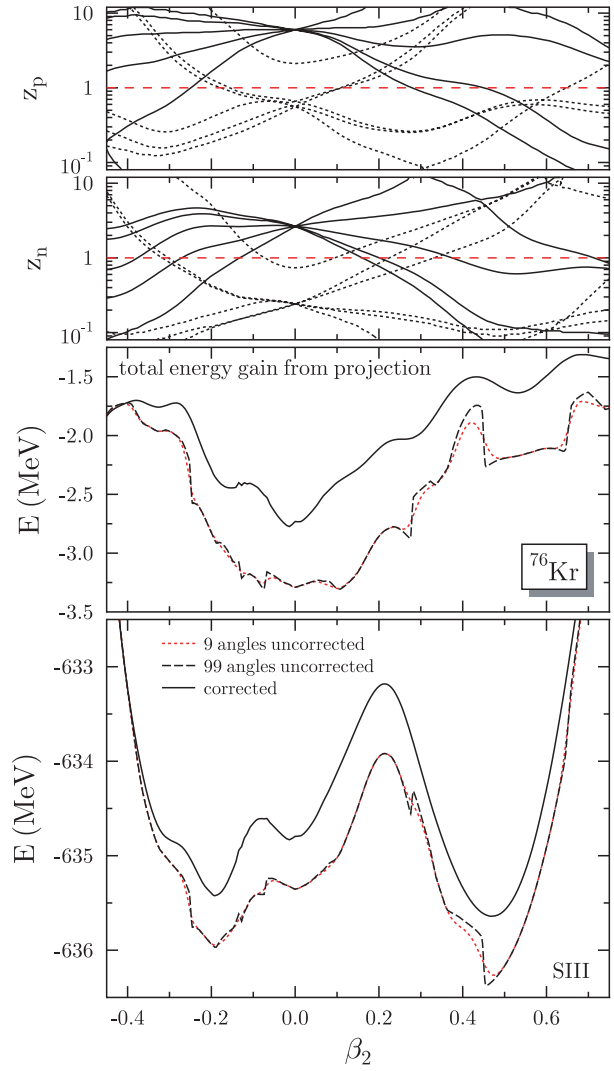

FIG. 13. (Color online) Spectrum of poles $z_\mu = |u_\mu/v_\mu|$ for protons and neutrons, the uncorrected and corrected energy gain from projection and the particle-number-projected quadrupole deformation energy for $L = 9$ and 99 discretization points of the integral in gauge space for ^{76}Kr.

a consequence, most of the steps visible in Fig. 13 are much smaller than those found for ^{18}O in Fig. 4. Notable exceptions are the ones on both sides of the prolate minimum at $\beta_2 \approx 0.43$, which indeed correspond to the crossings of proton levels that are well separated from other poles. The correction is not of the same magnitude in the various minima; in fact, the variation of the correction between the various minima is of the same order as the difference in total energy of the latter. Correcting for spurious energies might have a visible impact on the excitation spectrum of this nucleus obtained from a GCM mixing over quadrupole shapes of particle-number- and angular-momentum-restored states.

F. ^{186}Pb

As the last example, we present in Fig. 14 results obtained for ^{186}Pb, a nucleus exhibiting triple shape coexistence

[11]The deformation energy surface obtained with SIII also displays shape coexistence, although its topography is quite different from the one obtained with SLy6. With SIII, the deformed minima are much more pronounced and lower in energy compared to the spherical one. However, this is irrelevant for the present discussion.

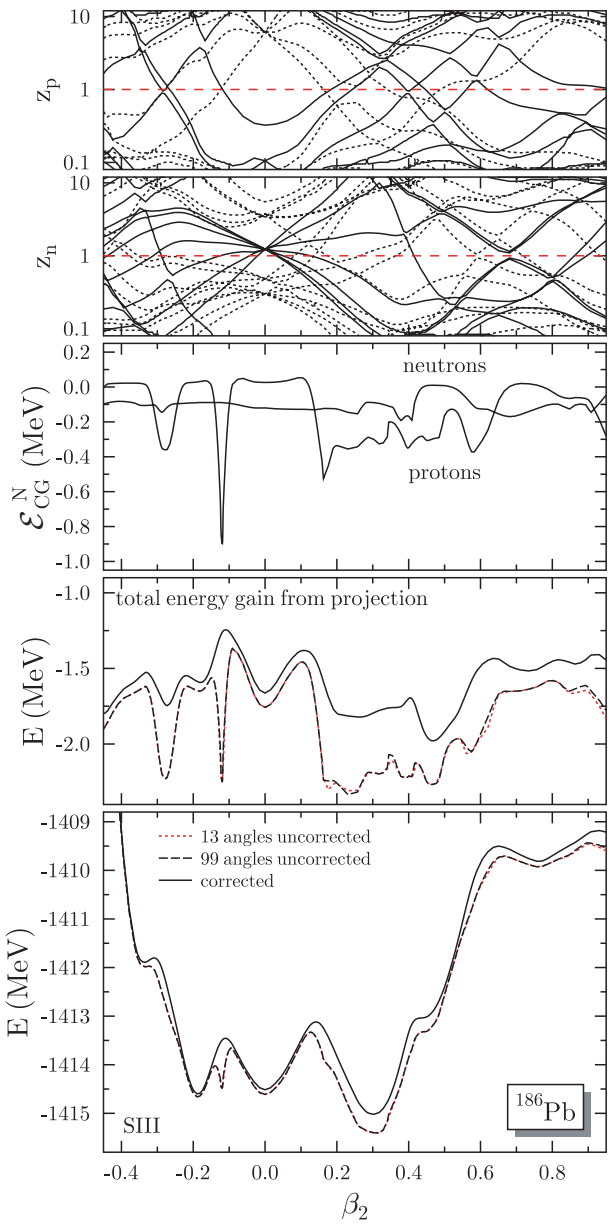

FIG. 14. (Color online) Spectrum of poles $z_\mu = |u_\mu/v_\mu|$ for protons and neutrons, the correction to the particle-number-restored EDF separately for protons and neutrons, the uncorrected and corrected energy gain from projection, and the particle-number-projected quadrupole deformation energy without and with correction for $L = 13$ and 99 discretization points of the integral in gauge space for ^{186}Pb.

of spherical, oblate, and prolate states studied earlier in Refs. [68,69] in a method that includes particle-number restoration using the Skyrme EDF SLy6.[12] In this heavy nucleus, the number of neutron poles $z^{\pm}_{\mu}$ in the vicinity of the Fermi level is even larger than for ^{76}Kr. When crossing the standard integration contour $R_n = 1$, those poles generate many steps that are, however, almost always of tiny size due to the closeness of other poles; the sole exception being the step at $\beta_2 = 0.4$. This is different for protons. As a consequence of the magic proton number $Z = 82$, the density of proton poles around the Fermi level is quite low for most deformations such that the few proton poles that cross in these regions have a much larger impact. This is illustrated by the second panel in Fig. 14 that shows the correction $\mathcal{E}^N_{CG}$ separately for protons and neutrons. The narrow peak at small oblate deformation $\beta_2 = 0.11$ is not a divergence but stems from the crossing of two proton levels at the Fermi energy in analogy to the structure found in ^{18}O around $\beta_2 = 0.67$. In both cases the double-crossing is a direct consequence of the shell closure: With all other levels being too far above or below to have occupation numbers significantly different from 0 or 1, the constraint on the average particle number dictates that two pairs of levels in the gap have an occupation of $v^2_\mu = 1/2$ simultaneously. Interestingly, the uncorrected deformation energy curve does not change much when increasing the number of integration points from $L = 13$ to 99. As for ^{18}O and ^{76}Kr, the correction varies strongly with deformation, has a different value in the various minima, and, most importantly, is on the same energy scale as the energy difference between those minima.

VII. SUMMARY, CONCLUSIONS, AND OUTLOOK

In the present article, we introduce the notion of spurious self-pairing. It appears as a generalization of spurious self-interaction processes, a well-known problem in electronic density-functional theory [6,29,60–62], to systems with pairing correlations that are modeled within EDF approaches using independent quasiparticle BCS states as auxiliary states of reference. Self-interaction and self-pairing processes appear for any energy functional that uses different vertices in the particle-hole and particle-particle channels and/or not fully antisymmetric vertices; e.g., as due to density dependencies. Neither self-interaction nor self-pairing appear when the many-body energy is strictly calculated as the expectation value of a Hamilton operator. Both are a price to pay when replacing the exact nuclear many-body problem by a system of coupled one-body problems in a EDF calculation, modeling higher-order in-medium correlations through a simple energy functional depending on one-body densities and currents. On the single-reference level, self-pairing gives a spurious contribution to the pairing field (and therefore influences all quantities it determines) and to the total binding energy.

Energy density functionals extended to perform multi-reference calculations, i.e., symmetry restoration or GCM-type configuration mixing, also contain unphysical contributions: First, the previously discussed self-interaction and self-pairing processes that continuously extend from SR energy functional to off-diagonal energy kernels, as well as a second and much more dangerous category of spuriosity that appears when the off-diagonal kernels are evaluated on the basis of the generalized Wick theorem. The use of a Wick theorem to evaluate a functional energy kernel that does not originate from a genuine Hamilton operator is not justified. Relying on the generalized Wick theorem to construct off-diagonal functional energy

[12]The deformation energy surface obtained with SIII is at variance with the experimental finding that the ground state is spherical with low-lying prolate and oblate bands seen as excitations [68,69]. However, this is irrelevant for the present discussion.

kernels has the unexpected particularity to provide previously discussed self-interaction and self-pairing contributions with unphysical weights that contain poles leading to divergences [18] and steps in the energy [25]. The latter have been noticed recently in the context of particle-number restoration whenever a single-particle level crosses the Fermi energy. As demonstrated in Article I [28], the weights of self-interaction and self-pairing terms obtained on the basis of the standard Wick theorem are different and present no problematic contributions. This feature can be exploited to unambiguously isolate the dangerous spuriosities and set up a correction scheme that regularizes unphysical divergences and steps in MR energy kernels [28]. In the present article, we have applied this correction scheme to the simplest and formally most transparent MR case of particle-number restoration after variation.

The complex-plane analysis performed in the present work reveals that each conjugated pair of single-particle levels $(\mu, \bar{\mu})$ provides an unphysical contribution to the physical pole at $z = 0$, in addition to generating unphysical poles at $z_\mu^\pm = \pm i|u_\mu|/|v_\mu|$. The latter cause the steps as they cross the integration contour [25]. The unphysical poles are also at the origin of the breaking of the shift invariance of PNR energies [25]. However, removing only the contribution from the poles at $z_\mu^\pm$ to the energy functional kernel leads to unphysical results. Instead, the spurious contribution from a given pair of single-particle levels to the pole at $z = 0$ has to be removed simultaneously, as both are very large, of opposite sign, and nearly cancel.

The correction scheme proposed in Article I does indeed remove both contributions; thereby it eliminates the divergences and steps and restores the shift invariance of PNR energies $\mathcal{E}^N$ as well as standard sum rules that they can be expected to fulfill. The correction to $\mathcal{E}^N$ is of the order of 1 MeV, and in most cases reduces the energy gain from PNR. On the one hand, the correction is sufficiently small that PNR-EDF results published earlier are not meaningless. On the other hand, in extreme cases the correction might be as large as 50% of the energy gain from PNR, which casts some doubt on the reliability of published calculations performed within the EDF framework. The correction is also of the same order as the rms error of the mass residuals reached with the best available particle-number-restored EDF mass fits [19]. The correction varies rapidly with deformation and affect significantly the structure of complex nuclei presenting soft deformation energy surfaces and coexisting minima.

In the present article, we do not attempt to correct for the "true" self-interaction and self-pairing processes that contaminate the single-reference energy density functionals. This amounts to modify the underlying energy density functional, a task that we postpone to later works. In addition, a self-consistent correction is very cumbersome, as documented in the literature for self-interaction in the context of electronic DFT [6,29,60–62].

Particle-number restoration is not the only type of MR-EDF calculation where using the GWT as a basis to construct nondiagonal functional energy kernels causes problems. In fact, any symmetry restoration or GCM-type configuration mixing calculation is expected to be contaminated with similar spurious contributions; e.g., anomalies were encountered in Ref. [80] in angular-momentum-restoration calculations of cranked states without pairing and using a Skyrme EDF. The correction scheme proposed in Article I can be applied to any type of MR-EDF calculation. However, all others but particle-number restoration require the numerical construction of the canonical basis of the Bogoliubov transformation connecting the two different quasiparticle bases associated with the two vacua entering the construction of the functional energy kernel [28]. Work toward the numerical implementation of such a scheme is underway.

In the present study, we have limited ourselves to particle-number restoration after variation, where the correction can be subtracted from energy kernels *a posteriori*. With variation-after-symmetry-restoration EDF calculations becoming available [26,52], and the variational equations sometimes running into the divergences [25], setting up a correction scheme for those variational equations becomes an important issue and will be addressed in a forthcoming study [81].

The correction proposed in Article I [28] and discussed in the present one is limited to energy functionals depending on integer powers of the density matrices. Most functionals used in the literature, however, have a density dependence of noninteger power, both in the functional modeling the effective strong interaction and as an approximate Coulomb exchange term. Compared to the functionals discussed here, such noninteger powers of the density matrix pose two additional types of difficulties when extended to nondiagonal energy kernels on the basis of the GWT: (i) as transition densities are complex, taking their fractional power is ambiguous [25], and (ii) there is no well-defined basis at present to remove the spurious branch cuts that are generated by such terms. Both points are illustrated and examined further in Article III of this series [27].

In our opinion, the particular difficulties of functionals with noninteger density dependencies constitute a strong motivation to construct energy functionals with integer powers of the densities only in view of performing meaningful MR-EDF calculations in the future. At present, there are no such nonrelativistic functionals of high performance. Relativistic functionals have been constructed along these lines recently [76] with a different motivation and have already been used in PNR-EDF calculations [20]. The construction of correctable energy functionals for multi-reference applications becomes an urgent task for the future. A particular problem will be to find a suitable functional for the Coulomb interaction, as using the exact exchange term is incommensurately expensive in multidimensional MR-EDF calculations.

ACKNOWLEDGMENTS

We thank J. Dobaczewski, W. Nazarewicz, P.-G. Reinhard, and M. V. Stoitsov for providing us with their analysis of the PNR-HFB problem in the complex plane a very early stage that triggered the present work. Part of the work by M.B. was performed within the framework of the Espace de Structure Nucléaire Théorique (ESNT) at Saclay. This work was supported by the US National Science Foundation under Grant No. PHY-0456903. We also thank the (Department of Energy's) Institute for Nuclear Theory at the University of

Washington for its hospitality and the Department of Energy for partial support during the elaboration of this work.

APPENDIX A: THE ENERGY FUNCTIONAL

The energy is given as the sum of the noninteracting kinetic energy, the Skyrme energy functional that models the strong particle-hole interaction, a pairing functional that models the particle-particle interaction, and the Coulomb energy functional

$$\mathcal{E} = \mathcal{E}_{\rm kin} + \mathcal{E}_{\rm Skyrme} + \mathcal{E}_{\rm Coulomb} + \mathcal{E}_{\rm pair} + \mathcal{E}_{\rm corr}. \tag{A1}$$

The kinetic energy is the mean value of a one-body operator; hence it does not pose problems. From the point of view of establishing the correction to the MR energy kernel, we identify in the following

$$\mathcal{E}^{\rho\rho} \equiv \mathcal{E}^{\rho\rho}_{\rm Skyrme} + \mathcal{E}^{\rm direct}_{\rm Coulomb}, \tag{A2a}$$

$$\mathcal{E}^{\rho\rho\rho} \equiv \mathcal{E}^{\rho\rho\rho}_{\rm Skyrme}, \tag{A2b}$$

$$\mathcal{E}^{\kappa\kappa} \equiv \mathcal{E}^{\kappa\kappa}_{\rm DI}, \tag{A2c}$$

making explicit the power of the density matrices entering a given term. Let us now specify these terms more explicitly.

A. The Skyrme energy functional

We restrict ourselves here to those terms of the Skyrme EDF depending on time-even densities and currents that contribute to the ground states of even-even nuclei in SR and MR-PNR calculations. Also, the functional given below corresponds to the particular Skyrme interaction SIII used throughout this article. For SIII, there are no density-dependent coupling constants, but the energy functional can be divided into a bilinear $\mathcal{E}^{\rho\rho}_{\rm Skyrme}$ and a trilinear term $\mathcal{E}^{\rho\rho\rho}_{\rm Skyrme}$. The Skyrme energy functional is usually represented either in terms of isoscalar and isovector densities [82] or in terms of the total density and the densities of the nucleon species [83]. In the context of particle-number restoration, the most convenient representation separates contributions that are bilinear in densities of the same isospin from those that are bilinear in densities of different isospin

$$\mathcal{E}^{\rho\rho}_{\rm Skyrme} = \int d^3r \left\{ \sum_{q=p,n} \left[A^{\rho\rho}\,\rho_q^2 + A^{\rho\tau}\,\rho_q\tau_q + A^{\rho\Delta\rho}\,\rho_q\Delta\rho_q + A^{\rho\nabla J}\,\rho_q\nabla\cdot\mathbf{J}_q \right] \right.$$
$$\left. + \sum_{\substack{q,q'=p,n \\ q\neq q'}} \left[B^{\rho\rho}\,\rho_q\rho_{q'} + B^{\rho\tau}\,\rho_q\tau_{q'} + B^{\rho\Delta\rho}\,\rho_q\Delta\rho_{q'} + B^{\rho\nabla J}\,\rho_q\nabla\cdot\mathbf{J}_{q'} \right] \right\}, \tag{A3}$$

$$\mathcal{E}^{\rho\rho\rho}_{\rm Skyrme} = \int d^3r \sum_{\substack{q,q'=p,n \\ q\neq q'}} A^{\rho\rho\rho}\,\rho_q^2\,\rho_{q'}. \tag{A4}$$

The $A^{ff'}$ and $B^{ff'}$ denote the coupling constants,[13] none of which are density dependent for SIII. In the canonical basis, the local densities entering the energy functional (A3) and (A4) are given by

$$\rho_q(\mathbf{r}) = 2\sum_{\mu>0} \phi^\dagger_\mu(\mathbf{r}q)\,\phi_\mu(\mathbf{r}q)\rho_{\mu\mu}$$
$$\tau_q(\mathbf{r}) = 2\sum_{\mu>0} [\nabla\varphi^\dagger_\mu(\mathbf{r}q)]\cdot[\nabla\phi_\nu(\mathbf{r}q)]\rho_{\mu\mu} \tag{A5}$$
$$\mathbf{J}_q(\mathbf{r}) = -i\sum_{\mu>0} \{\varphi^\dagger_\mu(\mathbf{r}q)[\nabla\times\hat\sigma\phi_\mu(\mathbf{r}q)] - \text{h.c.}\}\rho_{\mu\mu}$$

and denote, for the isospin $q = n, p$, the matter density, the kinetic density, and the spin-orbit current, respectively. The operator $\hat\sigma$ is the vector built out of the three cartesian Pauli matrices. The density matrix $\rho_{\mu\mu}$ is given either by Eq. (5) for the SR-EDF or by Eq. (16) or (38) for the PNR-MR-EDF. One can see from the expressions given above that any local density $f_q(\mathbf{r})$ can be written as:

$$f_q(\mathbf{r}) \equiv 2\sum_{\mu>0} W^f_{\mu\mu}(\mathbf{r}q)\rho_{\mu\mu}, \tag{A6}$$

where $f \in \{\rho, \tau, \mathbf{J}\}$ and where the explicit form of each $W^f_{\mu\mu}(\mathbf{r}q)$ can be easily extracted from Eq. (A5). This will facilitate the construction of the matrix elements needed to evaluate the correction $\mathcal{E}^N_{\rm CG}$.

B. The Coulomb energy functional

The standard Coulomb energy functional that is used in connection with most parametrizations of the Skyrme energy functional is given by

$$\mathcal{E}_{\rm Coulomb} = \frac{e^2}{2}\iint d^3r\,d^3r'\,\frac{\rho_p(\mathbf{r})\rho_p(\mathbf{r}')}{|\mathbf{r}-\mathbf{r}'|}$$
$$-\frac{3}{4}e^2\left(\frac{3}{\pi}\right)^{1/3}\int d^3r\,\rho_p^{4/3}(\mathbf{r}). \tag{A7}$$

[13] Superscripts ff' and fff' used on the right-hand side of Eqs. (A3) and (A4) refer to the local densities that appear in the functional, whereas the superscripts $\rho\rho$, $\kappa\kappa$, $\rho\rho\rho$, ... on the left-hand side of Eqs. (A3), (A4), and (A8) correspond to the powers in the density matrices.

The proton density entering Eq. (A7) is calculated as described in the preceding section. The energy functional (A7) provides the textbook example of an energy functional that is not self-interaction free [29].

The Coulomb exchange term in the Slater approximation, represented by the second term on the right-hand side of Eq. (A7), resembles the density-dependent terms of modern parametrizations of the Skyrme functional. As, at present, we do not have a correction scheme for terms depending on noninteger powers of the density, we drop it and consider the direct term only in the present work. Concerning absolute binding energies, the Coulomb exchange term is the smallest of all contributions to the energy functional for nuclei and states considered here; it does not exceed 2% of the total binding energy even in very heavy nuclei with a strong Coulomb field. What is even more important for the present study is that its value changes also by at most 2% when deforming a nucleus; its influence on potential energy surfaces is smaller than what can be resolved in the plots shown in Sec. VI.

C. Pairing energy functional

For pairing, we choose a local energy functional deduced from a simple delta interaction (DI), often referred to as "volume pairing"

$$\mathcal{E}_{\mathrm{DI}}^{\kappa\kappa} = \sum_{q} \int d^3r\, A^{\tilde{\rho}\tilde{\rho}}\, \tilde{\rho}_q^*(\mathbf{r})\tilde{\rho}_q(\mathbf{r}). \tag{A8}$$

More elaborate parametrizations of the pairing energy functional are frequently used in the literature. When enforcing time-reversal invariance as done here, the local pair densities entering the pairing functional are related to the pairing tensor through

$$\tilde{\rho}_q(\mathbf{r}) \equiv 2\sum_{\mu>0} W_{\mu\bar{\mu}}^{\tilde{\rho}}(\mathbf{r}q)\,\kappa_{\bar{\mu}\mu}^{\varphi\varphi'}, \tag{A9}$$

$$\tilde{\rho}_q^*(\mathbf{r}) \equiv 2\sum_{\mu>0} W_{\mu\bar{\mu}}^{\bar{\rho}\,*}(\mathbf{r}q)\,\kappa_{\bar{\mu}\mu}^{\varphi'\varphi*}, \tag{A10}$$

where $\kappa_{\mu\bar{\mu}}^{\varphi\varphi'}$ and $\kappa_{\mu\bar{\mu}}^{\varphi'\varphi*}$ are given by Eqs. (6) and (7) for SR-EDF calculations with $\varphi' = \varphi$ and by Eqs. (17) and (18), or Eqs. (39) and (40), respectively, for PNR-MR-EDF calculations. In the case of SR-EDF and PNR-MR-EDF calculations, $W_{\mu\bar{\mu}}^{\tilde{\rho}}(\mathbf{r}q)$ and $W_{\mu\bar{\mu}}^{\bar{\rho}}(\mathbf{r}q)$ are equal and given by

$$W_{\mu\bar{\mu}}^{\tilde{\rho}}(\mathbf{r}q) = W_{\mu\bar{\mu}}^{\bar{\rho}}(\mathbf{r}q) = g_\mu \sum_{\sigma=\pm1} \sigma\phi_\mu(\mathbf{r}\sigma q)\phi_{\bar{\mu}}(\mathbf{r}-\sigma q) \tag{A11}$$

and represent the spin-singlet part of the two-body wave function. This does not hold for other MR-EDF calculations. The notation $\sigma = \pm1$ denotes the spinor component with spin projection $\pm1/2$. The functions $W_{\mu\bar{\mu}}^{\tilde{\rho}}(\mathbf{r}q)$ and $W_{\mu\bar{\mu}}^{\bar{\rho}}(\mathbf{r}q)$ incorporate a cutoff g_μ to regularize the pairing problem, which is otherwise divergent in a variational calculation. In the SR calculations, we use the smooth phenomenological cutoff proposed in Ref. [84], whereas in the PAV-PNR MR calculations it is set to $g_\mu = 1$.

APPENDIX B: CORRECTION TERM

A. Bilinear terms

1. Matrix elements

We focus here on the case where the system is time-reversal invariant, which leads to

$$W_{\mu\mu}^{f} = W_{\bar{\mu}\bar{\mu}}^{f} \tag{B1}$$

for the time-even densities contributing to the Skyrme and Coulomb functionals. There is a minus sign in the left-hand side of Eq. (B1) when considering time-odd ones that we do not have to take into account here as the corresponding contributions from the two states $(\mu, \bar{\mu})$ cancel out both in the total energy and in the correction given by Eq. (29). For the state-dependent function entering the pair density we have

$$W_{\mu\bar{\mu}}^{\tilde{\rho}*}(\mathbf{r}q) = W_{\mu\bar{\mu}}^{\tilde{\rho}}(\mathbf{r}q) = -g_\mu W_{\mu\mu}^{\rho}(\mathbf{r}q). \tag{B2}$$

For the SIII energy functional, the matrix elements that match the definition of the bilinear part as given by Eq. (9) read as

$$\bar{v}_{\mu\nu\mu\nu}^{\rho\rho} = 2\int d^3r \sum_{f,f'} A^{ff'} W_{\mu\mu}^{f}(\mathbf{r}q)\, W_{\nu\nu}^{f'}(\mathbf{r}q), \tag{B3}$$

where the sum over f, f' runs over all terms appearing in Eq. (A3). The quasilocal form of the Skyrme energy functional simplifies the construction of the matrix elements $\bar{v}_{\mu\nu\mu\nu}^{\rho\rho}$ in two ways: on the one hand, they involve one triple integral only and, on the other, they contain products that are separable in μ and ν. This is of great help from the numerical point of view when coding the correction to the PNR energy as defined by Eq. (29).

The situation is different for the direct Coulomb term. Indeed, the corresponding matrix elements (not antisymmetric as Coulomb exchange was dropped altogether) are not separable

$$\bar{v}_{\mu\nu\mu\nu}^{\rho\rho} = 2e^2 \iint d^3r d^3r' \,\frac{W_{\mu\mu}^{\rho}(\mathbf{r}p)W_{\nu\nu}^{\rho}(\mathbf{r}'p)}{|\mathbf{r}-\mathbf{r}'|}. \tag{B4}$$

and they involve a sixfold integral. This considerably complicates their calculation compared to the matrix elements of the Skyrme functional. Instead, the Poisson equation for the Coulomb potential generated by the source $W_{\lambda\lambda}^{\rho}(\mathbf{r}p)$

$$U_{\lambda\lambda}^{\rho}(\mathbf{r}) = -4\pi e\Delta W_{\lambda\lambda}^{\rho}(\mathbf{r}p), \tag{B5}$$

is solved first using boundary conditions constructed from the lowest-order terms in a multipole expansion of the state-dependent field $W_{\lambda\lambda}^{\rho}(\mathbf{r}p)$, and then the Coulomb energy of the other density in this field is obtained as

$$\bar{v}_{\mu\nu\mu\nu}^{\rho\rho} = 2e^2 \int d^3r\, W_{\mu\mu}^{\rho}(\mathbf{r}p)U_{\nu\nu}(\mathbf{r}). \tag{B6}$$

For all but very light nuclei, the calculation of the correction is much more costly than the calculation of the PNR direct Coulomb energy itself, as the correction $U_{\mu\mu}^{\rho}(\mathbf{r})$ has to be determined for each single-particle state solving Eq. (B5), whereas for the total Coulomb energy the Coulomb potential

has to be determined only for the summed up total charge density. However, $U^{\rho}_{\mu\mu}(\mathbf{r})$ entering the correction is independent of the gauge angle, whereas the Coulomb potential has to be determined for each gauge anglewhen calculating the total PNR Coulomb energy.

Last, but not least, the matrix elements entering the pairing functional are given by

$$\bar{v}^{\kappa\kappa}_{\mu\bar{\mu}\nu\bar{\nu}} = 4\int d^3r\; A^{\tilde{\rho}\tilde{\rho}}\, W^{\tilde{\rho}*}_{\mu\bar{\mu}}(\mathbf{r}q)\, W^{\tilde{\rho}}_{\nu\bar{\nu}}(\mathbf{r}q). \tag{B7}$$

2. Correction

Let us now write the spurious contribution $\mathcal{E}^N_C G$ that must be removed from the MR-PNR energy, defined by Eq. (29), for the functional introduced in Appendices A1, A2, and A3.

The spurious contributions only originate from interactions between particles of the same isospin. All contributions from the bilinear part of the energy functional to the correction contain the same occupation factor, for which we introduce the shorthand notation

$$\mathcal{V}^N_{SG\mu} \equiv (u_\mu v_\mu)^4 \int_0^{2\pi} d\varphi \frac{e^{-i\varphi N}}{2\pi c^2_N} \frac{(e^{2i\varphi}-1)^2}{\left(u^2_\mu + v^2_\mu e^{2i\varphi}\right)^2} \times \prod_{\substack{\nu>0\\ q_\nu=q_\mu}} \left(u^2_\nu + v^2_\nu e^{2i\varphi}\right). \tag{B8}$$

Hence, we obtain

$$\mathcal{E}^N_{\rm CG} = 4\int d^3r \sum_{\mu>0} \mathcal{V}^N_{{\rm SG}\mu} \Bigg[\sum_{\{f,f'\}} A^{ff'} W^f_{\mu\mu}(\mathbf{r}q)\, W^{f'}_{\mu\mu}(\mathbf{r}q) - A^{\tilde{\rho}\tilde{\rho}}\, \tilde{W}_{\mu\bar{\mu}}(\mathbf{r}q)\, \tilde{W}_{\mu\bar{\mu}}(\mathbf{r}q) + e^2\, W^{\rho}_{\mu\mu}(\mathbf{r}p) U_{\mu\mu}(\mathbf{r}) \Bigg], \tag{B9}$$

where it is understood that the Coulomb term only contributes to the sum over proton pairs. In the MR-PNR code, the calculation of Eq. (B9) constitutes an effort similar to the evaluation of a local one-body operator, as it can be reduced to a single sum over half of the single-particle states adding up a local function in space that is integrated over afterward.

B. Trilinear terms

1. General expression

We have restricted ourselves here to the special case of the Skyrme SIII functional. The zero-range three-body force that it originates from has the particular property that it gives an energy functional composed of terms that are bilinear in densities of one isospin times a density of the other isospin. The absence of terms trilinear in densities of one isospin greatly simplifies the correction term (see Article I), which reduces to

$$\begin{aligned}\mathcal{E}^N_{\rm CG} = \frac{1}{6}\sum_{\mu>0}\sum_{\substack{\lambda\gtrless 0\\ q_\lambda\neq q_\mu}} &\left(\bar{v}^{\rho\rho\rho}_{\mu\mu\lambda\mu\mu\lambda} + \bar{v}^{\rho\rho\rho}_{\bar{\mu}\mu\lambda\bar{\mu}\mu\lambda} + \bar{v}^{\rho\rho\rho}_{\mu\bar{\mu}\lambda\mu\bar{\mu}\lambda} + \bar{v}^{\rho\rho\rho}_{\bar{\mu}\bar{\mu}\lambda\bar{\mu}\bar{\mu}\lambda} + \bar{v}^{\rho\rho\rho}_{\mu\lambda\mu\mu\lambda\mu} + \bar{v}^{\rho\rho\rho}_{\bar{\mu}\lambda\mu\bar{\mu}\lambda\mu}\right.\\ &\left. + \bar{v}^{\rho\rho\rho}_{\mu\lambda\bar{\mu}\mu\lambda\bar{\mu}} + \bar{v}^{\rho\rho\rho}_{\bar{\mu}\lambda\bar{\mu}\bar{\mu}\lambda\bar{\mu}} + \bar{v}^{\rho\rho\rho}_{\lambda\mu\mu\lambda\mu\mu} + \bar{v}^{\rho\rho\rho}_{\lambda\bar{\mu}\mu\lambda\bar{\mu}\mu} + \bar{v}^{\rho\rho\rho}_{\lambda\mu\bar{\mu}\lambda\mu\bar{\mu}} + \bar{v}^{\rho\rho\rho}_{\lambda\bar{\mu}\bar{\mu}\lambda\bar{\mu}\bar{\mu}}\right) \mathcal{V}^{N_\mu}_{{\rm SG}\,\mu}\\ &\times v^2_\lambda \left[\int_0^{2\pi} d\phi\; \frac{e^{-i\phi N_\lambda}}{2\pi c^2_{N_\lambda}} \frac{e^{2i\phi}}{u^2_\lambda + v^2_\lambda e^{2i\phi}} \prod_{\substack{\nu>0\\ q_\nu=q_\lambda}} \left(u^2_\nu + v^2_\nu e^{2i\phi}\right)\right],\end{aligned} \tag{B10}$$

where $(N_\lambda = N, N_\mu = Z)$ or $(N_\lambda = Z, N_\mu = N)$ depending on the isospin of the states $(\mu, \bar{\mu})$.

2. Matrix elements

The matrix elements of the trilinear term appearing in the SIII Skyrme functional are given by

$$\bar{v}^{\rho\rho\rho}_{\mu\nu\lambda\mu\nu\lambda} = 6\int d^3r A^{\rho\rho\rho}\, W^{\rho}_{\mu\mu}(\mathbf{r}q_\mu)\, W^{\rho}_{\nu\nu}(\mathbf{r}q_\nu)\, W^{\rho}_{\nu\nu}(\mathbf{r}q_\lambda). \tag{B11}$$

3. Correction

Finally, the spurious term to be removed from the trilinear part of the SIII Skyrme functional is

$$\mathcal{E}^N_{\rm CG} = 12\sum_{\mu>0} \mathcal{V}^{N_\mu}_{{\rm SG}\mu} \int d^3r \left[W^{\rho}_{\mu\mu}(\mathbf{r}q_\mu)\right]^2 \times \left[\int_0^{2\pi} d\phi\; \frac{e^{-i\phi N_\lambda}}{2\pi c^2_{N_\lambda}} \rho_{q_\lambda}(\mathbf{r}\phi) \prod_{\substack{\nu>0\\ q_\nu=q_\lambda}} \left(u^2_\nu + v^2_\nu e^{2i\varphi}\right)\right], \tag{B12}$$

where the last term in square brackets $[\cdots]$ is nothing but the particle-number-projected local density of nucleons with isospin $q_\nu \neq q_\mu$.

[1] M. Bender, P.-H. Heenen, and P.-G. Reinhard, Rev. Mod. Phys. **75**, 121 (2003).
[2] P. Hohenberg and W. Kohn, Phys. Rev. **136**, B864 (1964).
[3] R. M. Dreizler and E. K. U. Gross, *Density Functional Theory: An Approach to the Quantum Many-Body Problem* (Springer-Verlag, Berlin, 1990).
[4] R. G. Parr and W. Yang, *Density-Functional Theory of Atoms and Molecules* (Clarendon, Oxford, UK, 1989).
[5] C. Fiolhais, F. Nogueira, and M. Marques, eds., *Lecture Notes in Physics: A Primer in Density Functional Theory* (Springer, Berlin/Heidelberg, 2003), Vol. 620.
[6] W. Koch and M. C. Holthausen, *A Chemist's Guide to Density Functional Theory* (Wiley-VCH, Weinheim, 2001).
[7] A. Nagy, Phys. Rep. **298**, 1 (1998).
[8] W. Kohn, Rev. Mod. Phys. **71**, 1253 (1998).
[9] J. Engel, Phys. Rev. C **75**, 014306 (2007).
[10] B. G. Giraud, B. K. Jennings, and B. R. Barrett, Phys. Rev. A **78**, 032507 (2008).
[11] B. G. Giraud, Phys. Rev. C **77**, 014311 (2008).
[12] P.-G. Reinhard and W. Otten, Nucl. Phys. **A420**, 173 (1984).
[13] S. Åberg, H. Flocard, and W. Nazarewicz, Annu. Rev. Nucl. Part. Sci. **40**, 439 (1990).
[14] W. Nazarewicz, Prog. Part. Nucl. Phys. **28**, 307 (1992).
[15] W. Nazarewicz, Int. J. Mod. Phys. E **2**, 51 (1993).
[16] P. G. de Gennes, *Superconductivity of Metals and Alloys* (Benjamin, New York, 1966).
[17] P.-H. Heenen, P. Bonche, J. Dobaczewski, and H. Flocard, Nucl. Phys. **A561**, 367 (1993).
[18] M. Anguiano, J. L. Egido, and L. M. Robledo, Nucl. Phys. **A696**, 467 (2001).
[19] M. Samyn, S. Goriely, M. Bender, and J. M. Pearson, Phys. Rev. C **70**, 044309 (2004).
[20] T. Nikšić, D. Vretenar, and P. Ring, Phys. Rev. C **74**, 064309 (2006).
[21] L. M. Robledo, Int. J. Mod. Phys. E **16**, 337 (2007).
[22] N. Tajima, H. Flocard, P. Bonche, J. Dobaczewski, and P.-H. Heenen, Nucl. Phys. **A542**, 355 (1992).
[23] F. Dönau, Phys. Rev. C **58**, 872 (1998).
[24] D. Almehed, S. Frauendorf, and F. Dönau, Phys. Rev. C **63**, 044311 (2001).
[25] J. Dobaczewski, M. V. Stoitsov, W. Nazarewicz, and P. G. Reinhard, Phys. Rev. C **76**, 054315 (2007).
[26] T. R. Rodriguez and J. L. Egido, Phys. Rev. Lett. **99**, 062501 (2007).
[27] T. Duguet, M. Bender, K. Bennaceur, D. Lacroix, and T. Lesinski, Phys. Rev. C **79**, 044320 (2009).
[28] D. Lacroix, T. Duguet, and M. Bender, Phys. Rev. C **79**, 044318 (2009).
[29] J. P. Perdew and A. Zunger, Phys. Rev. B **23**, 5048 (1981).
[30] S. Stringari and D. M. Brink, Nucl. Phys. **A304**, 307 (1978).
[31] P. Bonche, J. Dobaczewski, H. Flocard, P.-H. Heenen, and J. Meyer, Nucl. Phys. **A510**, 466 (1990).
[32] P.-G. Reinhard and C. Toepffer, Int. J. Mod. Phys. E **3**, 435 (1994).
[33] N. Onishi and S. Yoshida, Nucl. Phys. **80**, 367 (1966).
[34] R. Balian and E. Brezin, Nuovo Cimento B **64**, 37 (1969).
[35] G. C. Wick, Phys. Rev. **80**, 268 (1950).
[36] P. Ring and P. Schuck, *The Nuclear Many-Body Problem* (Springer-Verlag, New York, 1980).
[37] J. Blaizot and G. Ripka, *Quantum Theory of Finite Systems* (MIT Press, Cambridge, MA, 1986).
[38] H. J. Mang, Phys. Rep. **18**, 327 (1975).
[39] P. Ring, R. Beck, and H. J. Mang, Z. Phys. **231**, 10 (1970).
[40] A. L. Goodman, in *Advances in Nuclear Physics*, edited by J. W. Negele and E. Vogt (Plenum Press, New York, 1979), Vol. 11, p. 263.
[41] D. Vautherin and D. M. Brink, Phys. Rev. C **5**, 626 (1972).
[42] J. Dechargé and D. Gogny, Phys. Rev. C **21**, 1568 (1980).
[43] P.-G. Reinhard and H. Flocard, Nucl. Phys. **A584**, 467 (1995).
[44] E. Chabanat, P. Bonche, P. Haensel, J. Meyer, and R. Schaeffer, Nucl. Phys. **A635**, 231 (1998); [Erratum-*ibid.* **A643**, 441 (1998)].
[45] M. Bender, J. Dobaczewski, J. Engel, and W. Nazarewicz, Phys. Rev. C **65**, 054322 (2002).
[46] S. A. Fayans, S. V. Tolokonnikov, E. L. Trykov, and D. Zawischa, Nucl. Phys. **A676**, 49 (2000).
[47] M. Anguiano, J. Egido, and L. Robledo, Nucl. Phys. **A683**, 227 (2001).
[48] D. Vretenar, A. V. Afanasjev, G. A. Lalazissis, and P. Ring, Phys. Rep. **409**, 101 (2005).
[49] J. A. Sheikh and P. Ring, Nucl. Phys. **A665**, 71 (2000).
[50] M. Anguiano, J. L. Egido, and L. M. Robledo, Phys. Lett. **B545**, 62 (2002).
[51] J. A. Sheikh, P. Ring, E. Lopes, and R. Rossignoli, Phys. Rev. C **66**, 044318 (2002).
[52] M. V. Stoitsov, J. Dobaczewski, R. Kirchner, W. Nazarewicz, and J. Terasaki, Phys. Rev. C **76**, 014308 (2007).
[53] T. R. Rodriguez, J. L. Egido, and L. M. Robledo, Phys. Rev. C **72**, 064303 (2005).
[54] G. Ripka and R. Padjen, Nucl. Phys. **A132**, 489 (1969).
[55] C. D. Siegal and R. A. Sorensen, Nucl. Phys. **A184**, 81 (1972).
[56] M. Bender and T. Duguet, Int. J. Mod. Phys. E **16**, 222 (2007). The correction used is this article is not exactly the same as the one used here and contains a part of the true multi-reference self-interaction and self-pairing.
[57] B. F. Bayman, Nucl. Phys. **15**, 33 (1960).
[58] B. Banerjee, H. J. Mang, and P. Ring, Nucl. Phys. **A215**, 366 (1973).
[59] T. Duguet (2006, unpublished).
[60] C. A. Ullrich, P.-G. Reinhard, and E. Suraud, Phys. Rev. A **62**, 053202 (2000).
[61] C. Legrand, E. Suraud, and P.-G. Reinhard, J. Phys. B **35**, 1115 (2002).
[62] A. Ruzsinsky, J. P. Perdew, G. I. Csonka, O. A. Vydrov, and G. E. Scuseria, J. Phys. Chem. **126**, 104102 (2007).
[63] E. Engel, *A Primer in Density Functional Theory*, edited by C. Fiolhais, F. Nogueira, and M. Marques, Lecture Notes in Physics **620** (Springer-Verlag, Berlin, Heidelberg, 2003), p. 56.
[64] S. Kümmel and L. Kronik, Rev. Mod. Phys. **80**, 3 (2008).
[65] K. Rutz, M. Bender, P.-G. Reinhard, and J. A. Maruhn, Phys. Lett. **B468**, 1 (1999).
[66] M. Bender and P.-G. Reinhard (unpublished discussion notes, 1999).
[67] M. Bender, H. Flocard, and P.-H. Heenen, Phys. Rev. C **68**, 044321 (2003).
[68] T. Duguet, M. Bender, P. Bonche, and P.-H. Heenen, Phys. Lett. **B559**, 201 (2004).
[69] M. Bender, P. Bonche, T. Duguet, and P.-H. Heenen, Phys. Rev. C **69**, 064303 (2004).
[70] M. Bender, G.-F. Bertsch, and P.-H. Heenen, Phys. Rev. C **73**, 034322 (2006).

[71] M. Bender and P.-H. Heenen, Nucl. Phys. **A713**, 390 (2003).
[72] A. P. Severyukhin, M. Bender, H. Flocard, and P.-H. Heenen, Phys. Rev. C **75**, 064303 (2007).
[73] M. Bender, P. Bonche, and P.-H. Heenen, Phys. Rev. C **74**, 024312 (2006).
[74] K. Dietrich, H. J. Mang, and J. H. Pradal, Phys. Rev. **135**, B22 (1964).
[75] V. N. Fomenko, J. Phys. G **3**, 8 (1970).
[76] T. Bürvenich, D. G. Madland, J. A. Maruhn, and P.-G. Reinhard, Phys. Rev. C **65**, 044308 (2002).
[77] M. Beiner, H. Flocard, N. V. Giai, and P. Quentin, Nucl. Phys. **A238**, 29 (1975).
[78] M. Baldo, P. Schuck, and X. Viñas, Phys. Lett. **B663**, 390 (2008).
[79] H. Flocard and N. Onishi, Ann. Phys. (NY) **254**, 275 (1997).
[80] H. Zdunczuk, J. Dobaczewski, and W. Satuła, Int. J. Mod. Phys. E **16**, 377 (2007).
[81] M. V. Stoitsov *et al.* (2007, unpublished).
[82] E. Perlinska, S. G. Rohozinski, J. Dobaczewski, and W. Nazarewicz, Phys. Rev. C **69**, 014316 (2004).
[83] P. Bonche, H. Flocard, and P.-H. Heenen, Nucl. Phys. **A467**, 115 (1987).
[84] P. Bonche, H. Flocard, P.-H. Heenen, S. J. Krieger, and M. S. Weiss, Nucl. Phys. **A443**, 39 (1985).